Of all the communities available to us there is not one I would want to devote myself to, except for the society of the true searchers, which has very few living members at any time...

Albert Einstein (1879-1955)

University of Alberta

Distorted Black Holes and Black Strings

by

Andrey A. Shoom

A thesis submitted to the Faculty of Graduate Studies and Research
in partial fulfillment of the requirements for the degree of

Doctor of Philosophy

Department of Physics

Fall 2009
Edmonton, Alberta

Examining Committee

Valeri P. Frolov, Physics

Robert B. Mann, Physics & Applied Mathematics, University of Waterloo

Richard Marchand, Physics

Marc de Montigny, Campus Saint-Jean

Don N. Page, Physics

Dmitri Pogosyan, Physics

To

My Parents

Abstract

The main objective of this thesis is to study the behavior of black objects in external fields, for example black holes and black strings in 4 and 5-dimensional spacetimes respectively. In particular, to analyze how external fields affect horizons and the internal structure of such objects, to study their properties, and to understand how the spacetime fabric works.

The thesis contains three chapters. In Chapters 1 and 2 we study the interior of 4-dimensional static, axisymmetric, electrically neutral and electrically charged distorted black holes. We analyze how external static and axisymmetric distortions affect the interior of such black holes. In particular, we study the behavior of the interior solution of an electrically neutral black hole near its horizon and singularity. The analysis shows that there exists a certain duality between the event horizon and the singularity. As a special example, we study the interior of a compactified 4-dimensional Schwarzschild black hole. In the case of an electrically charged black hole, a similar duality exists between its event and Cauchy horizons. The duality implies that the Cauchy horizon remains regular, provided the distortion is regular at the event horizon.

Extension of the general theory of relativity to higher dimensional spacetimes brings a large variety of black objects whose boundary, the event horizon, may be of a complicated structure. One such object is a black string. In Chapter 3 we discuss the so-called Gregory-Laflamme instability of 5-dimensional black strings in a spacetime with one compact dimension and their topological phase transitions. Here we consider black strings with electric or magnetic charge. Linear static perturbations of these objects indicate the presence of a threshold unstable mode.

An analysis of such mode shows that an electrically charged black string is less stable than a neutral one. The situation is opposite for a magnetically charged black string. An analysis of 5-dimensional extremal black string with electric charge shows a continuous spectrum of unstable threshold modes.

The results presented in this thesis may have applications in the theory of classical 4-dimensional black holes and in the modern theoretical models of higher dimensions.

Preface

The physical objects we shall discuss in this thesis are black holes and black strings. These objects are solutions of the Einstein theory of general relativity. We shall discuss static black holes and black strings in asymptotically flat (or analytically extendable to asymptotically flat), predictable spacetimes. The characteristic feature of such objects is their boundary, which is called the event horizon. Any physical object, for example, a particle, which travels in the future direction outside such a black object and crosses its event horizon cannot return back to the same region of space. The black hole event horizon is a spatially compact null hyper-surface. The event horizon of a black string is a null hyper-surface, which may be not spatially compact. Here we consider two known types of black holes, the Schwarzschild black hole, which is one-parameter solution of the vacuum Einstein equations, and the Reissner-Nordström (RN) black hole, which is two-parameter solution of the Einstein-Maxwell equations. The parameter of the Schwarzschild black hole is its mass. The parameters of the RN black hole are its mass and electric (or magnetic) charge. Black strings are higher dimensional black objects. We shall discuss 5-dimensional black strings with electric or magnetic charge. The objective of this thesis is to study such black holes and black strings distorted by static external fields.

We begin with a 4-dimensional Schwarzschild black hole, which is the simplest black-hole solution of the Einstein equations. This solution is vacuum, static, spherically symmetric, and asymptotically flat. It is of Petrov type-D. The black hole has a spacetime curvature singularity located behind its event horizon. The singularity is spacelike and topologically $\mathbb{R}^1 \times S^2$ (see, e.g., [51]). The interior of the black hole represents an anisotropic universe collapsing towards the black hole singularity.

The Schwarzschild black hole is stable against external gravitational perturbations. The evolution of linear gravitational perturbations shows the presence of quasi-normal modes in the black hole radiation spectrum. According to the Israel uniqueness theorem, the Schwarzschild black hole is the only vacuum, static, asymptotically flat solution which has a regular, simply connected event horizon [77]. Such properties of the Schwarzschild black hole make it quite an interesting object to study.

Recent astronomical observations and their analysis suggest that each galaxy, including our Milky Way, may contain at its center a supermassive black hole which strongly interacts with external matter (see, e.g., [28, 35]). To study properties of such a black hole, especially its interior structure, is a formidable problem. At the beginning it is better to start with less complicated model. Namely, to study how the interaction of the Schwarzschild black hole with external matter

and fields affects its properties. This question is important not only from astrophysical point of view. Studying the interaction of black holes with surrounding matter and fields allows us to understand deeper their thermodynamic behavior, what is particularly important in connection with string theory. In addition, black holes play an important role as backgrounds for quantum fields. Finally, analysis of black hole solutions may let us understand some geometrical and causal properties of spacetime within the scope of general relativity. However, due to the nonlinear nature of the Einstein equations, study of black hole interactions is a very complicated problem, which, in most cases, is tractable only numerically. To find an exact, analytical solution which describes the interaction of the Schwarzschild black hole with external objects seems to be possible only for highly symmetrical models. But even such idealized models allow us to draw some important conclusions about properties the Schwarzschild black hole. One of such cases, representing the Schwarzschild black hole distorted by static, axisymmetric gravitational fields due to remote masses, we consider in Chapter 1 of the thesis. We study how such type of distortion affects the Schwarzschild black hole interior. To do this, we ask the following questions. Does the distortion change the topology of the singularity of the Schwarzschild black hole? How does such a distortion affects the maximal proper time of free fall from the event horizon to the singularity? Does the event horizon of the distorted black hole have regions of high spacetime curvature, and if so, what is their location? This question is important for study of the validity of the semiclassical approximation which is used in the analysis of the Schwarzschild black hole quantum evaporation. As it is well known, such an approximation leads to the information paradox (see, e.g., [52, 103] and references therein). In addition, a compactified Schwarzschild black hole can be considered as a topological phase in the black string − black hole topological phase transition, which we discuss in Chapter 3. Studying the analytical model of the 4-dimensional compactified Schwarzschild black hole, which is a particular type of distorted black hole, one can analyze whether the classical theory of general relativity can properly describe the merger points of the topological phase transition, where the spacetime curvature is extremely high. Finally, one can ask if there is any relation between the distortion of the event horizon and the interior of the Schwarzschild black hole. To address this question more clearly, we remind the reader that the interior of the Schwarzschild black hole is a dynamical region; thus, a distortion of its event horizon can be considered as initial Cauchy data for the corresponding dynamical evolution. Chapter 1 of this thesis clarifies some of these questions.

In Chapter 2, we study the interior of a distorted 4-dimensional RN black hole. The undistorted RN black hole is a static, spherically symmetric, asymptotically flat solution of the Einstein-Maxwell equations. It has many properties similar to those of the Schwarzschild black hole. Namely, it is of Petrov type-D. It radiates the quasi-normal modes; however, they are always both gravitational and electro-

magnetic. The Israel uniqueness theorem for the Schwarzschild black hole admits generalization to the RN black hole. Namely, the RN solution is the only static, asymptotically flat solution to the Einstein-Maxwell equations, which has a regular, simply connected event horizon [78]. However, due to the presence of electric charge, the interior of the RN black hole is remarkably different from that of the Schwarzschild black hole. The principal difference is that the RN black hole has an inner, Cauchy horizon, which is a null hyper-surface beyond which predictability of evolution based on the past initial data breaks down. The RN black hole curvature singularity located in its centre, behind the Cauchy horizon, is topologically $\mathbb{R}^1 \times S^2$ (see, e.g., [51]). However, in contrast to the Schwazschild black hole, this singularity is timelike. The singularity can be avoided by timelike and null curves. A maximal analytic extension of the RN spacetime, which makes it geodesically complete, results in an infinite sequence of new universes which may be explored by adventurers who succeeded in crossing the Cauchy horizon (see Figure 2.1). However, crossing the Cauchy horizon causes its perturbations and, as a result, is fraught with danger. An analysis of the Cauchy horizon stability against gravitational perturbations, in particular, the mass inflation phenomenon, suggests that the spacetime curvature grows infinitely near a perturbed Cauchy horizon [107]. Thus, it is important to understand what types of perturbations, if any, preserve the regular Cauchy horizon. For example, does the Cauchy horizon of the RN black hole distorted by certain external axisymmetric fields remain regular? This is the main question among others we address here. In Chapter 2, we discuss the interior region of such a distorted RN black hole which is located between its event and Cauchy horizons. We ask the following questions. Is there any relation between the distortion of the event and Cauchy horizons of the RN black hole? How much does the distortion affect the maximal proper time of free fall from the event to the Cauchy horizon of the RN black hole? Do the horizons have regions of high spacetime curvature, and if so, what is their location? Answers to these questions, which we present in Chapter 2 of the thesis, may help us understand physical properties of the RN black hole, which is very similar in its internal structure to the rotating (Kerr) black hole which is a more realistic candidate for an astrophysical black hole than the Schwarzschild one is.

In Chapter 3, we discuss black strings which are solutions of higher dimensional theory of general relativity. Consideration of higher dimensions has at least two reasons. One is mathematical. We want to understand deeper the mathematical structure of general relativity. In other words, we want to understand, using the language of general relativity, how the spacetime fabric works. Another reason originates from attempts to solve the hierarchy problem, which is a hot issue of modern theoretical physics. In attempts to resolve the hierarchy problem, modern theoretical models suggest that our world may have large extra spatial dimensions (see, e.g., [6, 8]). If such a suggestion is true, we may have an interesting possibility

of mini black hole production in the future LHC experiments.

In a higher dimensional spacetime a large variety of topologically different black objects may exist, for example black holes, black rings, black branes and black strings (for a review see, e.g., [66]). So the rich variety of higher dimensional black objects makes their study especially interesting. Black branes and black strings are low energy solutions of string theory. Infinitely long black branes and black strings are unstable against small gravitational perturbations. The classical instability of black branes and black strings, the so-called Gregory-Laflamme instability, is analogous to the Jeans instability of gravitating systems. In addition, there is an interesting relation between the gravitational instability of black branes and black strings and the off-shell instability of the corresponding Euclidean black holes, known as gravitational instantons.

Here we consider a black string in a 5-dimensional spacetime which has one large compact spatial dimension. A spacelike cross section of such a black string horizon has topology $S^2 \times S^1$. In contrast, a spacelike cross section of the corresponding compactified 5-dimensional black hole horizon has the topology of a 3-dimensional hyper-sphere, S^3. As we mentioned before, the black string and black hole can be considered as different topological phases of a topological phase transition diagram. Black strings, as well as black holes, are thermodynamic systems, which have temperature and entropy. Using a global thermodynamic argument, one can show that for a fixed asymptotic size of the compact dimension there is a critical value of mass of a neutral black string below which such a string becomes thermodynamically unstable, and may likely undergo a topological phase transition to the corresponding compactified black hole. Such thermodynamic instability is closely related to gravitational instability of the black string.

In Chapter 3 of the thesis, we shall study a black string with electric charge, which is a solution of 5-dimensional Einstein-Maxwell equations. We consider linear, static gravitational perturbations and search for a threshold unstable mode. We are interested how the presence of an electric charge affects the black string stability. This is the main question we address here. Such a problem was already considered for black strings with magnetic charge and with, or without, dilaton field. As it was illustrated, magnetic charge tends to stabilize black string. Thus, it is important to understand the role of black string parameters in its thermodynamic and dynamic properties. Here we study dynamic and thermodynamic properties of a 5-dimensional electrically charged black string and compare our results with the properties of a 5-dimensional magnetically charged black string. In addition, we consider an extremal 5-dimensional black string with electric charge and study its linear, static gravitational perturbations.

This thesis is organized as follows.

In Chapter 1, we discuss a 4-dimensional distorted Schwarzschild black hole. In Section 1.3 we discuss the Weyl solution representing a distorted Schwarzschild

black hole and focus on its interior region. In Section 1.4 we discuss properties of the distorted black hole solution and establish duality relations between the black hole horizon and singularity. In Section 1.5, we discuss how the black hole distortion affects the maximal proper time of free fall of a test particle moving along the axis of symmetry from the horizon to the singularity. An asymptotic form of metric near the black hole horizon and singularity is obtained in Section 1.6 and Section 1.7 respectively. Special examples of exact solutions and their properties are considered in Section 1.8. In Section 1.9, we consider properties of the interior and singularity of 4-dimensional compactified black holes. Section 1.10 contains a summary and discussions of our results. Additional technical details and calculations used in this chapter are collected in Appendixes A, B, C and D.

In Chapter 2 we consider a 4-dimensional distorted electrically charged black hole. Section 2.3 of this chapter collects the results concerning the charged distorted black hole solution generated by the Harrison-Ernst transformation. We present these results mainly in order to fix the notations which we use in the main part of this chapter. In Section 2.4, we establish special duality relations between properties of the outer (event) and the inner (Cauchy) horizons of the charged distorted black hole. In Sections 2.5 and 2.6, we study the Gaussian curvature of the horizon surfaces and present their isometric embedding diagrams. In Section 2.7, we discuss how the black hole distortion affects the maximal proper time of free fall of a test particle moving along the axis of symmetry from the outer to the inner horizon. In Section 2.8, we establish a relation between the spacetime curvature invariants near the black hole horizons and their Gaussian 2-dimensional curvatures. We summarize and discuss our results in Section 2.9. Necessary details are included in Appendix E.

In Chapter 3 we discuss the Gregory-Laflamme instability of a 5-dimensional black string with electric charge. In Section 3.2, we present the metric of the 5-dimensional electric black string and discuss its properties. In Section 3.3, we consider the static S-wave perturbation of the charged string and derive the corresponding master equation. In Section 3.4, we integrate numerically the master equation and construct the critical curve in the topological phase transition diagram. In Section 3.5, we derive a similar curve using the global thermodynamic equilibrium argument. In Section 3.6 we study the static S-wave perturbations of the 5-dimensional extremal electric black string. In Section 3.7, we discuss and compare the phase diagrams for the electric and magnetic black strings. Section 3.8 contains a discussion of our results.

A summary of the results derived and future perspectives are presented in the Conclusion.

The results presented in this doctoral thesis were obtained during the course of the author's Ph.D. program at the University of Alberta between September 2005

and August 2009. The thesis is based on the following published papers in peer reviewed journals:

1. Interior of distorted black holes,
   Valeri P. Frolov and Andrey A. Shoom, Phys. Rev. D **76**, 064037 (2007); arXiv: 0705.1570.

2. Interior of a charged distorted black hole,
   Shohreh Abdolrahimi, Valeri P. Frolov, and Andrey A. Shoom, Phys. Rev. D **80**, 024011 (2009); arXiv: 0905.0178.

3. Gregory-Laflamme instability of 5D electrically charged black strings,
   Valeri P. Frolov and Andrey A. Shoom, Phys. Rev. D **79**, 104002 (2009) arXiv: 0903.2893.

Acknowledgements

I am very much grateful to my supervisor, Professor Valeri P. Frolov, from whom I learnt much more than I could imagine, for his inspiration and encouragement, for fruitful discussions and advices, and for his constant support during my Ph.D. program. It has been a great privilege to be his student and to work with such a True Master. I am very much thankful to Professor Don N. Page for his humanity, for his enthusiasm to discuss physics and many other things, for his advice and encouragement, and for his illuminating and lucid explanations of delicate strands of physics. I am very happy that I had an opportunity to communicate with a person of such intellect and knowledge, that is always a very enjoyable and fascinating journey of mind. I would like to thank Professor Richard Marchand for his kindness and enthusiasm to discuss interesting aspects of physics. It has been a very enjoyable time to be his student and to learn form him many interesting details of statistical physics. My cordial thanks to Professor Sharon Morsink for introducing to me basic physics of neutron stars, and to Professor Dmitri Pogosyan for his interesting lectures on Cosmic Microwave Background radiation.

Last but not least, I thank to the members of the Theoretical Physics Institute, as well as to my colleagues, teachers, and friends, Shohreh Abdolrahimi, Massimo Boninsegni, Patrick Connell, Long Dinh Dang, Dan Gorbonos, Rituparno Goswami, Stepan Grinyok, Werner Israel, Faqir Khanna, Burkhard Kleihaus, David Kubizňák, Jutta Kunz, Robert B. Mann, Marc de Montigny, Eric Poisson, Frans Pretorius, Rodrigo Rocha Cuzinatto, Suneeta Vardarajan, Eric Woolgar, Xing Wu, Shima Yaghoobpour Tari, Hirotaka Yoshino and Andrei Zel'nikov, for valuable and numerous discussions of physics and mathematics.

Finally, I would like to thank Elizabeth Berends, Gordana Brouilette, Patty Chu, Lee Grimard, Sandra Hamilton, Linda Jacklin, Nandi Khanna, Mary Jean Smallman, Carolyn Steinborn, Ruby Swanson, Roseann Whale, Maya Wheelock and Dr. Isaac Isaac for their numerous help and support. My especial thanks to Sarah Derr for her kindness, constant help, and advices during my Ph.D. program.

Table of Contents

List of Figures

List of Symbols and Abbreviations

Here, we present some symbols and notations, and give definitions which are used in the thesis. Other notations and definitions are explained in the text.

Abbreviations

The abbreviation const is used for 'constant'. The capital D is used for 'dimensional', e.g., 4D should be read as 4-dimensional. The number of dimensions is denoted by D, if arbitrary. The gravitational constant in a spacetime of arbitrary dimensions is denoted as $G_{(D)}$. In particular, in 4D spacetime the gravitational constant is denoted as $G_{(4)}$, which we write as G.

Units

The following units convention is used in this thesis: $c = \hbar = k_B = 1$. In Chapters 1 and 2, we take $G = 1$, and in Chapter 3 we take, for convenience, $16\pi G = 1$. Here, the fundamental constants are [4]:

the gravitational constant:	$G = 6.67428(67) \times 10^{-11}\ kg^{-1}\, m^3\, s^{-2}$
the speed of light in vacuum:	$c = 299792458\ m\, s^{-1}$
the reduced Planck constant:	$\hbar = 1.054571628(53) \times 10^{-34}\ kg\, m^2\, s^{-1}$
the Boltzmann constant:	$k_B = 1.3806504(24) \times 10^{-23}\ kg\, m^2\, s^{-2} K^{-1}$

The Planck distance is

$$l_{Pl} = \sqrt{\hbar G/c^3} = 1.616253 \times 10^{-35}\ m.$$

The Planck time is

$$\tau_{Pl} = \sqrt{\hbar G/c^5} = 5.391241 \times 10^{-44}\ s.$$

Symbols and sign conventions

The signature of the spacetime metric $g_{\alpha\beta}$ is: $(-\ +\ +\cdots+)$, i.e., it is $+(D-2)$.
The time coordinate index is 0: $t \equiv x^0$.
Balance of indices and the Einstein summation convention are assumed.
The following special symbols are used:

$\sim$	order of magnitude estimate
$\approx$	approximately equal
$\equiv$	identity
$i = \sqrt{-1}$	imaginary unit, if it sits on the baseline
$a \to b$	a goes to b
$a \longleftrightarrow b$	a goes to b, or b goes to a
$f\|_{x=a}$	value of $f = f(x)$ evaluated at $x = a$
$\|a\|$	absolute value of a
$\mathrm{Re}\,\{a\}$	real part of a
$\wedge$	wedge product
$\boldsymbol{v} \cdot \boldsymbol{w}$	scalar product of vectors $\boldsymbol{v}$ and $\boldsymbol{w}$
$T^{\alpha\beta} = \mathrm{diag}(T^{00}, ...)$	represents a geometrical object $T^{\alpha\beta}$, whose off-diagonal components are zeros
$\lfloor x \rfloor$	the floor function of x, which is the largest integer not greater than x
$\Gamma(x)$	the Gamma function
$\delta(x)$	the Dirac delta function
$H(x) = \begin{cases} 1, & x > 0 \\ 0, & x < 0 \end{cases}$	the Heaviside step function

Basic definitions

Components of geometrical objects are defined with respect to a coordinate basis, e.g., $T_{\alpha_1\alpha_2\cdots}{}^{\beta_1\beta_2\cdots}$. In a local orthonormal frame these components are $T_{\hat{\alpha}_1\hat{\alpha}_2\cdots}{}^{\hat{\beta}_1\hat{\beta}_2\cdots}$.
Antisymmetrization of indices of a tensor $T_{\alpha_1\cdots\alpha_n}{}^{\beta_1\cdots\beta_m}$ is defined by square brackets as follows:

$$T_{[\alpha_1\cdots\alpha_n]}{}^{\beta_1\cdots\beta_m} = \frac{1}{n!}\left(\text{alternating sum of } T_{\alpha_1\cdots\alpha_n}{}^{\beta_1\cdots\beta_m} \text{ over all permutations of } \alpha_i\text{'s}\right).$$

The Kronecker symbol $\delta_\alpha{}^\beta$ is

$$\delta_\alpha{}^\beta = \delta^\beta{}_\alpha = \begin{cases} 1, & \text{if } \alpha = \beta \\ 0, & \text{otherwise.} \end{cases}$$

The partial derivative with respect to coordinate x^α is defined by comma in front of subscript α as follows:

$$f_{,\alpha} \equiv \frac{\partial f}{\partial x^\alpha}\,, \quad f_{,\alpha\beta} \equiv \frac{\partial^2 f}{\partial x^\alpha \partial x^\beta}\,, \quad \text{etc.}$$

The Lie derivative of a tensor $\boldsymbol{T}$ with respect to a vector field $\boldsymbol{v}$ is defined as follows:

$$\begin{aligned} (\mathcal{L}_{\boldsymbol{v}}\boldsymbol{T})_{\alpha_1\alpha_2\cdots}{}^{\beta_1\beta_2\cdots} &= v^\gamma T_{\alpha_1\alpha_2\cdots}{}^{\beta_1\beta_2\cdots}{}_{,\gamma} - T_{\alpha_1\alpha_2\cdots}{}^{\gamma\beta_2\cdots} v^{\beta_1}{}_{,\gamma} - T_{\alpha_1\alpha_2\cdots}{}^{\beta_1\gamma\cdots} v^{\beta_2}{}_{,\gamma} - \cdots \\ &+ T_{\gamma\alpha_2\cdots}{}^{\beta_1\beta_2\cdots} v^\gamma{}_{,\alpha_1} + T_{\alpha_1\gamma\cdots}{}^{\beta_1\beta_2\cdots} v^\gamma{}_{,\alpha_2} + \cdots\,. \end{aligned}$$

The covariant derivative of a tensor $T_{\alpha_1\cdots\alpha_n}{}^{\beta_1\cdots\beta_m}$ is defined by the symbol nabla,

$$\begin{aligned} \nabla_\gamma T_{\alpha_1\cdots\alpha_n}{}^{\beta_1\cdots\beta_m} &= T_{\alpha_1\cdots\alpha_n}{}^{\beta_1\cdots\beta_m}{}_{,\gamma} + \Gamma^{\beta_1}{}_{\delta\gamma} T_{\alpha_1\cdots\alpha_n}{}^{\delta\cdots\beta_m} + \cdots + \Gamma^{\beta_m}{}_{\delta\gamma} T_{\alpha_1\cdots\alpha_n}{}^{\beta_1\cdots\delta} \\ &- \Gamma^\delta{}_{\alpha_1\gamma} T_{\delta\cdots\alpha_n}{}^{\beta_1\cdots\beta_m} - \cdots - \Gamma^\delta{}_{\alpha_n\gamma} T_{\alpha_1\cdots\delta}{}^{\beta_1\cdots\beta_m}\,. \end{aligned}$$

Here, the Christoffel symbols $\Gamma^\alpha{}_{\beta\gamma}$ are

$$\Gamma^\alpha{}_{\beta\gamma} = \frac{1}{2} g^{\alpha\delta}(g_{\delta\beta,\gamma} + g_{\gamma\delta,\beta} - g_{\beta\gamma,\delta})\,.$$

The main conventions for geometrical objects are these adopted in [94]. Namely, the Riemann tensor is

$$R^\alpha{}_{\beta\gamma\delta} = \Gamma^\alpha{}_{\beta\delta,\gamma} - \Gamma^\alpha{}_{\beta\gamma,\delta} + \Gamma^\alpha{}_{\sigma\gamma}\Gamma^\sigma{}_{\beta\delta} - \Gamma^\alpha{}_{\sigma\delta}\Gamma^\sigma{}_{\beta\gamma}\,.$$

The Ricci tensor is defined by $R_{\alpha\beta} = R^\gamma{}_{\alpha\gamma\beta}$. The Ricci scalar is $R = g^{\alpha\beta}R_{\alpha\beta} = R^\alpha{}_\alpha$. The Einstein equations are ($G_{(D)} = 1$)

$$G_{\alpha\beta} = R_{\alpha\beta} - \frac{1}{2} g_{\alpha\beta} R = 8\pi\, T_{\alpha\beta}\,,$$

or

$$R_{\alpha\beta} = 8\pi \left(T_{\alpha\beta} - \frac{1}{D-2} g_{\alpha\beta} T \right)\,, \quad T = g^{\alpha\beta} T_{\alpha\beta}\,.$$

Here, the energy-momentum tensor $T_{\alpha\beta}$ is defined by

$$T_{\alpha\beta} = -\frac{2}{\sqrt{-g}}\left(\frac{\delta(\sqrt{-g}\Lambda_m)}{\delta g^{\alpha\beta}} - \left[\frac{\delta(\sqrt{-g}\Lambda_m)}{\delta(g^{\alpha\beta}{}_{,\gamma})}\right]_{,\gamma}\right),$$

where Λ_m is the Lagrangian density of matter. For our purposes it is sufficient to consider the energy-momentum tensor whose components in a local orthonormal frame are given by

$$T^{\hat{\alpha}\hat{\beta}} = \mathrm{diag}(\varepsilon\,,\ p_i)\,,\ \ i = 1, ..., D-1\,,$$

where ε is the energy density, and p_i's are the $(D-1)$ principal pressures. Here, we define the following energy conditions.
The *null energy condition* is that for any null vector n^α, $T_{\alpha\beta}n^\alpha n^\beta \geqslant 0$, i.e.,

$$\varepsilon + p_i \geqslant 0\,,\ \ \text{for any } i.$$

The *weak energy condition* is that for any timelike vector k^α, $T_{\alpha\beta}k^\alpha k^\beta \geqslant 0$, i.e.,

$$\varepsilon \geqslant 0\,,\ \ \text{and}\ \ \varepsilon + p_i \geqslant 0\,,\ \ \text{for any } i.$$

The weak energy condition implies the null energy condition.
The *strong energy condition* is that for any timelike vector k^α, $T_{\alpha\beta}k^\alpha k^\beta \geqslant \frac{T}{D-2}k^\alpha k_\alpha$, i.e.,

$$\varepsilon + p_i \geqslant 0\,,\ \ \text{and}\ \ \varepsilon + \frac{1}{D-3}\sum_{i=1}^{D-1} p_i \geqslant 0\,,\ \ \text{for any } i.$$

The strong energy condition implies the null energy condition. It does not, in general, imply the weak energy condition.
The *dominant energy condition* is that for any timelike vector k^α, $T_{\alpha\beta}k^\alpha k^\beta \geqslant 0$, and $T_{\alpha\beta}k^\beta$ is not spacelike, i.e.,

$$\varepsilon \geqslant 0\,,\ \ \text{and}\ \ p_i \in [-\varepsilon, \varepsilon]\,,\ \ \text{for any } i.$$

The dominant energy condition implies the weak and the null energy conditions. It does not, in general, imply the strong energy condition.

The corresponding averaged energy conditions can be defined by integrating the null energy condition along a null curve, and by integrating the weak and the strong energy conditions along a timelike curve (for details see, e.g., [120]).

The Weyl tensor is given by

$$C_{\alpha\beta\gamma\delta} = R_{\alpha\beta\gamma\delta} - \frac{2}{D-2}\left(g_{\alpha[\gamma}R_{\delta]\beta} - g_{\beta[\gamma}R_{\delta]\alpha}\right) + \frac{2}{(D-1)(D-2)}Rg_{\alpha[\gamma}g_{\delta]\beta}\,.$$

The Kretschmann scalar is

$$\mathcal{K} = R_{\alpha\beta\gamma\delta}R^{\alpha\beta\gamma\delta} = C_{\alpha\beta\gamma\delta}C^{\alpha\beta\gamma\delta} + \frac{4}{D-2}R_{\alpha\beta}R^{\alpha\beta} - \frac{2}{(D-1)(D-2)}R^2\,.$$

Chapter 1

4D distorted Schwarzschild black hole

1.1 Introduction

The uniqueness theorem proved by Israel [77] tells us that the only static vacuum black hole solution of the Einstein equations in an asymptotically flat spacetime is the Schwarzschild one. In the application to a real astrophysical problem this solution, even in the absence of rotation, is highly idealized. For instance, the presence of matter, e.g., in the form of accretion disk, distorts the metric. If a static distribution of matter is localized outside the black hole horizon, the spacetime in the vicinity of the horizon remains vacuum. We call such a solution a *distorted black hole*. The metric near the horizon of a general (not necessary axisymmetric) static distorted black hole was studied in [44].

If the distribution of matter outside a black hole is axisymmetric, the metric of the distorted black hole allows a detailed description. The reason is that the vacuum metric outside the matter is the Weyl solution. This metric contains two functions of two variables. One of these functions, which has the meaning of the gravitational potential, obeys the linear Laplace equation in a flat 3D space, while the other can be obtained from it by a simple integration. Axially symmetric distorted black holes were studied in several publications (see, e.g., [22, 34, 50, 79, 80, 99, 106]). Such axially symmetric distorted black holes arise naturally in the models were one of the (large) spatial dimensions is compactified. For the general discussion of such solutions in higher dimensions see, e.g., [67, 97]. In 4D spacetime, such compactified black hole solutions admit the Weyl form of metric. The properties of 4D compactified black holes were studied in [11, 40].

In the previous studies of distorted black holes the attention has mainly been focused on the properties of the black hole exterior. However, any distribution of matter in the black hole exterior region distorts the metric not only outside the

black hole, but also in its interior. Our purpose is to study this effect. Namely, we consider the interior of an axially symmetric distorted black hole. In particular, we study the structure of the spacetime in the vicinity of the black hole singularity. We start with an analysis of a general axially symmetric solution which is static outside the black hole and has a regular horizon. The external metric is determined by the solution of the 3D flat Laplace equation for the corresponding gravitational potential. The latter can be uniquely characterized by its multipole moments. We demonstrate that these multipole moments determine both the shape of the horizon of the distorted black hole and the spacetime structure near its singularity. As a special example, we consider an application of the obtained results to the case of the compactified black hole. For such a black hole the distortion multipole moments are fixed by the regularity condition of the compactified spacetime, and they depend only on the ratio of the black hole size to the size of the compactified dimension. We discuss the internal structure of compactified black holes. The main results presented here were published in [45].

1.2 Schwarzschild spacetime

We begin with a short review of the Schwarzschild spacetime (an excellent description can be found, e.g., in [22, 43, 72, 94]). The Schwarzschild solution is given by

$$ds^2 = -\left(1-\frac{2M}{r}\right)dt^2 + \left(1-\frac{2M}{r}\right)^{-1} dr^2 + r^2(d\theta^2 + \sin^2\theta\, d\phi^2)\,. \qquad (1.1)$$

It is the static, asymptotically flat, spherically symmetric solution of the vacuum Einstein equations, which has one parameter, M. For $r > 2M$ this solution represents spacetime outside a spherically symmetric distribution of electrically neutral matter which has zero net angular momentum. For large values of the coordinate r the gravitational field of the matter becomes weak and can be compared with its Newtonian description. The comparison shows that the parameter $M > 0$ is the gravitational mass of the matter. For $r > 2M$ the coordinate t is timelike; it measures proper time of observers resting at asymptotic infinity ($r \to +\infty$). The coordinate r is a measure of the surface area $4\pi r^2$ of spacelike 2D surfaces defined by $r = const > 2M$. According to the Birkhoff theorem, the Schwarzschild solution is unique: any spherically symmetric solution of the vacuum Einstein equations is locally isometric to the Schwarzschild solution. Algebraically, the Schwarzschild solution is of Petrov type-D, i.e., the Schwazschild spacetime has two double principal null directions: the only non-zero Weyl scalar is $\Psi_2 = -Mr^{-3}$.

If the matter of mass M has collapsed within the surface $r = 2M$, which is called the Schwarzschild sphere, then a closed trapped spacelike 2D surface $\mathscr{S}$

forms in the region $r < 2M$ surrounding the matter. By definition, ingoing and outgoing null geodesics orthogonal to $\mathscr{S}$ always converge at $\mathscr{S}$. This is the result of a gravitational pull, which is so strong that even outgoing light rays are dragged backward. As far as the matter cannot travel faster than light, it will eventually contract to a smaller and smaller volume. The existence of a closed trapped surface implies that the spacetime singularity forms in the region $r < 2M$ (see, e.g., [72]). The final stage of the collapse is the Schwarzschild black hole described by the metric (1.1), where

$$t \in (-\infty, \infty)\,, \;\; r \in (0, \infty)\,, \;\; \theta \in [0, \pi]\,, \;\; \phi \in [0, 2\pi). \tag{1.2}$$

This metric is singular at $r = 0$ and at $r = 2M$. It has additional trivial coordinate singularities at $\theta = 0$ and $\theta = \pi$. Calculation of the spacetime invariant, the Kretschmann scalar,

$$\mathcal{K}_{\rm Sch} = R_{\alpha\beta\gamma\delta} R^{\alpha\beta\gamma\delta} = \frac{48M^2}{r^6}, \tag{1.3}$$

shows that the singularity at $r = 0$ is true spacetime singularity. An analysis of the metric and null geodesics near the singularity shows that this singularity is spacelike and topologically $\mathbb{R}^1 \times S^2$ (see, e.g., [51]). The singularity at $r = 2M$ is just a coordinate singularity: the spacetime invariant (1.3) does not diverge there. This singularity indicates that the Schwarzschild coordinates (1.2) do not cover the whole the spacetime manifold: there are two disconnected regions defined by $r \in (0, 2M)$ and $r \in (2M, +\infty)$. Using different coordinates one can present the Schwarzschild metric in a form which is not singular at $r = 2M$. In other words, one can extend, by an appropriate choice of coordinates, the exterior Schwarzschild manifold $r \in (2M, +\infty)$ beyond the Schwarzschild sphere $r = 2M$. One of such well established, maximal, time symmetric extension is given by the Kruskal-Szekeres coordinates (see, e.g., [94]),

$$u \in (-\infty, \infty)\,, \;\; v \in (-\infty, \infty)\,, \;\; \theta \in [0, \pi]\,, \;\; \phi \in [0, 2\pi), \tag{1.4}$$

where

$$\text{for } \; r > 2M \qquad \begin{cases} u = \pm \left(\frac{r}{2M} - 1\right)^{1/2} e^{r/4M} \cosh\left(\frac{t}{4M}\right) \\ v = \pm \left(\frac{r}{2M} - 1\right)^{1/2} e^{r/4M} \sinh\left(\frac{t}{4M}\right), \end{cases} \tag{1.5}$$

$$\text{for } \; r < 2M \qquad \begin{cases} u = \pm \left(1 - \frac{r}{2M}\right)^{1/2} e^{r/4M} \sinh\left(\frac{t}{4M}\right) \\ v = \pm \left(1 - \frac{r}{2M}\right)^{1/2} e^{r/4M} \cosh\left(\frac{t}{4M}\right). \end{cases} \tag{1.6}$$

The Schwarzschild metric (1.1) in these coordinates reads

$$ds^2 = -\frac{32M^3}{r}e^{-r/2M}(-dv^2 + du^2) + r^2(d\theta^2 + \sin^2\theta\, d\phi^2)\,, \tag{1.7}$$

where $r = r(u, v)$ is defined by

$$\left(\frac{r}{2M} - 1\right) e^{r/2M} = u^2 - v^2. \tag{1.8}$$

Obviously, the metric (1.7) is regular at $r = 2M$. The spacetime singularity $r = 0$ is defined in the Kruskal-Szekeres coordinates by $v^2 - u^2 = 1$. In fact, there are two singularities defined by

$$v = +(1 + u^2)^{1/2}\,,\ \ v = -(1 + u^2)^{1/2}. \tag{1.9}$$

This is the result of the maximal analytic extension of the Schwarzschild spacetime manifold, which is achieved by the choice of the Kruskal-Szekeres coordinates, which give the 'complete picture'. The original, Schwarzschild coordinates (1.1) cover only part of the extended manifold, and, as a result, reveal only one spacetime singularity at $r = 0$.

To demonstrate the causal structure of the Schwarzschild spacetime (1.7) we apply the conformal transformations

$$v + u = \tan\left(\frac{\mathscr{T} + \mathscr{R}}{2}\right)\,,\ \ v - u = \tan\left(\frac{\mathscr{T} - \mathscr{R}}{2}\right), \tag{1.10}$$

which map the spacetime (1.7), (1.4) into the corresponding Carter-Penrose conformal diagram, which is illustrated in Figure 1.1. The spacetime singularities are presented by the segments

$$\mathscr{T} = \pm\frac{\pi}{2}\,,\ \ \mathscr{R} \in \left(-\frac{\pi}{2}, \frac{\pi}{2}\right). \tag{1.11}$$

This diagram demonstrates causal connections between the different regions, horizons, infinities and singularities of the Schwarzschild spacetime (1.7). Here, the

following Penrose definitions are used:

$$\begin{aligned}
\mathcal{I}^- &\quad \text{is past timelike infinity corresponding to } t \to -\infty \text{ and finite } r,\\
\mathcal{I}^+ &\quad \text{is future timelike infinity corresponding to } t \to +\infty \text{ and finite } r,\\
\mathcal{I}^0 &\quad \text{is spacelike infinity corresponding to } r \to +\infty \text{ and finite } t,\\
\mathscr{I}^- &\quad \text{is past null infinity corresponding to } t - r \to -\infty \text{ and finite } t + r,\\
\mathscr{I}^+ &\quad \text{is future null infinity corresponding to } t + r \to +\infty \text{ and finite } t - r.
\end{aligned} \tag{1.12}$$

The regions I and I' are asymptotically flat. They represent two distinct but

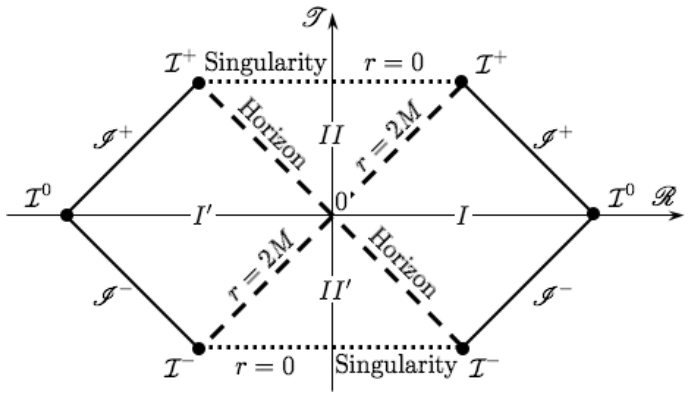

Figure 1.1: Carter-Penrose conformal diagram of the Schwarzschild spacetime. Each point in the diagram, except for the six vertices, represents a 2D sphere (θ, ϕ) defined by $(\mathscr{T}, \mathscr{R}) = const.$ Radial null geodesics are the lines $\mathscr{T} \pm \mathscr{R} = const.$

identical universes, each of which is located on one side of the Einstein-Rosen bridge, which evolves so rapidly that no null rays can pass through it [94]. Thus, these universes are causally disconnected.

Region II is the Schwarzschild black hole interior. It represents an anisotropic collapsing universe of infinite spatial volume, which expands in the spatial t direction and contracts in the θ and ϕ directions. Each point in this region in the diagram represents a closed 2D trapped surface. The radial coordinate r is time like in this region. Thus, the propagation in the black hole interior towards its singularity is time evolution. Particles moving along causal lines and entering the black hole interior can never escape outside, as they can never move backward in time.

Region II' is region II with the reversed direction of time. This region is the interior of the white hole. It represents an expanding anisotropic universe, which can never be entered from the outside by causal particles. Particles moving inside

of the region inevitably escape with the flow of time. Each point in this region represents a reversed-in-time closed 2D trapped surface. Thus, all particles in region II' came in fact out from the singularity in their past.

The Schwarzschild spacetime cannot be mathematically extended beyond the spacetime singularity (1.9), for the singularity does not belong to the spacetime manifold. In the language of general relativity, a spacetime singularity is the region where physical laws break down. It is common to reckon that the classical description of spacetime in the regions of a very high (Planck) curvature, where $\mathcal{K} \sim l_{Pl}^{-4}$, is invalid, and should be replaced with a quantum one.

In the following sections we shall discuss the Schwarzschild black hole distorted by external, static, axisymmetric gravitational fields. We shall study how such distortions affect the black hole interior.

1.3 Metric of a distorted black hole

The Israel uniqueness theorem [77] states: *among all static, asymptotically flat vacuum spacetimes with closed, simply connected equipotential surfaces $\boldsymbol{\xi}_{(t)}^2 = const$, where $\boldsymbol{\xi}_{(t)} = \partial_t$ is a timelike, surface-orthogonal Killing vector, the Schwarzschild solution is the only one which has a regular event horizon $\boldsymbol{\xi}_{(t)}^2 = 0$.*

Here we shall study how a Schwarzschild black hole is modified by the presence of static, axisymmetric external distribution of matter. There are two possible ways how to consider sources of such external matter. The first way is to include the sources into the Einstein equations; then the corresponding spacetime will not be vacuum. The second way is to move the sources to asymptotic infinity; then the corresponding spacetime will not be asymptotically flat. In both the cases the Israel uniqueness theorem is not applicable, and the corresponding black hole may have a regular horizon and differ from the Schwarzschild one. Here we consider the second way and study the spacetime at the vicinity of the black hole horizon. Such a solution is called a *local black hole*, which was studied in [50]. Our goal is to study the interior of such a local black hole. Following [50] we present the metric of a local black hole in the Weyl form

$$ds^2 = -e^{2U}dt^2 + e^{-2U}\left[e^{2V}(d\rho^2 + dz^2) + \rho^2 d\phi^2\right], \tag{1.13}$$

where $U = U(\rho, z)$, $V = V(\rho, z)$, and the coordinate ranges are

$$t \in (-\infty, \infty)\,,\ \ \rho \in (0, \infty)\,,\ \ z \in (-\infty, \infty)\,,\ \ \phi \in [0, 2\pi). \tag{1.14}$$

The Weyl spacetime has two commuting, orthogonal, surface-orthogonal Killing vectors: $\boldsymbol{\xi}_{(t)} = \partial_t$, which is timelike, and $\boldsymbol{\xi}_{(\phi)} = \partial_\phi$, which is rotational and spacelike. In a general case, static, axisymmetric vacuum solutions can be written in

the Weyl form (for details see [50]).

In principle, there might exist two types of local black holes which horizon surface is sphere or torus [50]. According to results by Hawking [71], the surface topology of a stationary 4D black hole must be a two-sphere, provided the dominant energy condition is satisfied. In addition, black holes with toroidal horizon surface violate topological censorship [37]. According to the theorem by Jacobson and Venkataramani [81], a black hole event horizon topology must be a two-sphere if it is stable for a long time and the averaged null energy condition is satisfied. Numerical simulations of formation of a temporarily toroidal horizon support this point of view [2, 76, 113]. Here, we shall consider only stable, spherical black holes.

To begin with, let us present the Schwarzschild metric (1.1) in the Weyl form. Matching the metrics (1.1) and (1.13), we derive for $r > 2M$:

$$U_S(r,\theta) = \frac{1}{2}\ln\left(1-\frac{2M}{r}\right)\,,\;\; V_S(r,\theta) = -\frac{1}{2}\ln\left(1+\frac{M^2\sin^2\theta}{r(r-2M)}\right). \tag{1.15}$$

The relation between the Schwarzschild (1.2) and Weyl (1.14) coordinates is

$$\rho = \sqrt{r(r-2M)}\sin\theta\,,\;\; z=(r-M)\cos\theta\,,\;\; r>2M. \tag{1.16}$$

Using the following transformation:

$$r = M+\frac{1}{2}(l_+ + l_-)\,,\;\; l_\pm = \sqrt{\rho^2+(z\pm M)^2}, \tag{1.17}$$

we derive

$$U_S(\rho,z) = \frac{1}{2}\ln\left(\frac{l_+ + l_- - 2M}{l_+ + l_- + 2M}\right)\,,\;\; V_S(\rho,z) = \frac{1}{2}\ln\left(\frac{(l_+ + l_-)^2 - 4M^2}{4l_+ l_-}\right). \tag{1.18}$$

Thus, the external region of the Schwarzschild black hole can be presented in the Weyl form.

So far, the Weyl form does not appear very suitable for a description of the Schwarzschild spacetime, for it covers only its exterior region. However, powerful properties of the the Weyl form are manifested in the corresponding vacuum Einstein equations

$$U_{,\rho\rho} + \frac{1}{\rho}U_{,\rho} + U_{,zz} = 0, \tag{1.19}$$

$$V_{,\rho} = \rho(U_{,\rho}^2 - U_{,z}^2)\,,\;\; V_{,z} = 2\rho\, U_{,\rho}U_{,z}. \tag{1.20}$$

Here, Eq. (1.19) for the U metric function is the Laplace equation associated with

the 3D flat metric

$$dl^2 = d\rho^2 + dz^2 + \rho^2 d\phi^2, \tag{1.21}$$

and it is the integrability condition for the other two Einstein equations (1.20). Once the solution U is known, V can be determined by simple quadratures. The Laplace equation for the potential U does not, in fact, correspond to the Newtonian limit, and it can be considered as a Euclidean map of the corresponding nonlinear equations.

An analysis of the Schwarzschild solution in the Weyl form shows that U_S corresponds in Newtonian theory to gravitational potential of an infinitesimally thin rod of length $2M$ and the uniform mass density $1/2$ which is located in a fictitious flat 3D space. The location of the rod in Weyl coordinates is given by $\rho = 0$, and $z \in [-M, M]$. The rod corresponds to the Schwarzschild black hole horizon. One can use the Poisson equation corresponding to the Laplace equation (1.19) with the source due to the rod, and apply the method of Green's function to construct

$$U_S(\rho, z) = \frac{1}{2} \ln \left(\frac{l_+ - M - z}{l_- + M - z} \right). \tag{1.22}$$

This is another representation of the Schwarzschild solution U_S which is equivalent to (1.18). Such a construction seems to violate spherical symmetry of the Schwarzschild solution. However, taking the appropriate Newtonian limit of U_S, one can see that U_S leads to the Newtonian potential of a spherically symmetric mass distribution (see, e.g., [110] and [30], p. 65-84).

We shall study the interior of a distorted Schwarzschild black hole. To do this, we have to consider the inner region $r \in (0, 2M)$ of the Schwarzschild black hole. However, this region in the Weyl coordinates corresponds to an imaginary ρ coordinate, and contains an additional coordinate singularities. Thus, an analytical continuation in (ρ, z, ϕ) coordinates is not suitable for us. Instead of (ρ, z, ϕ) coordinates we can use prolate spheroidal coordinates (η, θ, ϕ) related to the Weyl canonical coordinates in the following way (see, e.g., [126]):

$$\rho = M\sqrt{\eta^2 - 1}\sin\theta\,, \;\; z = M\eta\cos\theta, \tag{1.23}$$

where

$$\eta \in [1, \infty)\,, \;\; \theta \in [0, \pi], \tag{1.24}$$

and M is the mass of the Schwarzschild black hole, which defines location of focal points of the prolate spheroidal coordinates. Thus,

$$d\rho^2 + dz^2 = M^2(\eta^2 - \cos^2\theta)[(\eta^2 - 1)^{-1}d\eta^2 + d\theta^2]. \tag{1.25}$$

The spherical Schwarzschild coordinates (r, θ, ϕ) are related to the prolate spheroidal

coordinates (η, θ, ϕ) as follows:

$$r = M(\eta + 1)\,, \;\; \theta = \theta\,, \;\; \phi = \phi. \tag{1.26}$$

Using (1.23)-(1.25), we write the Weyl metric (1.13) representing the Schwarzschild black hole in the following form:

$$ds^2 = -e^{2U_S}dt^2 + M^2 e^{-2U_S}\left[e^{2V_S}(\eta^2 - \cos^2\theta)\left[\frac{d\eta^2}{\eta^2-1} + d\theta^2\right] + (\eta^2-1)\sin^2\theta\, d\phi^2\right], \tag{1.27}$$

where

$$U_S = \frac{1}{2}\ln\left(\frac{\eta-1}{\eta+1}\right)\,, \;\; V_S = \frac{1}{2}\ln\left(\frac{\eta^2-1}{\eta^2-\cos^2\theta}\right). \tag{1.28}$$

The vacuum Einstein equations (1.19), (1.20) in the prolate spheroidal coordinates take the following form:

$$(\eta^2-1)U_{,\eta\eta} + 2\eta\, U_{,\eta} + U_{,\theta\theta} + \cot\theta\, U_{,\theta} = 0, \tag{1.29}$$

$$V_{,\eta} = N\left(\eta\left[(\eta^2-1)U_{,\eta}^2 - U_{,\theta}^2\right] + 2(\eta^2-1)\cot\theta\, U_{,\eta}U_{,\theta}\right), \tag{1.30}$$

$$V_{,\theta} = N\left(\cot\theta\left[U_{,\theta}^2 - (\eta^2-1)U_{,\eta}^2\right] + 2\eta\, U_{,\eta}U_{,\theta}\right). \tag{1.31}$$

Here, $N = \sin^2\theta(\eta^2 - \cos^2\theta)^{-1}$. According to [50] the Schwarzschild black hole distorted by external sources is defined by

$$U = U_S + \hat{U}\,, \;\; V = V_S + \hat{V}, \tag{1.32}$$

where $\hat{U}$ and $\hat{V}$ are the distortion fields. The corresponding metric representing an axisymmetric Schwarzschid black hole distorted by an external, static gravitational field is

$$ds^2 = -\frac{\eta-1}{\eta+1}e^{2\hat{U}}dt^2 + M^2(\eta+1)^2 e^{-2\hat{U}}\left[e^{2\hat{V}}\left(\frac{d\eta^2}{\eta^2-1} + d\theta^2\right) + \sin^2\theta\, d\phi^2\right]. \tag{1.33}$$

Because of linearity of the Laplace equation for U, the distortion field $\hat{U}$ solves the same equation

$$(\eta^2-1)\hat{U}_{,\eta\eta} + 2\eta\,\hat{U}_{,\eta} + \hat{U}_{,\theta\theta} + \cot\theta\,\hat{U}_{,\theta} = 0. \tag{1.34}$$

The equation for $\hat{V}$ can be derived using Eqs. (1.30), (1.31) and (1.28),

$$\hat{V}_{,\eta} = N\left(\eta[(\eta^2-1)\hat{U}_{,\eta}^2 - \hat{U}_{,\theta}^2] + 2(\eta^2-1)\cot\theta\hat{U}_{,\eta}\hat{U}_{,\theta} + 2\eta\hat{U}_{,\eta} + 2\cot\theta\hat{U}_{,\theta}\right), \tag{1.35}$$

$$\hat{V}_{,\theta} = N(\eta^2-1)\left(\cot\theta[\hat{U}_{,\theta}^2 - (\eta^2-1)\hat{U}_{,\eta}^2 - 2\hat{U}_{,\eta}] + 2\eta\hat{U}_{,\theta}[\hat{U}_{,\eta} + (\eta^2-1)^{-1}]\right). \tag{1.36}$$

In what follows, we shall study properties of this metric, focusing on the distorted Schwarzschild black hole interior.

The black hole horizon $\mathcal{H}$ is defined by

$$\mathcal{H}: \ \eta = 1\,, \ \ \theta \in [0,\pi]. \tag{1.37}$$

Following [50] and [22] in order to guarantee regularity of the distorted black hole horizon we choose $\hat{U}$ to be finite and smooth in the vicinity and on the horizon $\mathcal{H}$. Thus, we have to find a regular solution to Eq. (1.34). This equation allows a separation of variables $\hat{U}(\eta,\theta) = \hat{F}(\eta)S(\theta)$, which gives

$$S_{,\theta\theta} + \cot\theta\, S_{,\theta} + \lambda S = 0\,, \tag{1.38}$$

$$(\eta^2-1)\hat{F}_{,\eta\eta} + 2\eta\hat{F}_{,\eta} - \lambda\hat{F} = 0, \tag{1.39}$$

where $\lambda \in \mathbb{R}^1$ is the separation constant. Since the polar points $\theta = 0, \pi$ are regular, the function $S(\theta)$ must be finite at these points. The solutions of this eigenvalue problem are the following:

$$\lambda = n(n+1)\,, \ \ S(\theta;n) = P_n(\cos\theta)\,, \ \ n = 0,1,\dots\,, \tag{1.40}$$

where $P_n(\cos\theta)$'s are the Legendre polynomials of the first kind (see, e.g., [3], p. 331). Expanding $\hat{U}$ over the complete set of the Legendre polynomials $P_n(\cos\theta)$, we derive

$$\hat{U}(\eta,\theta) = \sum_{n\geqslant 0}\hat{F}_n(\eta)P_n(\cos\theta)\,. \tag{1.41}$$

Since at the horizon surface $\hat{U}$ must be finite and regular, one must omit solutions of Eq. (1.39) that are infinitely growing at $\eta = 1$. Thus, we obtain the following regular solution for $\hat{U}$:

$$\hat{U}(\eta,\theta) = \sum_{n\geqslant 0} a_n P_n(\eta)P_n(\cos\theta), \tag{1.42}$$

where a_n are the expansion coefficients, which we call the Weyl multipole moments.

For a given value of $\hat{U}$ on the black hole horizon $\mathcal{H}$, the Weyl multipole moments are defined by

$$a_n = \frac{2n+1}{2}\int_0^\pi d\theta \sin\theta\, \hat{U}(\eta,\theta)|_{\eta=1} P_n(\cos\theta)\,. \tag{1.43}$$

Equation (1.39) has another class of solutions represented in terms of the Legendre polynomials of the second kind (see, e.g., [3], p. 331). However, this class of solutions diverges at $\eta = 1$, and hence, does not represent a regular horizon. A particular type of such solutions representing the exterior gravitational field of a static deformed mass with axial symmetry was considered in [110] and, in a different form, in [90]. Here we consider the distortions of the type given by Eq. (1.42). It is convenient to present the solution (1.42) in a different form, which allows to derive a solution to equations (1.35) and (1.36) in a closed form,

$$\hat{U} = \sum_{n\geqslant 0} c_n R^n P_n\left(\eta\cos\theta/R\right)\,,\quad R = (\eta^2 - \sin^2\theta)^{1/2}. \tag{1.44}$$

The coefficients c_n's define the distortion field $\hat{U}$. We shall call these coefficients the Weyl multipole moments, or briefly, the multipole moments. The relation between the Weyl multipole moments a_n's and c_n's is given in Appendix A. The relation of the Weyl multipole moments to their relativistic analogues was discussed in [118] for the Schwarzschild black hole distorted by an external field. The general formalism, which includes both the Thorne [119] and the Geroch-Hansen (see [48, 49, 65, 110]) relativistic multipole moments is presented in [117]. For a relation between the Thorne [119] and the Geroch-Hansen relativistic multipole moments see [10, 61].

The solution to Eqs. (1.35), (1.36) for $\hat{U}$ given by expression (1.44) was presented in [15],

$$\hat{V} = \hat{V}_1 + \hat{V}_2, \tag{1.45}$$

$$\hat{V}_1 = \sum_{n\geqslant 1} c_n \sum_{l=0}^{n-1}\left[\cos\theta - \eta - (-1)^{n-l}(\eta+\cos\theta)\right] R^l P_l\left(\eta\cos\theta/R\right), \tag{1.46}$$

$$\hat{V}_2 = \sum_{n,k\geqslant 1} \tfrac{nkc_nc_k}{n+k} R^{n+k}\left[P_n\left(\eta\cos\theta/R\right) P_k\left(\eta\cos\theta/R\right)\right.$$
$$\left. - P_{n-1}\left(\eta\cos\theta/R\right) P_{k-1}\left(\eta\cos\theta/R\right)\right]. \tag{1.47}$$

Here $\hat{V}_1$ is linear and $\hat{V}_2$ is quadratic in the c_n's.

Expressions (1.44)-(1.47) guarantee that the distortion fields $\hat{U}$ and $\hat{V}$ are smooth and finite at the horizon. Geroch and Hartle [50] demonstrated that if $\hat{U}$ is a regular smooth function in any small open neighborhood of the horizon $\mathcal{H}$

(including $\mathcal{H}$) determined by expression (1.37), which takes the same values, u_0, on both ends of the segment (1.37),

$$\hat{U}(\eta = 1, \theta = 0) = \hat{U}(\eta = 1, \theta = \pi) = u_0, \tag{1.48}$$

then the solution is regular at the horizon, and describes a distorted black hole. This is the black hole equilibrium condition. We can rewrite this condition in terms of the multipole moments. Using Eq. (1.44) and the property of the Legendre polynomials,

$$P_n(\pm 1) = (\pm 1)^n, \tag{1.49}$$

we present the equilibrium condition in the following form:

$$\sum_{n \geqslant 0} c_{2n+1} = 0, \tag{1.50}$$

and one has

$$u_0 = \sum_{n \geqslant 0} c_n = \sum_{n \geqslant 0} c_{2n}\,. \tag{1.51}$$

If the distortion source obeys the strong energy condition, u_0 has to be non-positive [50]. Thus, a static, axisymmetric, distorted black hole is at equilibrium if the sum of the coefficients of the odd multipole moments of the distortion field $\hat{U}$ vanishes. The black hole equilibrium conditions (1.50) and (1.51) can be presented in terms of a_n Weyl multipole moments as follows (for details see Appendix A):

$$\sum_{k \geqslant 0} a_{2n+1} = 0\,, \;\; u_0 = \sum_{n \geqslant 0} a_n = \sum_{n \geqslant 0} a_{2n}\,. \tag{1.52}$$

The equilibrium condition implies local flatness (absence of conical singularities) along the symmetry axis of the black hole. Namely,

$$\hat{V}(\eta, \theta)|_{\theta=0} = \hat{V}(\eta, \theta)|_{\theta=\pi} = 0. \tag{1.53}$$

Because the metric (1.33) is regular at the distorted black hole horizon $\eta = 1$, we can do analytical continuation of the metric and consider the values $\eta < 1$. One can check by calculating spacetime invariants that the spacetime (1.33) has a spacelike singularity at $\eta = -1$. Thus, the distorted black hole interior corresponds to $\eta \in (-1, 1)$.

Let us emphasize that Eq. (1.34) for the distortion field $\hat{U}$ in the interior region $\eta \in (-1, 1)$ is of the hyperbolic type, in accordance with the general property of black holes. Namely, the direction to the singularity in the interior region is the direction to the future, and the evolution of the metric in this region obeys dynamical equations.

In what follows, we consider the dimensionless form of the metric dS^2, related to the metric ds^2, [see Eq.(1.33)],

$$ds^2 = \frac{M}{\kappa_0} dS^2 \,, \;\; \kappa_0 = \frac{e^{2u_0}}{4M} \,, \tag{1.54}$$

where κ_0 is the surface gravity of the distorted Schwarzschild black hole. For the dimensionless metric dS^2 we define

$$T = \kappa_0 t \,, \;\; \mathcal{U} = \hat{U} - u_0 \,. \tag{1.55}$$

One can write the metric dS^2 in the form

$$dS^2 = -4\frac{\eta-1}{\eta+1} e^{2\mathcal{U}} dT^2 + \frac{1}{4}(\eta+1)^2 e^{-2\mathcal{U}} \left[e^{2\hat{V}} \left(\frac{d\eta^2}{\eta^2-1} + d\theta^2 \right) + \sin^2\theta \, d\phi^2 \right] . \tag{1.56}$$

In the next section, we shall study the metric (1.56) and its properties. In order to obtain the corresponding characteristics of the 'physical' solution (1.33), it is sufficient to use the scaling transformations (1.55).

1.4 Duality relations between the horizon and the singularity

In this section, we describe special symmetry relations between the Schwarzschild black hole horizon and its singularity. As we already mentioned in the previous section, the spacetime (1.56) has two Killing vectors corresponding to the T and ϕ coordinates, $\boldsymbol{\xi}_{(T)}$ and $\boldsymbol{\xi}_{(\phi)}$. Thus, the essential part of the spacetime geometry is confined to the (η, θ) plane. The metric on this plane is defined by (1.56) for $T = const$ and $\phi = const$,

$$d\Sigma_+^2 = \frac{1}{4}(\eta+1)^2 e^{-2\mathcal{U}} \left[e^{2\hat{V}} \left(\frac{d\eta^2}{\eta^2-1} + d\theta^2 \right) \right] . \tag{1.57}$$

To study the geometry of this plane it is customary to define

$$\eta = \cos\psi \,, \;\; \psi \in (0, \pi), \tag{1.58}$$

for $\eta \in (-1, 1)$ corresponding to the black hole interior. The metric (1.57) takes the following form:

$$d\Sigma_+^2 = \frac{1}{4}(1+\cos\psi)^2 e^{-2\mathcal{U}+2\hat{V}} \left[-d\psi^2 + d\theta^2 \right] . \tag{1.59}$$

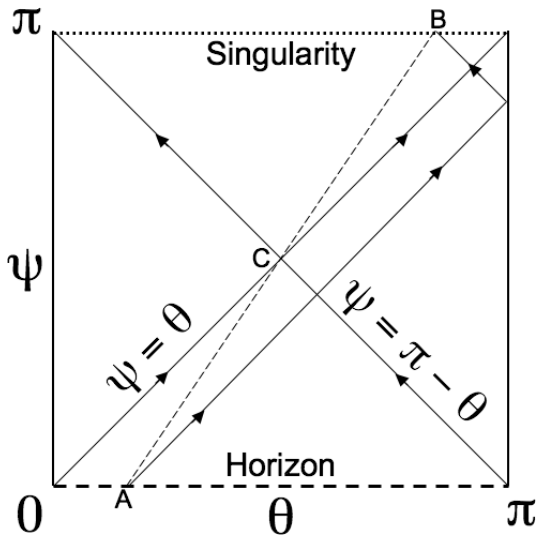

Figure 1.2: Carter-Penrose conformal diagram for the Schwarzschild black hole interior, the $(\psi,\, \theta)$ sector. The arrows illustrate propagation of three future directed null rays. Points A and B connected by one of such rays are symmetric with respect to the central point $C(\pi/2, \pi/2)$.

Thus, ψ is a timelike coordinate. The Carter-Penrose conformal diagram presented in Figure 1.2 illustrates the geometry of the Schwarzschild black hole interior. The lines $\psi \pm \theta = const$ are null rays propagating within the 2D plane (ψ, θ) defined by $(T, \phi) = const$ section of the 4D Schwarzschild spacetime (1.56). Three of such rays are illustrated in Figure 1.2 by the arrows. For example, one of the rays starts at point A on the horizon $\mathcal{H}$, goes through the 'south' pole at $\theta = \pi$, and terminates at point B, at the singularity. Note, that this diagram is different from the usual Carter-Penrose diagram for the radial sector (t, r) of the Schwarzschild black hole (see Figure 1.1).

Consider a transformation R_C representing the reflection of coordinates (ψ, θ) with respect to the 'central point' C in the black hole interior region

$$R_C : \qquad (\psi, \theta) \to (\pi - \psi, \pi - \theta). \tag{1.60}$$

This transformation determines a map R_C^* between functions defined in the interior region and on its boundaries

$$f^* = R_C^*(f)\,, \quad f^*(\psi, \theta) = f(\pi - \psi, \pi - \theta)\,. \tag{1.61}$$

Using expressions (1.44)-(1.47) we obtain

$$\mathcal{U}^*(\psi,\theta) \equiv \mathcal{U}(\pi-\psi,\pi-\theta) = \mathcal{U}(\psi,\theta), \tag{1.62}$$
$$\hat{V}_1^*(\psi,\theta) \equiv \hat{V}_1(\pi-\psi,\pi-\theta) = -\hat{V}_1(\psi,\theta)\,, \tag{1.63}$$
$$\hat{V}_2^*(\psi,\theta) \equiv \hat{V}_2(\pi-\psi,\pi-\theta) = \hat{V}_2(\psi,\theta)\,. \tag{1.64}$$

It is easy to see that coordinates of the points A and B are related by the reflection R_C. Thus, the transformation R_C determines a map between functions on the horizon and on the singularity. Now we demonstrate that for the distortion fields $\mathcal{U}$ and $\hat{V}$ this is a symmetry transformation. In other words, the values of $\mathcal{U}$ and $\hat{V}$ on the singularity, $\psi=\pi$, are determined by their values on the horizon, $\psi=0$.

Using Eqs. (1.62), (1.44), and the properties of the Legendre polynomials (1.49) we derive

$$\mathcal{U}(\pi,\pi-\theta) \;=\; \mathcal{U}(0,\theta) = \sum_{n\geqslant 0} c_n \cos^n\theta - u_0. \tag{1.65}$$

Expressions (1.44)-(1.47) and (1.49) give

$$\begin{aligned}\hat{V}_1(\psi,\theta)|_{\psi=0} &= -(1-\cos\theta)\sum_{n\geqslant 1} c_n \sum_{l=0}^{n-1}\cos^l\theta \\ &- (1+\cos\theta)\sum_{n\geqslant 1}(-1)^n c_n \sum_{l=0}^{n-1}(-\cos\theta)^l = 2\mathcal{U}(0,\theta), \qquad (1.66)\\ \hat{V}_2(\psi,\theta)|_{\psi=0} &= 0. \qquad (1.67)\end{aligned}$$

Thus, using Eqs. (1.63) and (1.64) we have

$$\hat{V}(\pi,\pi-\theta) \;=\; -\hat{V}(0,\theta) = -2\mathcal{U}(0,\theta). \tag{1.68}$$

The above expressions (1.65) and (1.68) allow one to establish special symmetry relations between the horizon and the singularity. We call the relations (1.65), (1.68) the *duality relations*.

Let us denote

$$u_\pm(\theta) = \sum_{n\geqslant 0}(\pm 1)^n c_n \cos^n\theta - u_0. \tag{1.69}$$

As we shall see below, this function defines boundary values of the distortion fields. It is easy to check that

$$u_\pm(\theta) \;=\; u_\mp(\pi-\theta)\,,\;\; u_\pm(0) = u_\pm(\pi) = 0. \tag{1.70}$$

Expression (1.70) implies that the functions $u_+(\theta)$ and $u_-(\theta)$ transform into each other under reflection with respect to the point $\theta = \pi/2$. This transformation property is directly related to the properties of the distortion field $\mathcal{U}$. Namely, using Eqs. (1.65), (1.69), (1.70) and (1.44), we derive the following *boundary values* of $\mathcal{U}$ [see Figure 1.3]:

$$\mathcal{U}(\psi,\theta)|_{\psi=0} = u_+(\theta), \qquad \mathcal{U}(\psi,\theta)|_{\psi=\pi} = u_-(\theta), \tag{1.71}$$

$$\mathcal{U}(\psi,\theta)|_{\theta=0} = u_+(\psi), \qquad \mathcal{U}(\psi,\theta)|_{\theta=\pi} = u_-(\psi). \tag{1.72}$$

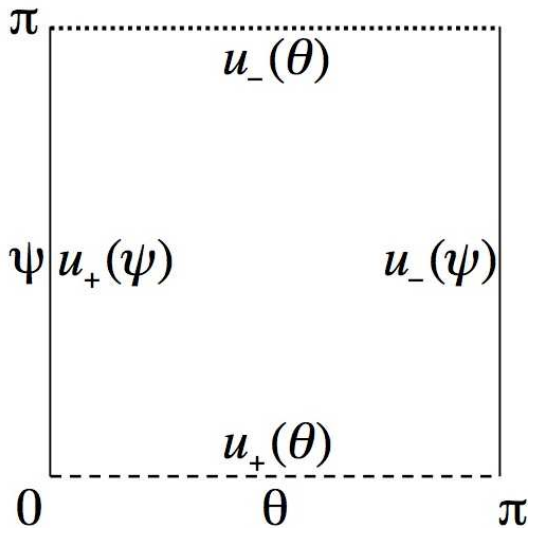

Figure 1.3: Boundary values of $\mathcal{U}$ for the interior of the distorted black hole. The dashed line, $\psi = 0$, is the horizon, and the dotted line, $\psi = \pi$, is the singularity.

Analogously, using Eqs. (1.68), (1.71), (1.70) and (1.53) we derive the *boundary values* of $\hat{V}$ [see Figure 1.4]

$$\hat{V}(\psi,\theta)|_{\psi=0} = 2u_+(\theta), \qquad \hat{V}(\psi,\theta)|_{\psi=\pi} = -2u_-(\theta), \tag{1.73}$$

$$\hat{V}(\psi,\theta)|_{\theta=0} = 0, \qquad \hat{V}(\psi,\theta)|_{\theta=\pi} = 0. \tag{1.74}$$

The boundary values of the distortion fields $\mathcal{U}$ and $\hat{V}$ define symmetry properties of the metrics on the black hole horizon and at the singularity. Thus, the distortion fields calculated at the singularity are expressed through those calculated on the horizon. This fact greatly simplifies the study of the spacetime structure near the singularity. We return to this point in Section 1.7.

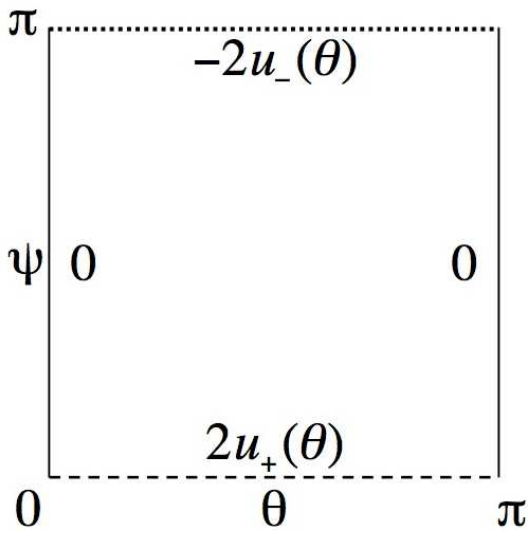

Figure 1.4: Boundary values of $\hat{V}$ for the interior of the distorted black hole. The dashed line, $\psi = 0$, is the horizon, and the dotted line, $\psi = \pi$, is the singularity.

Using expression (1.42) one can present expression (1.69) in the following way:

$$u_{\pm}(\theta) = \sum_{n \geqslant 0} (\pm 1)^n a_n P_n(\cos\theta) - u_0. \tag{1.75}$$

Obviously, all the relations presented in this section hold for (1.42). We shall use both the presentations of $\hat{U}$ throughout this thesis. Referring to Appendix A helps to switch from one representation to another.

1.5 Free fall from the horizon to the singularity

It is interesting to check how distortion of the Schwarzschild black hole affects proper time of free fall from the black hole horizon to its singularity. In the case of undistorted Schwarzschild black hole of mass M, the maximal proper time is πM (see, e.g., [94], p. 836). Let us consider, for example, motion of a test particle of zero angular momentum which moves from the horizon to the singularity of the distorted black hole along its symmetry axis. The dimensionless proper time of this free fall calculated for the dimensionless metric (1.56), with the aid of Eqs. (1.53) and (1.72) is given by

$$\tau_{\pm}(E) = \frac{1}{2}\int_0^{\pi} d\psi \frac{(1+\cos\psi)(1-\cos\psi)^{1/2} e^{-u_{\pm}(\psi)}}{\left[1-\cos\psi + E^2(1+\cos\theta)e^{-2u_{\pm}(\psi)-2u_0}\right]^{1/2}}\,. \tag{1.76}$$

Here, $\pm$ signs are for $\theta = 0$ and $\theta = \pi$ axes respectively, and E is the energy of the test particle,

$$E = 2\frac{\eta - 1}{\eta + 1} e^{2u_\pm(\psi)+u_0} \frac{dT}{d\tau_\pm}. \tag{1.77}$$

The maximal proper time corresponds to $E = 0$. Thus, we derive

$$\tau_\pm = \tau_\pm(0) = \frac{1}{2}\int_0^\pi d\psi(1 + \cos\psi)e^{-u_\pm(\psi)}. \tag{1.78}$$

The dimensional proper time is $2Me^{-u_0}\tau_\pm$ [see Eq. (1.54)].

To illustrate how distortion of the black hole affects this time, we consider two simple examples. As the first example, we consider the quadrupole distortion when only a_0 and a_2 do not vanish. Taking into account that $a_0 = u_0 - a_2$ [see Eq. (1.52)] one has

$$u_\pm(\psi) = -\frac{3}{2}a_2 \sin^2\psi\,. \tag{1.79}$$

The integral (1.78) can be evaluated analytically,

$$\tau_\pm = \frac{\pi}{2}e^{3a_2/4} I_0(3a_2/4)\,, \tag{1.80}$$

where $I_0(z)$ is the modified Bessel function (see, e.g., [3], p. 374). The plot of $\tau_\pm$ as a function of the quadrupole moment a_2 is shown in Figure 1.5(**a**).

As the second example we consider the octupole distortion when only a_1 and a_3 do not vanish. Because of the condition (1.52) one has $a_1 = -a_3$, and

$$u_\pm(\psi) = \mp\frac{5}{2}a_3\, \cos\psi\, \sin^2\psi\,. \tag{1.81}$$

To obtain $\tau_\pm$ we used numerical integration. The plot of τ_+ as a function of the octupole moment a_3 is shown in Figure 1.5(**b**).

1.6 Near horizon geometry

1.6.1 Shape of a distorted horizon

The form of the horizon surface for the metric (1.56) and the boundary values (1.71) and (1.73) is determined by the following line element (see also [50]):

$$d\sigma_+^2 = e^{2u_+}d\theta^2 + e^{-2u_+}\sin^2\theta\, d\phi^2. \tag{1.82}$$

Here, and in what follows $u_\pm \equiv u_\pm(\theta)$. This metric is obtained from the metric (1.56) as the limit $\eta \to 1$, (or $\psi \to 0$), of the metric on the 2D section $T = const$,

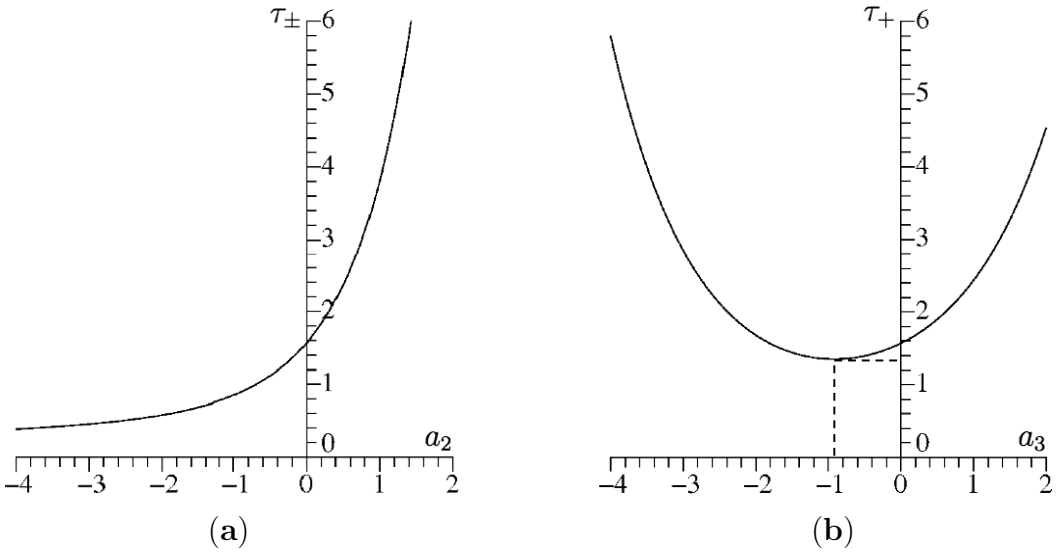

Figure 1.5: (**a**): Quadrupole distortion: the proper time, $\tau_\pm$, as a function of the quadrupole moment a_2. (**b**) Octupole distortion: the proper time, τ_+, as a function of the octupole moment a_3. The minimal value of $\tau_{+min} \approx 1.35$ corresponds to $a_{3min} \approx -0.917$. The similar plot for τ_- can be obtained by the reflection $a_3 \to -a_3$. The dimensionless proper time for the Schwarzschild black hole is $\tau_\pm = \pi/2 \approx 1.57$.

$\psi = const$. The dimensionless horizon area is equal to 4π.

A natural measure of intrinsic curvature of a 2D surface is its Gaussian curvature K. Gaussian curvature of a horizon surface was studied by several authors (see, e.g., [38, 89, 114, 122, 123]). The Gaussian curvature of the metric $d\sigma_+^2$ is $K_+ = R/2$, where R is the Ricci scalar curvature. It is given by the following expression:

$$K_+ = e^{-2u_+}\left(1 + u_{+,\theta\theta} + 3\cot\theta u_{+,\theta} - 2u_{+,\theta}^2\right) . \tag{1.83}$$

As special examples, we consider the quadrupole and octupole distortions with functions u_+ given by (1.79) and (1.81), respectively. The Gaussian curvature for these distortions is

$$K_+ = e^{3a_2\sin^2\theta}\left[1 + 3a_2(1 - 5\cos^2\theta) - 18a_2^2\cos^2\theta\sin^2\theta\right] , \tag{1.84}$$

$$K_+ = \frac{1}{2}e^{5a_3\cos\theta\,\sin^2\theta}\left[2 - 10a_3\cos\theta(9\cos^2\theta - 5) - 25a_3^2\sin^2\theta(1 - 3\cos^2\theta)^2\right] , \tag{1.85}$$

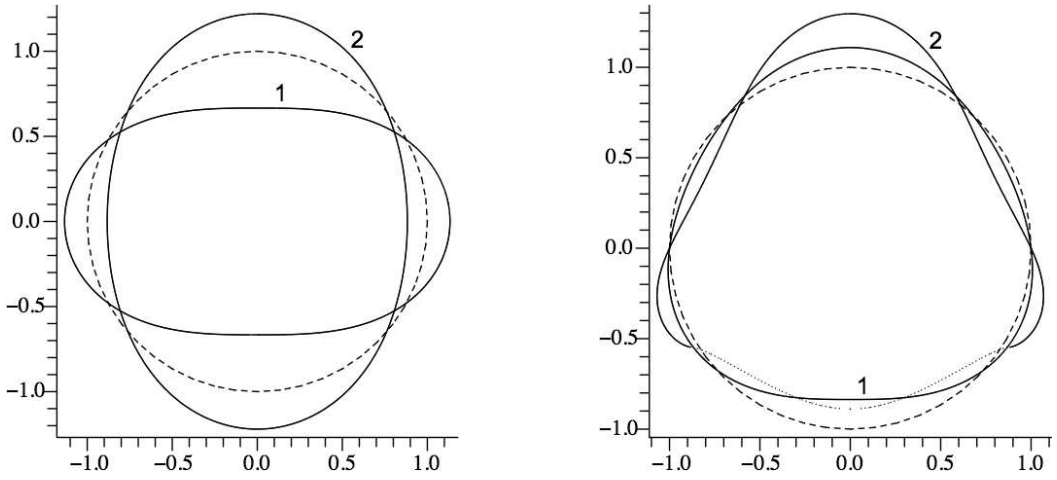

Figure 1.6: Shape of the horizon surface of the distorted black hole. The embedding diagram for the horizon surface can be obtained by rotation of the curves on the plots around the vertical axis. The left plot (**a**) shows the rotation curves for the quadrupole distortion of $a_2 = 1/12$, line (1) and $a_2 = -1/12$, line (2). The right plot (**b**) shows the rotation curves for the octupole distortion of $a_1 = -a_3 = 1/20$, line (1) and $a_1 = -a_3 = 1/6$, line (2). The region embedded into pseudo-Euclidean space is illustrated in plot (**b**) by the dotted line. The rotation curves for positive octupole moments a_3 can be obtained by the reflection of the rotational curves in plot (**b**) with respect to the horizontal axis at 0.0. The dashed lines in both the plots are round circles of radius 1 corresponding to the Schwarzschild black hole.

respectively. For the quadrupole distortion the Gaussian curvature becomes negative at both of the poles, $\theta = 0$ and $\theta = \pi$, for $a_2 > 1/12$. Similarly, for the octupole distortion, the Gaussian curvature becomes negative at one of the poles for $|a_3| > 1/20$. It means that for these values of the multipole moments the horizon surface of the distorted black hole cannot be isometrically embedded into a flat 3D space as a surface of revolution (see, e.g., [38] and references therein). For $a_2 \leqslant 1/12$ (in the quadrupole case) and $|a_3| \leqslant 1/20$ (in the octupole case) isometric embedding may be possible.

To construct the embedding we consider an axisymmetric 2D surface which is parametrized as follows:

$$\rho = \rho(\theta)\,, \quad z = z(\theta). \tag{1.86}$$

Let us embed this surface into a flat 3D space with the metric in cylindrical coor-

dinates (z, ρ, ϕ):

$$dl^2 = \epsilon dz^2 + d\rho^2 + \rho^2 d\phi^2, \tag{1.87}$$

where for Euclidean space $\epsilon = 1$, and for pseudo-Euclidean space $\epsilon = -1$. Note, that an axisymmetric 2D surface cannot be isometrically embedded into a 3D Euclidean space as a surface of revolution if its Gaussian curvature is negative at the vicinity of a fixed point of rotation [38]. However, a failure of the embedding does not generally imply that Gaussian curvature of the surface is negative. The geometry induced on the surface (1.86) is given by

$$dl^2 = (\epsilon z_{,\theta}^2 + \rho_{,\theta}^2) d\theta^2 + \rho^2 d\phi^2. \tag{1.88}$$

Matching the metrics (1.82) and (1.88) we derive the following embedding map:

$$\rho = e^{-u_+} \sin\theta\,, \quad z = \int_\theta^{\pi/2} \mathcal{Z}\, d\theta, \tag{1.89}$$

$$\mathcal{Z}^2 = \epsilon e^{2u_+} [1 - e^{-4u_+} (\cos\theta - u_{+,\theta} \sin\theta)^2]. \tag{1.90}$$

From Eq. (1.90) we see that if the expression in the square brackets is negative, an isometric embedding into 3D Euclidean space as a surface of revolution is not possible, and we should take $\epsilon = -1$. The embedding diagrams of the distorted event horizon surface for the quadrupole and octupole distortions are illustrated in Figure 1.6. Note that the change in sign from '+' to '−' of the quadrupole moment corresponds to a deformation of the rotational curve from oblate to prolate and vice versa. The change in sign of the octupole moment corresponds to an overturn of the rotational curve preserving its shape.

1.6.2 Kretschmann invariant

The Gaussian curvature discussed in the previous subsection characterizes the shape of the 2D surface of the distorted horizon. In this subsection we study the 4D curvature of the spacetime near the distorted horizon. We demonstrate that the 4D curvature is greater at the points where the horizon surface is sharper.

The components of the curvature tensor depend on the coordinate choice. Hence, to characterize the strength of the curvature one needs to consider curvature invariants. The simplest one is the Kretschmann scalar $\mathcal{K} = R_{\alpha\beta\gamma\delta} R^{\alpha\beta\gamma\delta}$. We demonstrate that there is a simple relation between the Kretschmann invariant and the Gaussian curvature at the surface of the distorted black hole.

The function $u_+(\theta)$, which specifies the geometry of the horizon surface, uniquely determines the geometry of the black hole interior. In particular, one can obtain expansion of $\mathcal{U}$ and $\hat{V}$ at the vicinity of the horizon (see Appendix B). The first

two terms of this expansion in the powers of ψ are

$$\mathcal{U} = u_+ - \frac{1}{4}u_+^{(2)}\psi^2 + \dots , \tag{1.91}$$

$$\hat{V} = 2u_+ - \frac{1}{2}(u_+^{(2)} - u_{+,\theta}^2 + 2\cot\theta u_{+,\theta})\psi^2 + \dots \tag{1.92}$$

Here and later we use the dots '...' for the omitted terms of higher order in ψ. We also defined

$$u_\pm^{(2)} = \sum_{n\geq 0}(\pm 1)^n a_n n(n+1)P_n(\cos\theta)\,. \tag{1.93}$$

In this approximation the metric near the black hole horizon reads

$$dS_+^2 = A_+ dT^2 + B_+(d\theta^2 - d\psi^2) + C_+ d\phi^2\,, \tag{1.94}$$

where

$$A_+ = \frac{1}{6}\psi^2 e^{2u_+}[6 - (3u_+^{(2)} - 1)\psi^2 + \dots]\,, \tag{1.95}$$

$$B_+ = \frac{1}{2}e^{2u_+}[2 - (u_+^{(2)} + 4\cot\theta u_{+,\theta} - 2u_{+,\theta}^2 + 1)\psi^2 + \dots]\,, \tag{1.96}$$

$$C_+ = \frac{1}{2}e^{-2u_+}\sin^2\theta[2 + (u_+^{(2)} - 1)\psi^2 + \dots]. \tag{1.97}$$

This expansion, for example, can be used to determine the value of the Kretschmann scalar $\mathcal{K} = R_{\alpha\beta\gamma\delta}R^{\alpha\beta\gamma\delta}$ at the horizon surface. Using Eqs. (1.94)-(1.97) we derive

$$\mathcal{K}_+ = 12e^{-4u_+}\left(1 + u_{+,\theta\theta} + 3\cot\theta u_{+,\theta} - 2u_{+,\theta}^2\right)^2. \tag{1.98}$$

For the Schwarzschild black hole $\mathcal{K}_{\mathrm{Sch},+} = 12$. Figure 1.7 illustrates the ratio, $k = \mathcal{K}_+/\mathcal{K}_{\mathrm{Sch},+}$, of the Kretschmann scalars of the distorted and Schwarzschild black holes.

Comparing expression (1.98) with expression (1.83), one arrives at the following relation valid on the horizon surface of a distorted black hole:

$$\mathcal{K}_+ = 12K_+^2\,. \tag{1.99}$$

This relation is valid not only for the axisymmetric case but also for an arbitrary static distorted black hole (see Appendix E, Eqs. (E.41), (E.1), for the electrically neutral case). The metric of distorted Schwarzschild black hole is of Petrov type-I. It is possible to show that this metric is of Petrov type-D both on the horizon and on the axis of azimuthal symmetry [104].

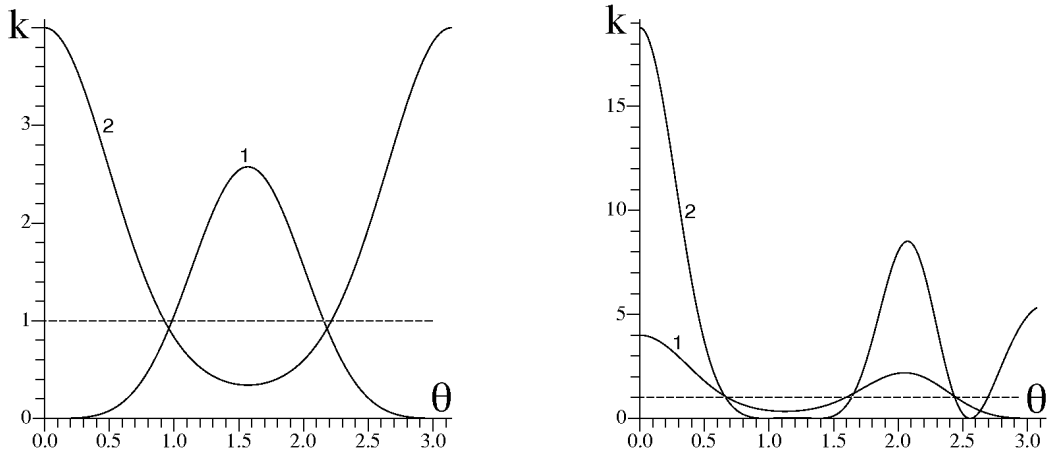

Figure 1.7: Ratio $k = \mathcal{K}_+/\mathcal{K}_{\rm Sch,+}$ of the Kretschmann scalar $\mathcal{K}_+$ on the horizon of the distorted black hole to its undistorted value $\mathcal{K}_{\rm Sch,+}$. Curves in plot (**a**) show k for the quadrupole distortion of $a_2 = 1/12$, line (1) and $a_2 = -1/12$, line (2). Similar curves in plot (**b**) show k for the octupole distortion of $a_1 = -a_3 = 1/20$, line (1) and $a_1 = -a_3 = 1/6$, line (2). The dashed horizontal lines at $k = 1$ correspond to the Schwarzschild black hole.

1.7 Spacetime near the singularity of a distorted black hole

1.7.1 Asymptotic form of the metric

Because of the symmetry property (1.62), the asymptotic form of $\mathcal{U}$ near the singularity $\psi = \pi$ can be easily obtained from its asymptotic expansion near the horizon $\psi = 0$. If the expansion of $\mathcal{U}$, [so $\hat{U}$, see (1.55)], is known, expansion of $\hat{V}$ can be found, for example, by simple integration of Eqs. (1.35), (1.36), or directly, by expansion of $\hat{V}$ given by Eqs. (1.45)-(1.47). The expansions for $\mathcal{U}$ and $\hat{V}$ near the singularity are given in Appendix B. Using these expansions one can obtain the asymptotic form of the metric (1.56) at the singularity, $\psi_- = \pi - \psi \to 0$,

$$dS_-^2 = A_- dT^2 + B_-(d\theta^2 - d\psi_-^2) + C_- d\phi^2\,, \tag{1.100}$$

where

$$A_- = \frac{8e^{2u_-}}{3\psi_-^2}[6 + (3u_{-,\theta\theta} + 3\cot\theta u_{-,\theta} - 1)\,\psi_-^2 \ldots]\,, \tag{1.101}$$

$$B_- = \frac{e^{-6u_-}}{96}\psi_-^4[6 - (9u_{-,\theta\theta} - 3\cot\theta u_{-,\theta} - 6(u_{-,\theta})^2 + 1)\psi_-^2 + \ldots]\,, \tag{1.102}$$

$$C_- = \frac{e^{-2u_-}}{96}\sin^2\theta\psi_-^4[6 - (3u_{-,\theta\theta} + 3\cot\theta u_{-,\theta} + 1)\psi_-^2 \ldots]\,. \tag{1.103}$$

Expressions (1.100)-(1.103) are sufficient to calculate the Kretschmann scalar near the singularity up to the second order in ψ_- corrections,

$$\mathcal{K}_- = \frac{12\cdot 2^{12}\,e^{12u_-}}{\psi_-^{12}}[1 + \tilde{\mathcal{K}}_-^{(2)}\psi_-^2 + \ldots]\,, \tag{1.104}$$

$$\tilde{\mathcal{K}}_-^{(2)} = \frac{1}{2}[1 + 3u_{-,\theta\theta} - 6(u_{-,\theta})^2 - 3\cot\theta u_{-,\theta}]\,. \tag{1.105}$$

Higher order terms can be obtained by using the relations given in Appendix B. In the absence of distortion, when $u_- = 0$, the Kretschmann scalar does not depend on θ,

$$\mathcal{K}_{\mathrm{Sch},-} = \frac{49152}{\psi_-^{12}}\,. \tag{1.106}$$

This is the value of $\mathcal{K}_-$ for the Schwarzschild geometry. Using the results of [104] it can be shown that the metric of a distorted black hole is of Petrov type-D at the singularity.

1.7.2 Stretched singularity

For the Schwarzschild geometry the metric near the singularity,

$$dS_-^2 \approx -\frac{1}{16}\psi_-^4 d\psi_-^2 + \frac{16}{\psi_-^2}dT^2 + \frac{\psi_-^4}{16}d\omega^2\,, \tag{1.107}$$

can be written in the form

$$dS_-^2 \approx -d\tau^2 + \frac{16}{(12\tau)^{2/3}}dT^2 + \frac{(12\tau)^{4/3}}{16}d\omega^2\,. \tag{1.108}$$

Here, $\tau = -\psi_-^3/12$ is the maximal proper time of a free fall to the singularity along the geodesic $T, \theta, \phi = const$. The quantity τ is negative, and it reaches 0 at the singularity. The metric (1.108) has the Kasner-like behavior with indices $(-1/3, 2/3, 2/3)$ (see, e.g., [115], p. 197). It describes a collapsing anisotropic universe that shrinks in the angular, θ and ϕ, directions and expands in the T

direction.

The Kretschmann invariant as a function of the maximal proper time has the following asymptotic form:

$$\mathcal{K}_{\mathrm{Sch},-} \approx \frac{64}{27\tau^4}\,. \tag{1.109}$$

This relation shows that the surface of constant $\mathcal{K}_{\mathrm{Sch},-}$ is, at the same time, a surface of constant τ.

Spacetime in the region where the curvature is of order of the Planck curvature requires quantum gravity for its description. For the Schwarzschild geometry at the surface where $\mathcal{K}_{\mathrm{Sch},-} \sim l_{Pl}^{-4}$ the proper time τ is of order of the Planck time τ_{Pl}. Since one cannot rely on the classical description in this domain, it is natural to cut the region where the curvature is higher than the Planck one and to consider its boundary as the *stretched* or *physical singularity*. For the Schwarzschild metric the *stretched singularity* hypersurface has the topology $\mathbb{R}^1 \times S^2$. Its metric is a direct sum of the metric of a round two-sphere and a line.

What happens to the *stretched singularity* when the metric of the black hole is distorted? To answer this question, we use the asymptotic form of the metric near the singularity, Eq. (1.100). Let us consider a timelike geodesic lying in the 'plane' $T = const$, $\phi = const$. We call such a geodesic 'radial'. It can be shown (see Appendix C) that a 'radial' geodesic is uniquely determined by the limiting value θ_0 of its angular parameter θ at which it crosses the singularity. Denote by τ the proper time along the 'radial' geodesic to its end point at the singularity. In coordinates (τ, θ_0) the metric dS_-^2 is given by (1.108) where $d\omega^2$ is replaced by

$$d\sigma_-^2 = e^{-2u_-} d\theta^2 + e^{2u_-} \sin^2\theta\, d\phi^2\,. \tag{1.110}$$

We can use (τ, θ_0) as new coordinates in the vicinity of the singularity. Expressions (C.14) and (C.15) relate these 'new' coordinates with the 'old' ones (ψ_-, θ). The Kretschmann scalar (1.104) in the 'new' coordinates reads

$$\mathcal{K}_- = \frac{64}{27\tau^4}[1 + \mathcal{K}_-^{(2)}\tau^{2/3} + O(\tau^{4/3})]\,, \tag{1.111}$$

$$\mathcal{K}_-^{(2)} = \frac{1}{2}(12)^{2/3} e^{2u_-(\theta_0)}[1 + 3u_{-,\theta_0\theta_0} - 6(u_{-,\theta_0})^2 - 3\cot\theta u_{-,\theta_0}]\,. \tag{1.112}$$

The expansion (1.111) coincides in the leading order with expression (1.109). Hence, in the presence of distortion, surfaces of equal $\mathcal{K}$ are again (in the leading order) surfaces of constant τ.

1.7.3 Shape of equicurvature surfaces

Let Σ_- be a surface where the Kretschmann scalar has constant value $\mathcal{K}_- = \mathcal{K}_c$. In the vicinity of the singularity (in the leading order in ψ_-) ψ_- and θ on Σ_- are related as follows [see Appendix C, Eq. (C.14) and Eq. (1.111)]:

$$\psi_- = \kappa_- e^{u_-} \,, \;\; \kappa_- = (49152/\mathcal{K}_c)^{1/12} \,, \tag{1.113}$$

and one has the relation $\psi_{-,\theta} = \psi_- u_{-,\theta}$.

Let us now consider the induced geometry on Σ_-. Using the relation (1.113), one can conclude that the $d\psi_-^2$ term in (1.100) gives quadratic in ψ_- corrections only. Neglecting all such terms in (1.100), we obtain the following expression for the leading asymptotic for the induced metric dl_-^2 on Σ_-:

$$dl_-^2 \approx \frac{16}{\kappa_-^2} dT^2 + \frac{\kappa_-^4}{16} d\sigma_-^2 \,, \tag{1.114}$$

where $d\sigma_-^2$ is given by (1.110). The surface Σ_- has the same topology $\mathbb{R}^1 \times S^2$ as in the absence of distortion, but its geometry is different. This difference manifests itself in the shape of $T = const$ 2D surfaces. The information about the shape is encoded in the 2D metric $d\sigma_-^2$. The total dimensionless area of the surface is 4π.

The metric (1.110) can be obtained from the horizon metric $d\sigma_+^2$, (1.82), by the transformation

$$u_+ \to -u_- . \tag{1.115}$$

This transformation implies the following *duality relations* between the horizon and the singularity [see Eq. (1.75)]:

$$a_{2n} \longleftrightarrow -a_{2n} \,, \;\; a_{2n+1} \longleftrightarrow a_{2n+1} . \tag{1.116}$$

Analogous relations hold for the c_n's Weyl multipole moments (see Appendix A). The embedding diagrams for the metric (1.110) are those with opposite value of the quadrupole moment a_2 and with the same value of a_3 [see Figure 1.6(**a**) and Figure 1.6(**b**), respectively].

1.8 Exact solutions: quadrupole and octupole distortions

In this section we consider the distorted Schwarzschild spacetime for quadrupole and octupole distortions. We truncate expressions (1.44)-(1.47) at the octupole approximation and using Appendix A, Eq. (A.24), rewrite the result in terms of

a_n's. The distortion field $\mathcal{U}$ has the following form:

$$\mathcal{U} = -\frac{3}{2}a_2\mathcal{P}_{3/2} - \frac{5}{2}a_3\cos\psi\cos\theta\mathcal{P}_{5/2}, \tag{1.117}$$

where

$$\mathcal{P}_q = \sin^2\psi + \sin^2\theta - q\sin^2\psi\sin^2\theta. \tag{1.118}$$

The corresponding distortion field $\hat{V}$ is

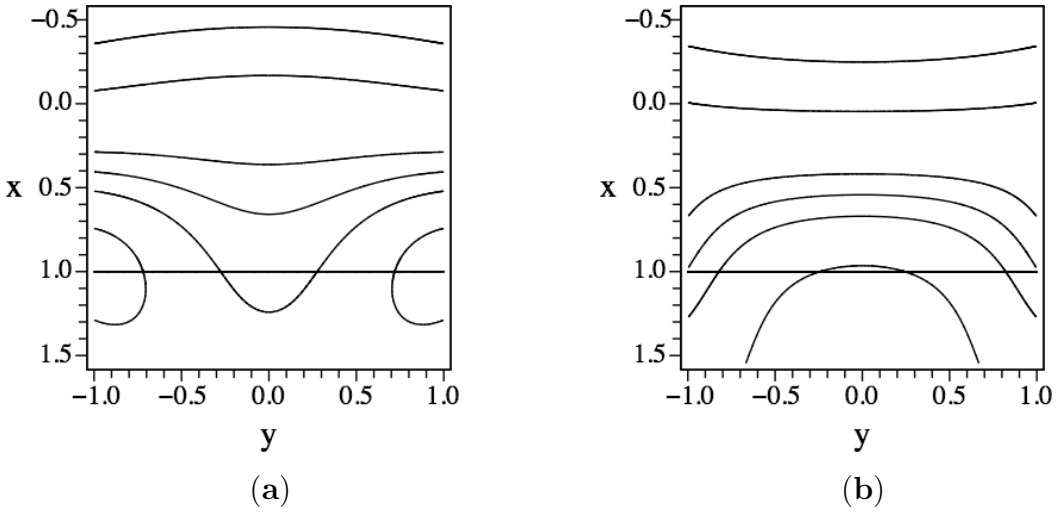

Figure 1.8: Contour lines of $\mathcal{K}$ for the quadrupole distortion of $a_2 = 1/12$ (**a**) and $a_2 = -1/12$ (**b**). The horizontal line $x = 1$ represents the event horizon.

$$\begin{aligned}\hat{V} &= \frac{1}{2}\sin^2\theta\left(\sin^2\psi\left[a_2^2\mathcal{V}_{22} + 2a_2a_3\mathcal{V}_{23} + a_3^2\mathcal{V}_{33}\right]\right.\\ &- \left. 6a_2\cos\psi + 5a_3\cos\theta\left[1 - 3\cos^2\psi\right]\right),\end{aligned} \tag{1.119}$$

where

$$\mathcal{V}_{22} = 9[1 - \mathcal{P}_{9/8}], \quad \mathcal{V}_{23} = \frac{15}{2}\cos\psi\cos\theta[2 - 3\mathcal{P}_{3/2}], \tag{1.120}$$

$$\mathcal{V}_{33} = \frac{25}{4}[4 - 12\mathcal{P}_{39/24} - 18\mathcal{P}_2^2 + 27\mathcal{P}_{11/6}^2]. \tag{1.121}$$

The exterior metric for a black hole distorted by a quadrupole field was derived in [29].

Using the GRTENSORII package we calculated the Kretschmann scalar $\mathcal{K}$ for

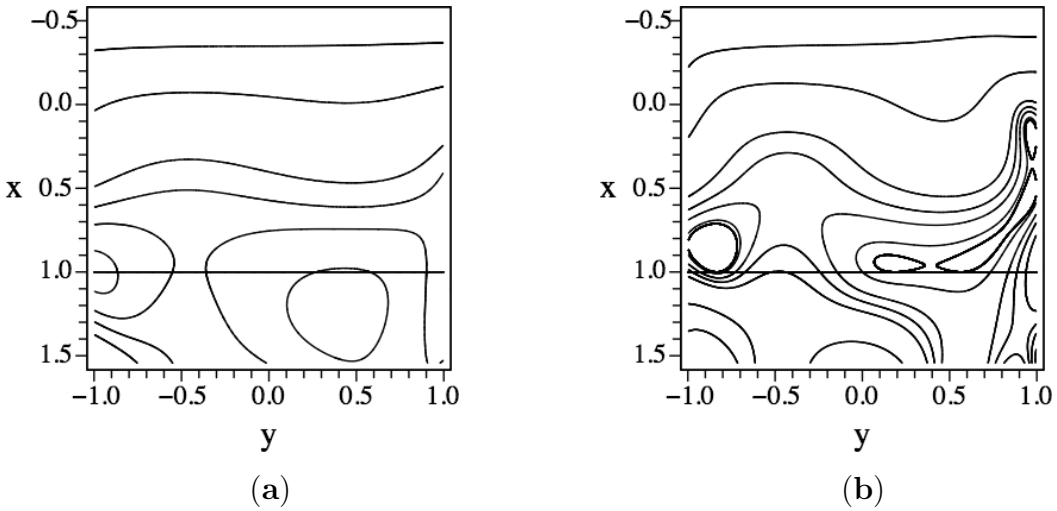

Figure 1.9: Contour lines of $\mathcal{K}$ for the octupole distortion of $a_1 = -a_3 = 1/20$ (**a**) and $a_1 = -a_3 = 1/6$ (**b**). The horizontal line $x = 1$ represents the event horizon.

this distortion. We did the calculations for both the interior and the exterior regions of the distorted Schwazschild black hole. Figures 1.8 and 1.9 illustrate the contour lines of $\mathcal{K}$ for the quadrupole and octupole distortions in the prolate spheroidal coordinates ($x = \eta\,,\ \ y = \cos\theta$), respectively. The spacetime singularity corresponds to $x = -1$.

1.9 Compactified Schwarzschild black hole

In this section we apply the obtained results to the special case of the Schwarzschild black hole in Kaluza-Klein spacetime, a *compactified Schwarzschild black hole*. Such a black hole is a solution of the vacuum Einstein equations for a spacetime where one (or more) spatial dimension(s) is compactified. The Schwarzschild black hole in 4D spacetime with one compact spatial coordinate was discussed in [40] (see also [11, 97]). As a result of compactification, the event horizon of the black hole is distorted. The metric is axisymmetric and is a special case of the Weyl solution. Such a black hole is schematically illustrated in Figure 1.10.

Here we review the construction of the compactified Schwarzschild black hole presented in [40]. As it was mentioned in Section 1.3, the metric function U_S of the Schwarzschild black hole of mass M corresponds to gravitational potential of an infinitesimally thin rod of the length $2M$ and the uniform mass density $1/2$. Thus, the metric function U_C of a compactified Schwarzschild black hole of mass

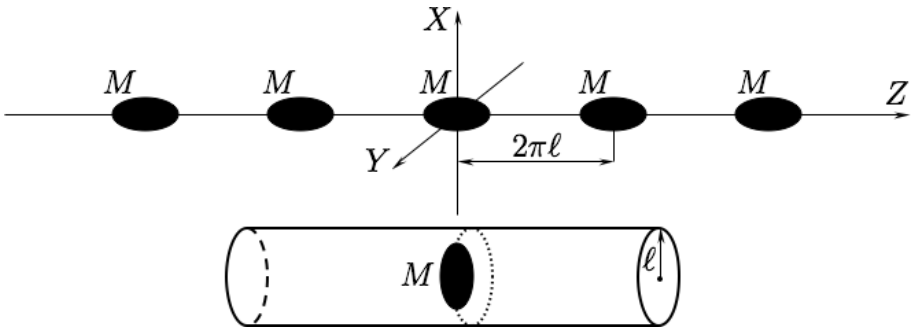

Figure 1.10: Compactified Schwarzschild black hole of mass M located in Kaluza-Klein spacetime of compactification radius ℓ. The corresponding covering space representing a sequence of Schwarzschild black holes situated along the Z-axis is shown above.

M corresponds to gravitational potential of an infinite sequence of infinitesimally thin rods, each of the length $2M$ and the uniform mass density $1/2$, which are situated along Z axis $2\pi\ell$ coordinate distance apart in the corresponding covering space (see Figure 1.10). Thus, the metric function U_C solves the following Poisson equation, which corresponds to the Laplace equation (1.19):

$$U_{,\rho\rho} + \frac{1}{\rho}U_{,\rho} + U_{,zz} = 4\pi h(\rho, z)\,. \tag{1.122}$$

Here, $h(\rho, z)$ is the source function which is, according to our construction, periodic in z and has the following form:

$$h(\rho, z) = \frac{\delta(\rho)}{4\pi\rho}\sum_{n=-\infty}^{\infty}\left[H(z+\mu-2\pi n) - H(z-\mu-2\pi n)\right], \tag{1.123}$$

where $H(x)$ is the Heaviside step function (see List of Symbols and Abbreviations). Here, and in what follows, the coordinates ρ and z are measured in units of ℓ, and $\mu = M/\ell$, where $0 < \mu < \pi$. To find a solution to Eqs. (1.122), (1.123) we can use either the method of Green's function, or Fourier's method. Both the methods are discussed in [40]. Here we apply Fourier's method, which gives a solution in more convenient form.

The source function $h(\rho, z)$ in the covering space can be easily mapped to the corresponding compactified space by identification of points on z axis which differ

by period 2π. Expansion of $h(\rho, z)$ in Fourier series reads

$$h(\rho, z) = \frac{\delta(\rho)}{4\pi\rho}\left[\frac{\mu}{\pi} + \sum_{n=1}^{\infty}\frac{2}{n\pi}\sin(n\mu)\cos(nz)\right]. \tag{1.124}$$

We shall look for a solution U to Eq. (1.122) in the following form:

$$U(\rho, z) = U_0(\rho) + \sum_{n=1}^{\infty} U_n(\rho)\cos(nz). \tag{1.125}$$

Substitution of expressions (1.124), (1.125) into (1.122) gives the following equations for the radial functions $U_n(\rho)$'s:

$$U_{0,\rho\rho} + \frac{1}{\rho}U_{0,\rho} = \frac{\mu}{\pi}\frac{\delta(\rho)}{\rho}\,, \tag{1.126}$$

$$U_{n,\rho\rho} + \frac{1}{\rho}U_{n,\rho} - n^2 U_n = \frac{2}{n\pi}\sin(n\mu)\frac{\delta(\rho)}{\rho}\,. \tag{1.127}$$

To find particular solutions to the equations, which correspond to the source function $h(\rho, z)$, we apply the method of variation of parameters (see, e.g., [83], p. 493). The fundamental set of solutions of the corresponding homogeneous equations and their Wronskians are given by

$$W[\ln|\rho|,\, 1] = -\frac{1}{\rho}\,, \tag{1.128}$$

$$W[I_0(n\rho),\, K_0(n\rho)] = -\frac{1}{\rho}\,, \tag{1.129}$$

respectively. Here, $I_0(n\rho)$ and $K_0(n\rho)$ are the modified Bessel functions (see, e.g., [3], p. 374). The method of variation of parameters gives

$$U_0(\rho) = \frac{\mu}{\pi}\int d\rho\frac{H(\rho)}{\rho}\,, \tag{1.130}$$

$$U_n(\rho) = \frac{2}{n\pi}\sin(n\mu)\left[H(\rho)K_0(n\rho)(I_0(n\rho)-1) - I_0(n\rho)\int d\rho H(\rho)\frac{dK_0(n\rho)}{d\rho}\right]. \tag{1.131}$$

For our coordinate range [see Eq. (1.14)] the Heaviside step function $H(\rho)$ is equal to 1, and the solutions above simplify to

$$U_0(\rho) = \frac{\mu}{\pi}\ln\rho\,,\;\; U_n(\rho) = -\frac{2}{n\pi}\sin(n\mu)K_0(n\rho). \tag{1.132}$$

Thus, we derive

$$U_C(\rho,z)=\frac{\mu}{\pi}\ln\rho-\sum_{n=1}^{\infty}\frac{2}{n\pi}\sin(n\mu)K_0(n\rho)\cos(nz). \tag{1.133}$$

We are interested in behavior of this function near the black hole horizon, which is defined by [cf. Eq. (1.37)]

$$\mathcal{H}:\ \ \rho=0\,,\ \ z\in[-\mu,\mu]. \tag{1.134}$$

We consider the expansion of the U_C function near the horizon. For $\rho\ll 1$ we have

$$K_0(n\rho)\approx-\ln\left(\frac{n\rho}{2}\right)-\gamma, \tag{1.135}$$

where $\gamma=0.57721566...$ is the Euler-Mascheroni constant (see, e.g., [3], p. 379). Substituting Eq. (1.135) into Eq. (1.133) we derive

$$U_C(\rho,z)\approx\ln\left(\frac{\rho}{2}\right)+\gamma+\frac{\mu}{\pi}(\ln 2-\gamma)+\frac{1}{\pi}\sum_{n=1}^{\infty}\frac{\ln n}{n}[\sin(n[\mu+z])+\sin(n[\mu-z])], \tag{1.136}$$

where $z\in[-\mu,\mu]$. To evaluate the sum in Eq. (1.136) we use the following relation (see equation 5.5.1.24 in [109]):

$$\sum_{n=1}^{\infty}\frac{\ln(na)}{n}\sin(nx)=\frac{1}{2}(x-\pi)\left[\gamma-\ln\left(\frac{a}{2\pi}\right)\right]+\frac{\pi}{2}\ln\left|\frac{1}{\pi}\sin\left(\frac{x}{2}\right)\Gamma^2\left(\frac{x}{2\pi}\right)\right|, \tag{1.137}$$

where $x\in(0,2\pi)$. Thus, we derive

$$U_C(\rho,z)\approx\ln\left(\frac{\rho}{4\pi}\right)+\frac{\mu}{\pi}\ln(4\pi)+\frac{1}{2}\ln\left(\frac{4\pi^2}{\mu^2-z^2}\right)+\frac{1}{2}\ln\left|f\left(\frac{\mu+z}{2}\right)f\left(\frac{\mu-z}{2}\right)\right|, \tag{1.138}$$

where

$$f(x)=\frac{1}{\pi^2}\,x\,\sin x\,\Gamma^2\left(\frac{x}{\pi}\right). \tag{1.139}$$

The function $f(x)$ has the following properties:

$$f(0)=1\,,\ \ f(\pi/2)=\frac{1}{2}\,,\ \ f(\pi)=0\,, \tag{1.140}$$

and in the interval $0 \leq x \leq \pi$ it can be approximated by a linear function,

$$f(x) \approx 1 - \frac{x}{\pi} \tag{1.141}$$

with an accuracy of 1%.

We can use expression (1.138) to derive the distortion field $\hat{U}$ at the compactified Schwarzschild black hole horizon. Because of the linearity of the corresponding Laplace equation, $\hat{U}$ can be calculated by simple subtraction of the Schwarzschild black hole metric function U_S, approximated at the vicinity of its horizon. An approximation of the U_S, given by expression (1.22), for $\rho \ll 1$ and $z \in [-\mu, \mu]$ reads

$$U_S(\rho, z) \approx \frac{1}{2} \ln \left(\frac{\rho^2}{4[\mu^2 - z^2]} \right). \tag{1.142}$$

Subtracting Eq. (1.142) from Eq. (1.138), and substituting $z = \mu \cos\theta$ at the horizon [see Eq. (1.16)] we derive

$$\hat{U}(\eta, \theta)|_{\eta=1} = \frac{\mu}{\pi} \ln(4\pi) + \frac{1}{2} \ln \left[f\left(\frac{\mu[1+\cos\theta]}{2} \right) f\left(\frac{\mu[1-\cos\theta]}{2} \right) \right]. \tag{1.143}$$

The multipole moments a_n's for the solution (1.143) can be obtained from (1.43). Let us emphasize that, since the function (1.143) is invariant under the transformation $\theta \to \pi - \theta$, the moments a_n's for odd n vanish [see Eqs. (1.75), (1.70)]. This implies that $u_- = u_+$, and the boundary value of $\hat{U}$ at $\eta = -1$, or $\psi = \pi$, coincides with the boundary value of this function at the horizon, $\eta = 1$, or $\psi = 0$ [see Eq. (1.71)], and we have [see Eq. (1.48)]

$$u_0 = \frac{\mu}{\pi} \ln(4\pi) + \frac{1}{2} \ln[f(\mu)]. \tag{1.144}$$

Using equations (1.143) and (1.144) we derive

$$u(\theta) = u_\pm(\theta) \approx \frac{1}{2} \ln \left[\frac{4\pi(\pi - \mu) + \mu^2 \sin^2\theta}{4\pi(\pi - \mu)} \right]. \tag{1.145}$$

The metric (1.82) on the surface of the horizon is

$$d\sigma_+^2 \approx \left[1 + \frac{\mu^2 \sin^2\theta}{4\pi(\pi - \mu)} \right] d\theta^2 + \left[1 + \frac{\mu^2 \sin^2\theta}{4\pi(\pi - \mu)} \right]^{-1} \sin^2\theta \, d\phi^2 . \tag{1.146}$$

Using equations (1.98), (1.99), (1.111) and (1.112), we can calculate the Kretschmann

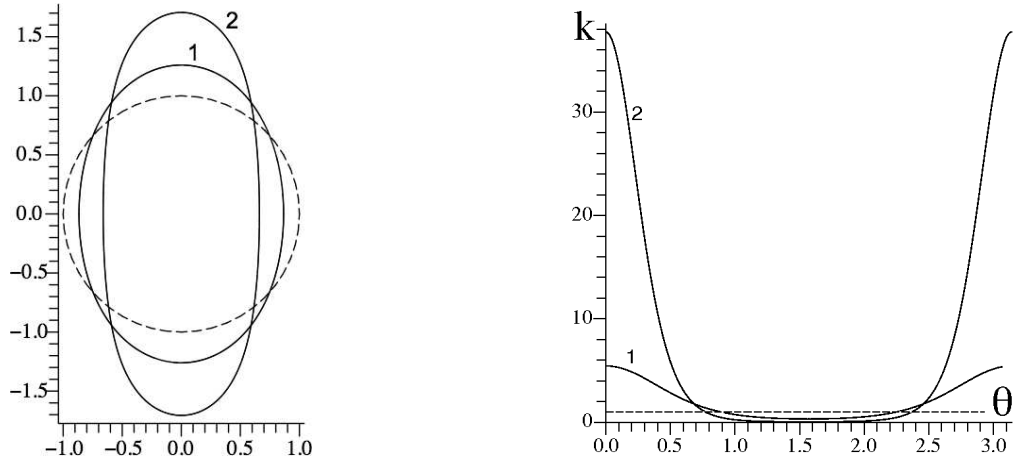

Figure 1.11: (**a**) Shape of the distorted event horizon surface for the compactified Schwarzschild black hole. Line (1): $\mu = 2/3\pi$; line (2): $\mu = 6/7\pi$. The dashed circle corresponds to the Schwarzschild black hole. The embedding surface is obtained by rotation of these curves around the vertical axis. (**b**) Kretschmann scalars ratio $k = \mathcal{K}_+/\mathcal{K}_{\text{Sch},+}$ on the horizon for the same values of μ, lines (1) and (2). The dashed horizontal line corresponds to the Schwarzschild black hole.

scalar at the horizon surface of the compactified Schwarzschild black hole,

$$\mathcal{K}_+ \approx 12\,[4\pi(\pi-\mu)]^4\,\frac{[4\pi(\pi-\mu)+\mu^2+3\mu^2\cos^2\theta]^2}{\left[4\pi(\pi-\mu)+\mu^2\sin^2\theta\right]^6}\,, \tag{1.147}$$

and in the vicinity of its *stretched singularity*,

$$\mathcal{K}_- \approx \frac{64}{27\tau^4}[1+\mathcal{K}^{(2)}\tau^{2/3}+O(\tau^{4/3})]\,, \tag{1.148}$$

$$\mathcal{K}_-^{(2)} \approx (12)^{2/3}\frac{\left[8\pi(\pi-\mu)-\mu^2\sin^2\theta\right]^2+3\mu^4\sin^2\theta(13\sin^2\theta-16)}{32\pi(\pi-\mu)\left[4\pi(\pi-\mu)+\mu^2\sin^2\theta\right]}\,. \tag{1.149}$$

Applying equations (1.89) and (1.90), and the transformation $u_+ \to -u_-$, respectively, we can construct an isometric embedding of these surfaces. Figure 1.11 illustrates the shapes of the distorted event horizon surface and the ratio of the Kretschmann scalars, $k = \mathcal{K}_+/\mathcal{K}_{\text{Sch},+}$, of the compactified Schwarzschild black hole and the Schwarzschild black hole. The metric (1.110) on the surface of the

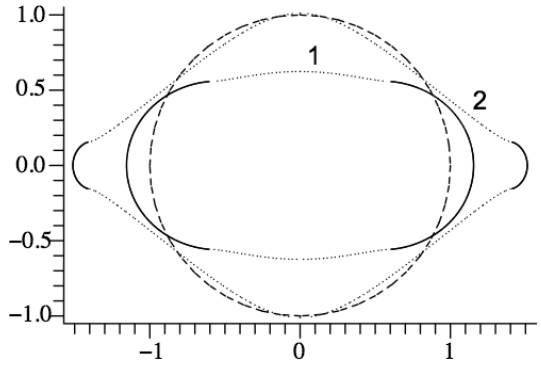

Figure 1.12: Shape of the distorted *stretched singularity* of the 4D compactified Schwarzschild black hole of $\mu = 2/3\pi$, line (1) and $\mu = 6/7\pi$, line (2). The regions embedded into pseudo-Euclidean space are illustrated by the dotted lines. The dashed circle corresponds to the Schwarzschild black hole. The embedding surface is obtained by rotation of these curves around the vertical axis.

stretched singularity is

$$d\sigma_-^2 \approx \left[1+\frac{\mu^2\sin^2\theta}{4\pi(\pi-\mu)}\right]^{-1} d\theta^2 + \left[1+\frac{\mu^2\sin^2\theta}{4\pi(\pi-\mu)}\right]\sin^2\theta\, d\phi^2\,. \quad (1.150)$$

The shape of the distorted *stretched singularity* is illustrated in Figure 1.12.

1.10 Discussion

Let us summarize the obtained results. We considered the geometry of static vacuum axisymmetric distorted black holes. We focused mainly on the properties of the horizon and interior of such black holes. The geometry of a distorted black hole is uniquely determined by the 'gravitational potential' U which is a solution of the 3D flat Laplace (in the exterior region) or d'Alembert (in the interior region) equation. After solving this 'master' equation, the second function V, which enters the metric, can be obtained by a simple integration.

The 'gravitational potential' U is a superposition of the Schwarzschild potential U_S and the distortion potential $\hat{U}$ [see Eq. (1.32)]. The distortion $\hat{U}$ is determined by the values of the multipole moments a_n's obeying the constraints (1.52). The distortion potential in the black hole interior possesses a remarkable discrete symmetry (1.62) which relates the values of $\hat{U}$ in the vicinity of the singularity to its values in the vicinity of the horizon. Thus, the functions $u_\pm(\theta)$ [see Eq. (1.69) or Eq. (1.75)] determine the shape of the horizon and the *stretched singularity*, as

well as the leading asymptotics of the metric and the curvature invariants near the horizon and singularity of a distorted black hole.

Qualitatively, the shape of the event horizon surface of a distorted black hole is similar to the shape of equipotential surfaces in linearized (Newtonian) gravity. Namely, consider a point-like mass M located at the coordinate center O (see Figure D.1 in Appendix D). In the presence of a quadrupole distortion its Newtonian gravitational potential reads (up to Newtonian monopole moment α_0)

$$U_N = -\frac{M}{\mathtt{r}} + \hat{U}_N\,,\ \ \hat{U}_N = \frac{\alpha_2}{2}\mathtt{r}^2(3\cos^2\vartheta - 1)\,, \tag{1.151}$$

where $\mathtt{r} = \sqrt{x^2+y^2+z^2}$ is the radial distance from the mass M, and α_2 is the Newtonian quadrupole moment. For positive α_2 such a distortion is generated, for example, by a ring of mass m and radius $\mathtt{r}_0 \gg \mathtt{r}$ located in the equatorial plane. For such a ring $\alpha_2 = m/(2\mathtt{r}_0^3)$ [see Appendix D, Eq. (D.3)]. Similarly, a negative quadrupole moment α_2 is generated, for example, by two point masses m_1 and m_2, located on the axis of symmetry on the opposite sides of the mass M at the distances $d_1 \gg \mathtt{r}$, and $d_2 \gg \mathtt{r}$, respectively. In this case $\alpha_2 = -m_1/d_1^3 - m_2/d_2^3$ [see Appendix D, Eq. (D.3)]. We consider $\mathtt{r} \sim M$ and assume that the distortion $\hat{U}_N$ is small. Then the change $\delta\mathtt{r}$ in the position of the equipotential surface of U_N given by Eq. (1.151) with respect to the position of the unperturbed surface of $\mathtt{r}_c = const$ is

$$\delta\mathtt{r} = -\frac{\alpha_2\mathtt{r}_c^4}{2M}(3\cos^2\vartheta - 1)\,. \tag{1.152}$$

Thus the quadrupole distortion deforms the equipotential surfaces and makes them either oblate (for $\alpha_2 > 0$) or prolate (for $\alpha_2 < 0$). This property is similar to the property of the horizon surface for the distorted black hole [see Figure 1.6(**a**)].

It should be emphasized that the linear approximation is not sufficient for the 'explanation' of the Kretschmann invariant properties. Indeed, in the linear approximation

$$ds^2 = -(1+2U_N)dt^2 + (1-2U_N)(dx^2+dy^2+dz^2)\,, \tag{1.153}$$

the Kretschmann scalar is

$$\mathcal{K} \approx 8U_{N,ij}U_N{}^{,ij} = 48\left[\alpha_2^2 - \frac{M(M+2\mathtt{r}U_N)}{\mathtt{r}^6}\right]. \tag{1.154}$$

Its variation under the small distortion $\hat{U}_N$ is

$$\delta\mathcal{K} = -\frac{2M^2}{\mathtt{r}_c^7}\delta\mathtt{r}\,. \tag{1.155}$$

Hence, in the weak field approximation, $\mathcal{K}$ is larger at the points where $\delta \mathtt{r} < 0$, such as at the poles of the oblate equipotential surface (for $\alpha_2 > 0$), and in the equatorial points of the prolate surface (for $\alpha_2 < 0$) than undistorted $\mathcal{K}$. This behavior of $\mathcal{K}$ in the weak field limit is opposite to the behavior of $\mathcal{K}$ on the horizon of the distorted black hole [see, e.g., Eq. (1.98) and Figure 1.7($\mathbf{a}$)]. This difference demonstrates that nonlinear effects and the spatial curvature play important role near the black hole horizon.

The property (1.99) has an important consequence for compactified black holes discussed in Section 1.9. For μ close to π, when the 'north' and 'south' poles of the compactified black hole are close to each other, the Gaussian curvature (and hence the Kretschmann invariant) becomes large at the poles. In other words, in the infinitely slow merger transition the region of a very high curvature 'leaks' through the horizon in the vicinity of the black hole poles. When this curvature reaches the Planck value, one can say that the *physical singularity* (as defined in Section 1.7) becomes naked. This may indicate that during the phase transition between black-hole and black-string phases one can expect the formation of a naked *physical singularity*. Whether this conclusion remains valid for higher dimensional compactified black holes and beyond the adiabatic approximation is an interesting open question.

Chapter 2

Interior of a charged distorted black hole

2.1 Introduction

In this chapter, we study how the distortion of a charged, static black hole generated by an axisymmetric, static matter distribution in its exterior region affects its interior. Here we present a direct generalization of a similar study for the distorted neutral black hole interior performed in the previous chapter.

The structure and properties of the charged and/or rotating black hole interior is a subject that has attracted a lot of interest during the past 30 years (see, e.g., [43], Chapter 14 and references therein). An analytic continuation of the Reissner-Nordström (RN) and Kerr solutions results in the existence of infinitely many new 'universes' in the black holes interior. However, the region containing these new universes lies in the future of the Cauchy horizon, a null hypersurface beyond which predictability of evolution based on the past initial data breaks down. A natural question is whether these universes are accessible to an observer traveling in the interior of the black hole. That is why the issue of the Cauchy horizon stability is so important. Observers traveling along a timelike world line receive an infinitely blueshifted radiation when they approach the horizon. Penrose [105] used these facts to argue that small perturbations produced in the black hole exterior grow infinitely near the Cauchy horizon. The evolution of small perturbations inside charged black holes was analyzed in [23, 92, 93]. These results confirm Penrose's intuitive arguments.

If one considers ingoing radiation only and neglects backscattered radiation, then the resulting Cauchy horizon singularity is weak. Namely, the Kretschmann invariant calculated on the Cauchy horizon is finite. A freely falling observer detects an infinite increase of energy density, but tidal forces remain finite as the observer crosses the Cauchy horizon (see [32, 85]). This singularity is called a

whimper singularity. However, in a realistic situation, when both incoming and outgoing radiation are present, the curvature grows infinitely near the Cauchy horizon. This was demonstrated by Poisson and Israel [107] who considered the ingoing and outgoing radiation simulated as two noninteracting radial streams of ingoing and outgoing lightlike particles following null geodesics. Poisson and Israel showed that this radiation results in an infinite growth of the black hole internal mass parameter and divergence of the Weyl scalar Ψ_2. They called this effect *mass inflation*. Mass inflation for a slowly rotating, charged black hole was discussed in [63]. Ori constructed an exact, simplified solution describing this effect [101]. Using his solution Ori showed that the *mass inflation* singularity is weak enough. Namely, the tidal forces calculated at the Cauchy horizon diverge in the reference frame of a freely falling observer, but their integral along the world line of the observer remains finite. It means that freely falling observers might in fact cross the Cauchy horizon. For a more detailed discussion see, e.g., [18–21, 63, 64]. Early numerical analysis of the Cauchy horizon stability predicted its destruction as a result of classical instability [54]. Later, analytical [12, 36], and numerical [14] discussions did not confirm this result. The mass inflation phenomenon may shed light on the Cauchy horizon stability problem. However, further investigation is necessary.

Although rotating black holes are of real astrophysical interest, charged black holes are often considered in publications. The reason for this is simple: a charged black hole also has a Cauchy horizon, but its spherical geometry makes an analysis easier. However, such a model is very simplified, for in the realistic world there always exists some matter outside the black hole. This matter distorts the gravitational field of the black hole. What is important is that this distortion generated by the matter distribution in the exterior of the black hole occurs not only outside the black hole, but also affects its interior. Since the region near the Cauchy horizon is 'fragile' and 'vulnerable,' it is interesting to analyze how such external matter affects the properties of the black hole Cauchy horizon. This is one of the questions we address here. We shall make several assumptions simplifying the analysis. Namely, we assume that the distortions of the black hole are static and axisymmetric. Moreover, we consider a special class of charged distorted black hole solutions which can be generated by the Harrison-Ernst transformation [33, 69] from a neutral distorted black hole metric. This class includes a large variety of solutions which can be presented in an explicit form.

We assume that in the vicinity of the black hole and in its interior the Einstein-Maxwell equations are satisfied, and the matter disturbing the black hole is located in the black hole exterior. The matter sources are described by the corresponding energy-momentum tensor which has to be included in the Einstein-Maxwell equations. To avoid this one can move these sources to infinity. The 'price' for this is that the corresponding spacetime is not asymptotically flat anymore. In our

description of a distorted black hole we follow [50] and adopt that approach.

Our main problem is to study how the black hole interior is distorted by the external fields. In particular, we shall study distortion of the inner (Cauchy) horizon and its relation to the distortion of the outer (event) horizon. Let us emphasize that our consideration is completely classical, and we do not consider quantum effects which may play an important role in the charged black hole interior. Discussion of these effects can be found, e.g., in [41, 42, 62, 100].

It should be emphasized that the study of the black hole interior is a dynamical problem. The geometry of the black hole interior is similar to the geometry of a collapsing, anisotropic, homogeneous universe. To study how the evolution of this universe is modified by an external influence, one must study first the modification of the external geometry of the black hole and use these results to find the corresponding modification of the geometry of the event horizon. This gives the initial data which determines the evolution of the black hole interior. Here we study a simple case when the distortion of the black hole in the exterior region is both static and axisymmetric. A similar problem for the neutral black hole was studied earlier in [45], (see Chapter 1). The results presented here are published in [1].

2.2 Reissner-Nordström spacetime

Before we proceed with the description of a charged distorted black hole, let us make a few remarks about the charged black hole solution in the absence of distortions. This is the well-known Reissner-Nordström (RN) solution representing electrically charged black hole (see, e.g., [22, 43, 72, 94])

$$ds^2 = -\left(1 - \frac{2M}{r} + \frac{Q^2}{r^2}\right) dt^2 + \left(1 - \frac{2M}{r} + \frac{Q^2}{r^2}\right)^{-1} dr^2 + r^2(d\theta^2 + \sin^2\theta d\phi^2),$$
$$A_\alpha = -\Phi_0 \delta_\alpha{}^t, \;\; \Phi_0 = \frac{Q}{r}. \tag{2.1}$$

Here, M is the black hole mass, and Q is its electric charge. The RN spacetime is static and asymptotically flat. It is of Petrov type-D, and it has spacetime singularity at $r = 0$, which is timelike. According to the generalized Birkhoff theorem, the RN solution is unique: any spherically symmetric solution of the Einstein-Maxwell equations (see Eq. (2.3) below) is locally isometric to the RN solution. We shall consider nonextremal black holes with $|Q| < M$. The RN black hole horizons are defined by $r_\pm = M \pm \sqrt{M^2 - Q^2}$, where the upper sign stands for the event horizon, and the lower sign stands for the Cauchy horizon. The horizons are coordinate singularities of the RN spacetime (2.1). The RN spacetime is regular

in the following regions:

$$\text{Region } I: r \in (r_+, +\infty), \ \text{Region } II: r \in (r_-, r_+), \ \text{Region } III: r \in (0, r_+). \tag{2.2}$$

In the regions I and III, the coordinate r is spacelike. These regions are static. In the region II, the coordinate r is timelike. This region is dynamic. It represents a contracting anisotropic homogeneous universe. As in the case of the Schwarzschild spacetime, one can find a maximal analytical extension of the RN manifold by appropriate choice of coordinates. However, in this case the maximally extended manifold is covered by analytic atlas consisting of two coordinate charts. One of the charts defines the RN metric analytic everywhere except $r = r_+$, and another chart defines the RN metric analytic everywhere except $r = r_-$. Figure 2.1 illus-

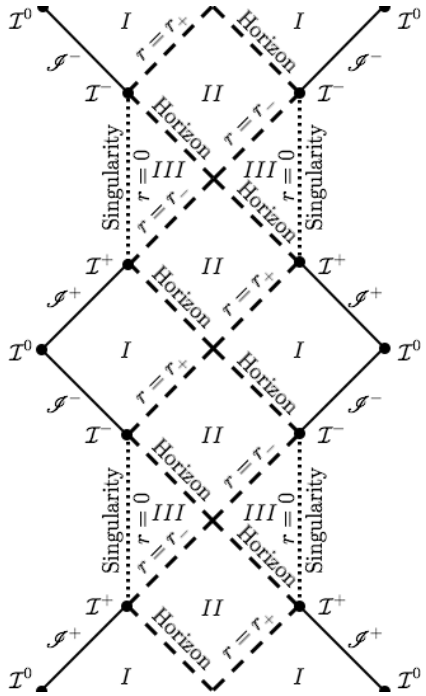

Figure 2.1: Part of the Carter-Penrose conformal diagram of the RN spacetime. Each point in the diagram, except for the vertices, represents a 2D sphere (θ, ϕ). The notations are defined in Section 1.1.

trates a part of the Carter-Penrose conformal diagram of the RN spacetime. The complete Carter-Penrose diagram consists of infinitely many such parts repeated in the vertical direction. Thus, it has an infinite number of asymptotically flat regions I, 'universes', and an infinite number of horizons and singularities. The RN spacetime singularity can be avoided by timelike and null curves. Even more,

this singularity is repulsive for timelike geodesics, which can never hit it. Thus, the spacetime manifold is timelike geodesically complete. However, nongeodesic timelike curves and radial null geodesics can terminate at the singularity.

The Carter-Penrose diagram suggests that observers might travel from one universe to another by passing though the regions II and III without hitting the timelike singularities. Such observers have to cross the event and Cauchy horizons. While crossing the event horizon, observers will appear to have an infinite redshift to observers located at the corresponding asymptotically flat region I. If they send an outgoing light signal to the region I at the moment when they cross the event horizon, it will be received in infinite time at $\mathcal{I}^+$. In the region II, where the observers travel after they crossed the event horizon, each point in the diagram represents a closed 2D trapped surface. Thus, traveling there is just time evolution, like in the Schwarzschild black hole interior. At the very end of this time evolution observers cross the Cauchy horizon and see, in a flash, the whole of the history of one of the regions I, in infinitely blueshifted ingoing null rays emerging from $\mathcal{I}^+$. Infinite blueshift suggests that small perturbations in the region I will be infinitely amplified at the Cauchy horizon. The amplified perturbations may destroy the Cauchy horizon and seal the door to other universes. According to the mass inflation effect proposed in [107], infinitely blueshifted ingoing radiation is only a necessary condition to destroy the Cauchy horizon. A sufficient condition is the outgoing flux, which is always present due to the backscattered ingoing radiation.

In the following sections we shall discuss the RN black hole distorted by external, static, axisymmetric matter. We shall study how such distortion affects the black hole interior, and, in particular, its Cauchy horizon.

2.3 Metric of a distorted RN black hole

2.3.1 Static, axisymmetric Einstein-Maxwell spacetime

In this section, following [15, 16, 34], we present a solution for a static, axisymmetric distorted charged black hole. This solution is obtained by applying the Harrison-Ernst transformation [33, 69] to the Weyl metric of a distorted vacuum black hole [see (1.27)]. Here we reproduce the basic relations, mainly in order to explain notations we shall use later. The metric of a charged distorted black hole, as the metric of the RN black hole [see Eq. (2.1)], is a special solution of the Einstein-

Maxwell equations

$$R_{\alpha\beta} = 8\pi\, T_{\alpha\beta}, \tag{2.3}$$
$$\nabla_\beta F^{\alpha\beta} = 0\,, \;\; \nabla_{[\alpha} F_{\beta\gamma]} = 0, \tag{2.4}$$
$$8\pi\, T_{\alpha\beta} = 2F_\alpha{}^\gamma F_{\beta\gamma} - \frac{1}{2} g_{\alpha\beta} F_{\gamma\delta} F^{\gamma\delta}. \tag{2.5}$$

Here, $F_{\alpha\beta} = \nabla_\alpha A_\beta - \nabla_\beta A_\alpha$, and A_α is the electromagnetic 4-potential. The nabla stands for the covariant derivative defined with respect to the metric $g_{\alpha\beta}$. It is convenient to make the following coordinate transformation [cf. Eq. (1.26)]:

$$r = M(1 + p\eta)\,, \;\; p = \frac{\sqrt{M^2 - Q^2}}{M}\,, \;\; \eta \in (-1/p, \infty), \tag{2.6}$$

and to rewrite the RN solution in the following form

$$ds^2 = -\frac{p^2(\eta^2 - 1)}{(1 + p\eta)^2} dt^2 + M^2(1 + p\eta)^2 \left[\frac{d\eta^2}{\eta^2 - 1} + d\theta^2 + \sin^2\theta d\phi^2\right], \tag{2.7}$$
$$\Phi_0 = \frac{\sqrt{1 - p^2}}{(1 + p\eta)}. \tag{2.8}$$

In these new coordinates, $\eta = \eta_\pm = \pm 1$ corresponds to the horizons of metric (2.7). We denote these horizons by $\mathcal{H}^{(\pm)}$, respectively. The black hole singularity is defined by $\eta = -1/p$.

The general form of a static, axisymmetric metric in prolate spheroidal coordinates $(\eta, \cos\theta, \phi)$ is given by

$$ds^2 = -e^{2\bar{U}} dt^2 + M^2 p^2 e^{-2\bar{U}} \left[e^{2\bar{V}} (\eta^2 - \cos^2\theta) \left[\frac{d\eta^2}{\eta^2 - 1} + d\theta^2\right] + (\eta^2 - 1)\sin^2\theta d\phi^2\right], \tag{2.9}$$

where the metric functions $\bar{U}$ and $\bar{V}$ depend on (η, θ) coordinates. The corresponding electrostatic 4-potential is

$$A_\alpha = -\Phi(\eta, \theta)\delta_\alpha{}^t. \tag{2.10}$$

2.3.2 Harrison-Ernst transformation

The Einstein-Maxwell equations for $\bar{U}$ and Φ are the Ernst equations [33], which in our case of static spacetime (2.9) take the following form:

$$\nabla\left(e^{-2\bar{U}} \nabla\bar{\mathcal{E}}\right) = 0\,, \quad \nabla\left(e^{-2\bar{U}} \nabla\Phi\right) = 0. \tag{2.11}$$

Here,

$$\bar{\mathcal{E}} = e^{2\bar{U}} - \Phi^2 \tag{2.12}$$

is the Ernst potential, and ∇ is the nabla operator defined with respect to the 3D flat metric

$$dl^2 = (\eta^2 - \cos^2\theta)\left[\frac{d\eta^2}{\eta^2-1} + d\theta^2\right] + (\eta^2-1)\sin^2\theta d\phi^2. \tag{2.13}$$

There exists a special class of solutions where the Ernst potential $\bar{\mathcal{E}}$ is an analytic function of Φ. Under this assumption Eqs. (2.11) imply

$$\frac{d^2\bar{\mathcal{E}}}{d\Phi^2} = 0. \tag{2.14}$$

If spacetime is asymptotically flat, we choose $\bar{U} = \Phi = 0$ at infinity. In this case a general solution of Eq. (2.14) can be written as

$$\bar{\mathcal{E}} = 1 - \frac{2}{\sqrt{1-p^2}}\Phi. \tag{2.15}$$

We shall keep this relation in our consideration. Following [33] it is convenient to parametrize $\bar{\mathcal{E}}$ and Φ as follows:

$$\bar{\mathcal{E}} = \frac{\bar{\xi}-1}{\bar{\xi}+1}, \qquad \Phi = \frac{\sqrt{1-p^2}}{\bar{\xi}+1}, \tag{2.16}$$

where $\bar{\xi}$ is the auxiliary Ernst potential. Using (2.11) one obtains the following equation for $\bar{\xi}$:

$$(\bar{\xi}^2 - p^2)\nabla^2\bar{\xi} - 2\bar{\xi}\,\nabla\bar{\xi}\cdot\nabla\bar{\xi} = 0. \tag{2.17}$$

In the absence of an electric field, $\Phi = 0$, the Ernst equation (2.11) is

$$\mathcal{E}\nabla^2\mathcal{E} = \nabla\mathcal{E}\cdot\nabla\mathcal{E}, \tag{2.18}$$

where $\mathcal{E} = e^{2U}$, and U corresponds to the vacuum uncharged solution. In this case one can also use the parametrization (2.16), which gives

$$\mathcal{E} = \frac{\xi-1}{\xi+1}, \tag{2.19}$$

and the Ernst equation (2.17) takes the form

$$(\xi^2 - 1)\nabla^2\xi - 2\xi\,\nabla\xi\cdot\nabla\xi = 0. \tag{2.20}$$

Comparing (2.17) and (2.20), we can derive the relation between the vacuum and the electrostatic Ernst potentials. This is the Harrison-Ernst transformation:

$$\bar{\xi} = p\xi. \tag{2.21}$$

Thus, if we know the solution U to the vacuum Einstein equations, we can apply the transformations (2.21) and (2.16) to obtain the corresponding solution $\bar{U}$, and the electrostatic potential Φ obeying the Einstein-Maxwell equations. Namely, using expressions (2.21), (2.19) and (2.16), we derive

$$e^{2\bar{U}} = \frac{4p^2e^{2U}}{[1+p-(1-p)e^{2U}]^2}\,,\quad \Phi = \frac{\sqrt{1-p^2}(1-e^{2U})}{1+p-(1-p)e^{2U}}. \tag{2.22}$$

These expressions determine the charged version of an electrically neutral, vacuum static solution. For example, starting with the Schwarzschild black hole solution, we can derive the RN black hole. If the Schwarzschild black hole is distorted by neutral exterior matter, these expressions electrically charge both, the black hole and the matter.

In the next subsection, we apply this 'charging' procedure to the Weyl static metric describing a vacuum, axisymmetric distorted black hole, and obtain an electrically charged distorted black hole. We discuss the corresponding metric in subsection 2.3.4.

2.3.3 Charged distorted black hole

Now we are ready to present a solution for a charged, axisymmetric distorted black hole. The Israel uniqueness theorem for distorted Schwarzschild black hole (see Chapter 1, Section 1.3) can be generalized to electrically charged distorted black hole [78]: *among all static, asymptotically flat, electro-vacuum solutions to the Einstein-Maxwell equations, which have closed, simply connected equipotential surfaces $\boldsymbol{\xi}^2_{(t)} = const$, where $\boldsymbol{\xi}_{(t)} = \partial_t$ is a timelike, surface-orthogonal Killing vector, the Reissner-Nordström solution is the only one which has a regular event horizon $\boldsymbol{\xi}^2_{(t)} = 0$.*

In analogy with the distorted Schwarzschild black hole, we consider a RN black hole distorted by static, axisymmetric external distribution of electrically charged matter whose sources are located at asymptotic infinity. The Israel theorem above is not applicable for such a black hole, for the corresponding spacetime is not asymptotically flat. Thus, we may have a charged distorted black hole which

differs from the RN one, and whose event horizon is regular. Following the procedure presented in the previous subsection, we can start with the vacuum solution representing an axisymmetric distorted Schwarzschild black hole (1.33), which we discussed in Chapter 1, Section 1.3. To obtain a charged version of the distorted neutral black hole, it is sufficient to derive $\bar{U}$ and Φ from U [see Eqs. (1.32), (1.28) and (1.44)] using the transformation (2.22). We have

$$e^{2\bar{U}} = \frac{4p^2(\eta^2-1)e^{2\hat{U}}}{[(1+p)(\eta+1)-(1-p)(\eta-1)e^{2\hat{U}}]^2}, \tag{2.23}$$

$$\Phi = \frac{\sqrt{1-p^2}[\eta+1-(\eta-1)e^{2\hat{U}}]}{(1+p)(\eta+1)-(1-p)(\eta-1)e^{2\hat{U}}}. \tag{2.24}$$

Remarkably, the transformation (2.22) does not alter Eqs. (1.35) and (1.36). Thus, $\bar{U}$ and Φ, given by Eqs. (2.23), (2.24), and V, which is determined by Eqs, (1.32), (1.28), and Eqs. (1.45)-(1.47), solve the corresponding Einstein-Maxwell equations. The axisymmetric distorted RN solution is given by (2.9), (2.10) together with (2.23), (2.24) and $\bar{V} = V$. Axisymmetric, distorted Schwarzschild black hole spacetime is of Petrov type-I, and is type-D on the horizon and on its axis of symmetry [104]. It can be checked that the transformation (2.22) does not alter these properties, and in addition the corresponding spacetime is of Petrov type-D on the Cauchy horizon.

A more general case of a distorted, electrically charged, rotating black hole was considered in [16]. Charged dilaton black hole distorted by the charged and dilatonic external matter was studied in [124].

2.3.4 Dimensionless form of the metric

The metric (2.9) contains only one essential dimensional parameter, say M, while all other parameters can be presented in dimensionless form. It is convenient to write the metric (2.9) in the following dimensionless form $dS_\pm^2$ adopted to analysis of the black hole horizons $\mathcal{H}^{(\pm)}$ [cf. Eq. (1.56)]:

$$ds^2 = \Omega_\pm^2 dS_\pm^2, \tag{2.25}$$

$$dS_\pm^2 = -\frac{\eta^2-1}{\Delta_\pm}e^{2\mathcal{U}}dT_\pm^2 + \frac{\Delta_\pm}{\eta^2-1}e^{-2\mathcal{U}+2\hat{V}}d\eta^2 + \Delta_\pm e^{-2\mathcal{U}}\left(e^{2\hat{V}}d\theta^2+\sin^2\theta d\phi^2\right), \tag{2.26}$$

$$\Omega_\pm = M(1\pm p)e^{\mp u_0} = M'(1\pm p'). \tag{2.27}$$

For the dimensionless metric $dS_\pm^2$, we define $T_\pm = \kappa_\pm t$, where $\kappa_\pm$ is the surface

gravity, which is given by

$$\kappa_{\pm} = \frac{p\, e^{\pm 2u_0}}{M(1\pm p)^2} = \frac{(1+p')e^{u_0} - (1-p')e^{-u_0}}{2M'(1\pm p')^2}\,. \tag{2.28}$$

We also use the following expressions for the metric functions $\Delta_{\pm}$ and $\mathcal{U}$:

$$\Delta_{\pm} = \frac{\delta^{\pm 1}}{4\delta}\left[\eta + 1 - \delta e^{2\mathcal{U}}(\eta - 1)\right]^2\,, \tag{2.29}$$

$$\mathcal{U} = \hat{U} - u_0\,,\ \ \delta = \delta_0 e^{2u_0} = \frac{1-p}{1+p}e^{2u_0} = \frac{1-p'}{1+p'}\,. \tag{2.30}$$

Together with the original parameters M and p it is convenient to use the related parameters

$$M' = \frac{M}{2}\left[(1+p)e^{-u_0} + (1-p)e^{u_0}\right]\,, \tag{2.31}$$

$$p' = \frac{\sqrt{M'^2 - Q^2}}{M'}\,. \tag{2.32}$$

In the absence of distortion $M' = M$ is the Komar mass of the RN black hole measured at asymptotic infinity. In the case when $Q = 0$, M' is the local mass of a distorted Schwarzschild black hole defined in [50].

The coordinate η changes from $\eta = +\infty$ (at spatial infinity) to the region of $\eta < -1$ where the spacetime singularity is located (see subsection 2.3.5). As in the case of the RN black hole (2.7), the horizons of metric (2.26) are defined by $\eta = \eta_{\pm} = \pm 1$. As we mentioned earlier, we shall use the notation $\mathcal{H}^{(\pm)}$ for the outer (+), and for the inner (−) horizons. To indicate that a dimensional quantity $(\ldots)$ is calculated at the black hole horizons $\mathcal{H}^{(\pm)}$, we shall use a superscript $(\pm)$, and denote this quantity as $(\ldots)^{(\pm)}$.

The metric (2.26) allows Wick's rotation $T_+ \to iT_E$, which transforms the exterior region $\eta \geq 1$ into that of the corresponding distorted Euclidean charged black hole. The Euclidean horizon surface $\eta = 1$ is a regular 2D totally geodesic surface. The corresponding electric field transforms as $\Phi_+ \to -i\Phi_E$.

As we shall see in the next section, the form of metric (2.26) is convenient for the analysis and comparison of the properties of the inner and outer black hole horizons. 2D metrics on the horizon surfaces can be obtained by taking $T = const$, and $\eta = \eta_{\pm} = \pm 1$ in the metric (2.26). In Section 2.4, we show that the surface area of the outer (event) horizon calculated for the dimensionless metric dS_+^2 is equal to 4π. Similarly, the surface area of the inner (Cauchy) horizon calculated for the metric dS_-^2 is also equal 4π. These normalization conditions specify the

form of the conformal factor $\Omega_\pm^2$ in (2.25). The 'real' (dimensional) areas of the horizon surfaces are

$$\mathcal{A}^{(\pm)} = 4\pi\Omega_\pm^2\,, \tag{2.33}$$

and the ratio of these areas is

$$\mathcal{A}^{(+)}/\mathcal{A}^{(-)} = (\Omega_+/\Omega_-)^2 = \left(\frac{1+p'}{1-p'}\right)^2 \equiv \delta^{-2}\,. \tag{2.34}$$

In what follows, we shall discuss different geometrical objects, such as the Kretschmann invariant $\mathcal{K}$, the Weyl scalar $\mathcal{C}^2$,

$$\mathcal{K} = R_{\alpha\beta\gamma\delta}R^{\alpha\beta\gamma\delta}\,, \quad \mathcal{C}^2 = C_{\alpha\beta\gamma\delta}C^{\alpha\beta\gamma\delta}\,, \tag{2.35}$$

and the Gaussian curvature K of the 2D horizon surfaces. We shall use the same notations with an index $\pm$ for an object calculated for the metric $dS_\pm^2$. One has

$$\mathcal{K} = \Omega_\pm^{-4}\mathcal{K}_\pm\,,\ \mathcal{C}^2 = \Omega_\pm^{-4}\mathcal{C}_\pm^2\,,\ K = \Omega_\pm^{-2}K_\pm\,. \tag{2.36}$$

To study the interior region we can use any of these two forms of the dimensionless metric $dS_\pm^2$. Certainly, the 'physical' result, calculated for the metric ds^2 will be the same.

The dimensionless electrostatic potential for metric (2.26) is given by

$$\Phi_\pm = \frac{\sqrt{\delta}\Delta_\pm^{-1/2}}{(e^{2u_0}-\delta)}\left[\eta+1-(\eta-1)e^{2\mathcal{U}+2u_0}\right]. \tag{2.37}$$

It is related to the electrostatic potential (2.24) as follows

$$\Phi = \Omega_\pm\kappa_\pm\,\Phi_\pm. \tag{2.38}$$

The non-vanishing dimensionless components of the electromagnetic field $F_{\mu\nu}$ are defined by

$$F_{\pm T_\pm\eta} = \Phi_{\pm,\eta} = \frac{\delta^{\pm1/2}}{\Delta_\pm}e^{2\mathcal{U}}[(1-\eta^2)\mathcal{U}_{,\eta}-1]\,, \tag{2.39}$$

$$F_{\pm T_\pm\theta} = \Phi_{\pm,\theta} = \frac{\delta^{\pm1/2}}{\Delta_\pm}e^{2\mathcal{U}}(1-\eta^2)\mathcal{U}_{,\theta}\,. \tag{2.40}$$

2.3.5 Singularities

Here, we mainly focus on the study of the horizons $\mathcal{H}^{(\pm)}$, and the inner domain located between the horizons. Since one cannot trust the metric obtained by the

analytical continuation of the exterior metric beyond the inner (Cauchy) horizon, it is reasonable to postpone study of the regions close to the spacetime singularity until the classical and quantum (in)stability will be proved. For this reason, we give only a couple of remarks about properties of the singularities in the analytic continuation of the charged distorted black hole solution.

Using expressions (2.25), (2.39), and (2.40) one can check that the curvature and the electromagnetic field invariants diverge for $\Delta_\pm = 0$, i.e., for

$$\eta \;=\; -\frac{1+\delta_0 e^{2\hat{U}}}{1-\delta_0 e^{2\hat{U}}}, \tag{2.41}$$

indicating the spacetime singularity. For the RN black hole, the singularity is located at $\eta = -1/p$, $p \in (0,1]$, corresponding to $r = 0$. Analyzing expression (2.41), we see that for $\hat{U} \leqslant 0$ the singularity is located in the region $\eta < -1$, whereas for $\hat{U} > 0$ the spacetime singularity is naked and located outside the outer horizon, $\eta > 1$. Thus, if the distortion field $\hat{U}$ satisfies the strong energy conditions, i.e., $\hat{U} \leqslant 0$ (for details see [50]), the spacetime outside the black hole outer horizon is regular, and the singularity is located behind the inner (Cauchy) horizon.

2.4 Duality relations between the inner and outer horizons

In this section, in analogy with the discrete symmetry between the event horizon and the singularity of distorted Schwarzschild black hole (1.65), (1.68), we describe special symmetry relations between the inner and outer horizons. Let us consider a 2D subspace $T_\pm = const$, $\phi = const$ orthogonal to the corresponding Killing vectors $\boldsymbol{\xi}_{(T_\pm)}$ and $\boldsymbol{\xi}_{(\phi)}$. In the coordinates

$$\eta = \cos\psi\,, \;\; \psi \in [0,\pi] \tag{2.42}$$

the subspace metrics are

$$d\Sigma^2_\pm = \Delta_\pm e^{-2\mathcal{U}+2\hat{V}}\left[-d\psi^2 + d\theta^2\right]. \tag{2.43}$$

Figure 2.4 illustrates the Carter-Penrose diagram for these metrics. Lines $\psi \pm \theta = const$ are null rays propagating from the outer to the inner horizon within the 2D subspace. Three of such null rays are shown in the figure. One of the rays starts at point A on the outer horizon $\mathcal{H}^{(+)}$, goes through the 'south' pole at $\theta = \pi$, and reaches point B at the inner horizon $\mathcal{H}^{(-)}$ (compare with Figure 1.2).

Consider a transformation R_C representing the reflection of coordinates (ψ, θ)

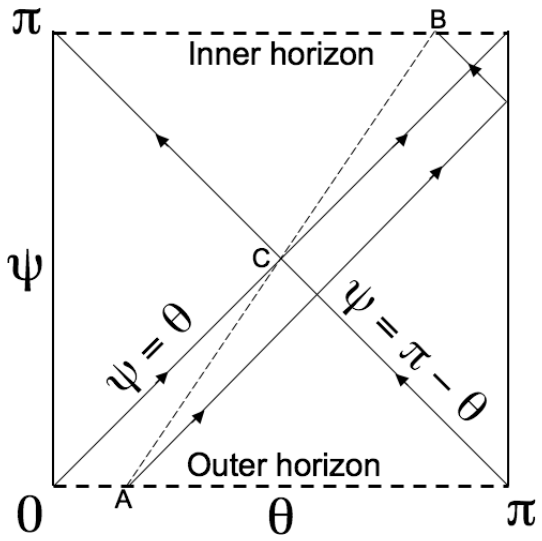

Figure 2.2: Carter-Penrose diagram for (ψ, θ) subspace of the charged distorted black hole interior. The arrows illustrate propagation of future directed null rays. Points A and B are symmetric with respect to the central point $C(\pi/2, \pi/2)$.

with respect to the 'central point' C in the interior region

$$R_C: \qquad (\psi, \theta) \to (\pi - \psi, \pi - \theta). \tag{2.44}$$

This transformation determines a map R_C^* between functions defined in the inner domain and on its boundaries

$$f^* = R_C^*(f)\,, \qquad f^*(\psi, \theta) = f(\pi - \psi, \pi - \theta)\,. \tag{2.45}$$

Such a transformation was considered for distorted Schwarzschild black hole between its event horizon and singularity [see Eqs. (1.62)-(1.64)]. It is easy to see that coordinates of the points A and B are related by the reflection R_C. Thus, the transformation R_C^* determines a map between functions on the inner and outer horizons. As in the case of distorted Schwarzschild black hole, this is a symmetry transformation for distortion fields $\mathcal{U}$ and $\hat{V}$. In other words, the values of $\mathcal{U}$ and $\hat{V}$ on the inner horizon, $\psi = \pi$, are determined by their values on the outer horizon, $\psi = 0$. Expressions (1.65) and (1.68), which we call the *duality relations*, allow one to establish special symmetry relations between the geometric properties of the inner and outer horizons. In this case, function (1.69) defines the boundary values (1.71), (1.72) and (1.73), (1.74) of the distortion fields $\mathcal{U}$ and $\hat{V}$, respectively, and as a result, the metric on the black hole horizons. Thus, the distortion fields calculated on the inner horizon are expressed through those calculated on

the outer horizon. This fact allows one to make important conclusions about the distortion of the Cauchy horizon (the details follow).

The boundary values of the distortion fields $\mathcal{U}$ and $\hat{V}$ define symmetry properties of the metric on the black hole horizon surfaces. The surface of the outer and the inner horizon is defined by $T_\pm = const$ and $\eta = \eta_\pm = \pm 1$, respectively. The corresponding dimensionless metrics derived from metric (2.26), by applying the transformation (2.42) and the boundary conditions (1.71) and (1.73), are

$$d\sigma_\pm^2 = e^{\pm 2u_\pm} d\theta^2 + e^{\mp 2u_\pm} \sin^2\theta d\phi^2. \tag{2.46}$$

The dimensional metrics on the horizon surfaces are [see Eq. (2.25)]

$$d\sigma^{(\pm)2} = \Omega_\pm^2 d\sigma_\pm^2. \tag{2.47}$$

Here, and in what follows $u_\pm \equiv u_\pm(\theta)$. The metric $d\sigma_+^2$ coincides with the metric on the distorted Schwarzschild black hole horizon surface (1.82). The dimensionless areas of the horizon surfaces are equal to 4π. The metrics $d\sigma_+^2$ and $d\sigma_-^2$ are related to each other by the transformation

$$u_+ \longleftrightarrow -u_-, \tag{2.48}$$

which according to (1.69) implies the following *duality relations* between the outer and the inner horizons

$$c_{2n} \longleftrightarrow -c_{2n}\,, \quad c_{2n+1} \longleftrightarrow c_{2n+1}. \tag{2.49}$$

These duality relations are exactly the same as the duality relations (1.115), (1.116) between the horizon and the singularity of the distorted Schwarzschild black hole (cf. Appendix A).

Thus, the metrics $dS_\pm^2$ are identical for distortions which have only odd multipole moments. The derived duality relations imply, in particular, that the inner (Cauchy) horizon of a distorted charged black hole solution obtained by the Harrison-Ernst transformation is regular, if the outer horizon is regular. This conclusion and its generalization to the case of rotating and charged black holes was proven recently in [5, 73].

2.5 Gaussian curvature

In this section we discuss the geometry of the distorted horizon surfaces. The gaussian curvature is a natural measure of the intrinsic curvature of a 2D surface (see, e.g., [38, 89, 114, 122, 123]). It is equal to 1/2 of its scalar curvature. For the

metrics (2.46) the Gaussian curvature is given by

$$K_{\pm} = e^{\mp 2u_{\pm}} \left(1 \pm u_{\pm,\theta\theta} \pm 3\cot\theta u_{\pm,\theta} - 2u_{\pm,\theta}^2\right). \tag{2.50}$$

The dimensional Gaussian curvatures associated with the metrics (2.47) are

$$K^{(\pm)} = \Omega_{\pm}^{-2} K_{\pm}. \tag{2.51}$$

We shall illustrate our analysis of the charged distorted black hole horizon surfaces considering simple examples of the lowest order multipole distortions. Namely, we shall consider quadrupole and octupole distortions for which the corresponding functions $u_{\pm}$ read

$$u_{\pm} \;\; = \;\; -c_2 \sin^2\theta\,, \;\; u_{\pm} = \mp c_3 \sin^2\theta\cos\theta. \tag{2.52}$$

Here, c_2 and c_3 are the quadrupole and the octupole moments, respectively.

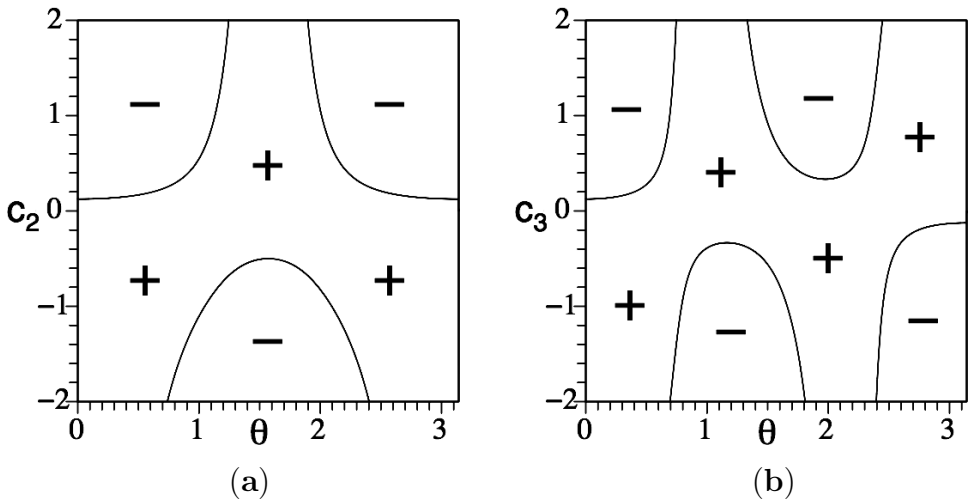

Figure 2.3: Regions of positive and negative Gaussian curvature for the outer horizon surface. Plot (**a**) illustrates the regions for different values of the quadrupole moment. Plot (**b**) illustrates the regions for different values of the octupole moment. Curves separating these regions correspond to zero Gaussian curvature.

Regions of positive and negative Gaussian curvature for different values of the quadrupole and octupole moments, for the outer horizon surface, are presented in Figure 2.3. From Figure 2.3(**a**) we see that for the quadrupole distortion regions of negative Gaussian curvature near the black hole poles ($\theta = 0, \pi$) correspond to

high positive values of c_2, and near its equator ($\theta = \pi/2$) to high negative values of c_2. Using Eqs. (2.50), (1.51), (1.69), and the auxiliary expressions

$$u_{\pm,\theta}(\theta) = -\sum_{n\geq 0}(\pm 1)^n c_n n \sin\theta \cos^{n-1}\theta, \tag{2.53}$$

$$u_{\pm,\theta\theta}(\theta) = \sum_{n\geq 0}(\pm 1)^n c_n n \cos^{n-2}\theta [n\sin^2\theta - 1], \tag{2.54}$$

we derive

$$K_{\pm}|_{\theta=0} = 1 \mp 2u^{(2)}_{\pm}, \;\; K_{\pm}|_{\theta=\pi} = 1 \mp 2u^{(2)}_{\mp}, \tag{2.55}$$

$$K_{\pm}|_{\theta=\pi/2} = e^{\pm 2(u_0 - c_0)}(1 \pm 2c_2 - 2c_3^2). \tag{2.56}$$

Here,

$$u^{(2)}_{\pm} = 2\sum_{n\geq 0}(\pm 1)^n c_n n, \tag{2.57}$$

in accordance with expression (1.93). Thus, the sign of the Gaussian curvature strictly depends on the distortion field. Using these expressions we see that for the quadrupole distortion Gaussian curvature of the outer horizon surface is positive at the poles for $c_2 < 1/8$, and on the equator for $c_2 > -1/2$. For $c_2 < -1/2$ we have a dumbbelled-shaped horizon. According to the duality relations (2.49) regions of positive and negative Gaussian curvature of the inner horizon surface can be constructed by mirror reflection of Figure 2.3 with respect to the line $c_2 = 0$.

Figure 2.3(**b**) illustrates that there is a symmetry between the regions of positive and negative Gaussian curvature and signs of the octupole moment. Namely, the transformation $c_3 \to -c_3$, $\theta \to \pi/2 - \theta$ does not change the figure. Using Eq. (2.55) we see that for $c_3 > 1/8$ Gaussian curvature is negative on the north pole and positive on the south pole, whereas for $c_3 < -1/8$ it is negative on the south pole and positive on the north. In addition, there are the regions of negative Gaussian curvature near the 'tropics' ($\pm 23^\circ 26' 22''$ from the equator), i.e., near $\theta_- \approx 1.165$ (corresponding to $\approx 23^\circ 16' 39''$ from the equator) for $c_3 < -0.333$, and $\theta_+ \approx 1.977$ (corresponding to $\approx -23^\circ 16' 39''$ from the equator) for $c_3 > 0.333$. According to the duality relations (2.49), the Gaussian curvature of the inner horizon surface is identical to that of the outer horizon surface. The dimensionless Gaussian curvature of the outer horizon surface for certain values of the quadrupole and octupole moments is plotted in Figure 2.4.

As we shall see in Section 2.8, the curvature and the electromagnetic field invariants calculated on and at the vicinity of the black hole horizons are expressed in terms of the corresponding Gaussian curvatures and their derivatives with respect to the angular coordinate θ.

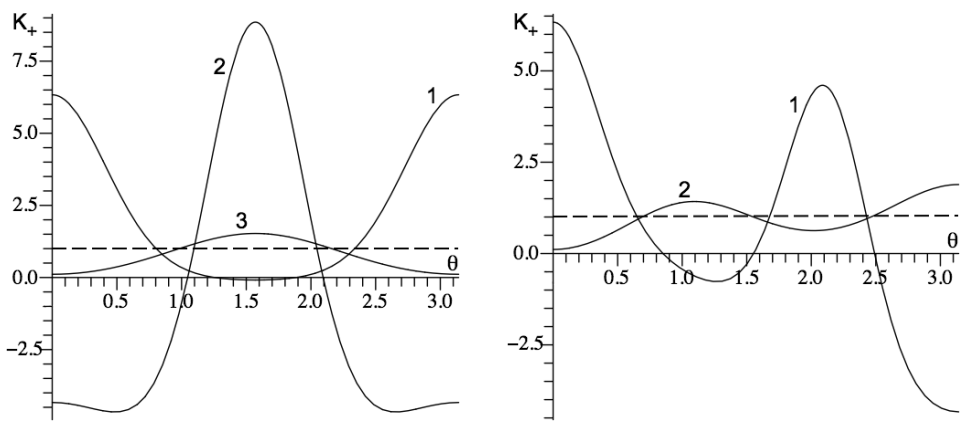

(**a**) (**b**)

Figure 2.4: Dimensionless Gaussian curvature K_+ of the outer horizon surface. (**a**) Quadrupole distortion: $c_2 = -2/3$, line (1), $c_2 = 2/3$, line (2), and $c_2 = 1/9$, line (3). (**b**) Octupole distortion: $c_3 = -2/3$, line (1), and $c_3 = 1/9$, line (2). The dashed horizontal lines at $K_+ = 1$ correspond to the RN black hole.

2.6 Embedding

To visualize the distorted horizon surfaces, we present their isometric embedding into a flat 3D space, in a way similar to the isometric embedding of the horizon surface of the distorted Schwarzschild black hole (see subsection 1.6.1). To construct the embedding we consider an axisymmetric 2D surface parametrized as follows:

$$\rho = \rho(\theta)\,, \quad z = z(\theta). \tag{2.58}$$

Let us embed this surface into a flat 3D space with the metric in cylindrical coordinates (z, ρ, ϕ):

$$dl^2 = \epsilon dz^2 + d\rho^2 + \rho^2 d\phi^2, \tag{2.59}$$

where for Euclidean space $\epsilon = 1$, and for pseudo-Euclidean space $\epsilon = -1$. The geometry induced on the surface is given by

$$dl^2 = (\epsilon z_{,\theta}^2 + \rho_{,\theta}^2) d\theta^2 + \rho^2 d\phi^2. \tag{2.60}$$

Matching the metrics (2.46) and (2.60) we derive the following embedding map:

$$\rho = e^{\mp u_\pm} \sin\theta\,, \quad z = \int_\theta^{\pi/2} \mathcal{Z}\, d\theta, \tag{2.61}$$

$$\mathcal{Z}^2 = \epsilon e^{\pm 2u_\pm}[1 - e^{\mp 4u_\pm}(\cos\theta \mp u_{\pm,\theta}\sin\theta)^2]. \tag{2.62}$$

From Eq. (2.62) we see that if the expression in the square brackets is negative, an isometric embedding into 3D Euclidean space using such a surface of revolution is not possible, and we should take $\epsilon = -1$.

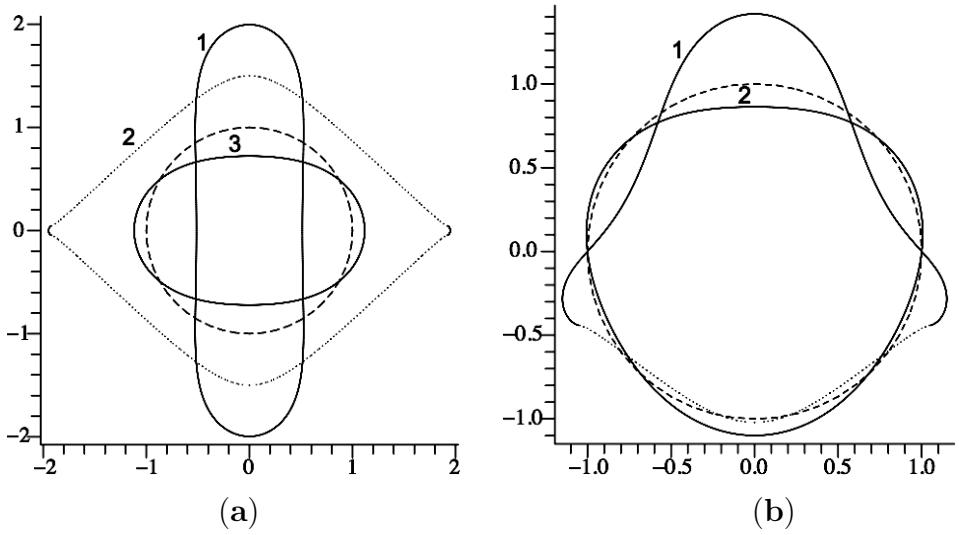

Figure 2.5: Shape of the outer horizon surface. The shape curves are shown in the (ρ, z) plane. (**a**) Quadrupole distortion: $c_2 = -2/3$, line (1), $c_2 = 2/3$, line (2), and $c_2 = 1/9$, line (3). (**b**) Octupole distortion: $c_3 = -2/3$, line (1), and $c_3 = 1/9$, line (2). Regions embedded into pseudo-Euclidian space are illustrated by the doted lines. The dashed circles of radius 1 correspond to the RN black hole.

According to the duality relations (2.49), it is enough to consider embedding of the outer horizon surface only. The shape curves of the outer horizon surface are presented in Figure 2.5. The embedding diagrams for the outer horizon surface can be obtained by rotation of the curves around the vertical axis of symmetry lying in the plane of the figure, parallel to the z axis. Note that the change in sign from '+' to '−' of the quadrupole moment corresponds to a deformation of the rotational curve from oblate to prolate and vice versa. This transformation corresponds to the duality relations (2.49) between the outer and inner horizon

surfaces. The change in sign of the octupole moment corresponds to an overturn of the rotational curve preserving its shape.

2.7 Free fall from the outer to the inner horizon

In Section 1.5 we studied how distortion of the Schwarzschild black hole affects proper time of a free fall from the black hole horizon to its singularity. It is interesting to check how the distortion changes the maximal proper time of free fall of a test particle from the outer to the inner horizon of the distorted RN black hole. Let us consider motion of a test particle of zero angular momentum which moves from the outer to the inner horizon along the axis of symmetry. Free fall from the north pole corresponds to $\theta = 0$, and free fall from the south pole corresponds to $\theta = \pi$. We use metric (2.25) with dS_+^2. Using Eq. (1.53) we derive the proper time of the free fall:

$$\tau(E) = \Omega_+ \int_{-1}^{+1} \frac{\Delta_+^{1/2} e^{-\mathcal{U}} d\eta}{(\Omega_+^{-2}\Delta_+ e^{-2\mathcal{U}} E^2 + 1 - \eta^2)^{1/2}}\Bigg|_{\theta=0,\pi}, \tag{2.63}$$

where E is the energy of the particle,

$$E = \kappa_+ \Omega_+^2 \frac{\eta^2 - 1}{\Delta_+} e^{2\mathcal{U}} \frac{dT_+}{d\tau}. \tag{2.64}$$

The maximal proper time corresponds to $E = 0$. Using the coordinate transformation (2.42) and applying the boundary values (1.72) we derive the maximal proper time for the free fall

$$\tau_{max} = \tau(0) = \tau_+ \Omega_+, \tag{2.65}$$

where Ω_+ is given by (2.27), and the dimensionless time τ_+ is

$$\tau_+ = \int_0^\pi \frac{d\psi}{2} \left[(\cos\psi + 1)e^{-u(\psi)} - \delta e^{u(\psi)}(\cos\psi - 1)\right]. \tag{2.66}$$

Here, $u(\psi) = u_+(\psi)$ for the fall from the north pole, and $u(\psi) = u_-(\psi)$ for the fall from the south pole. For the RN black hole we have $\tau_+ = \pi/(1+p)$, and $\tau_{max} = \pi M$, that is exactly the same as the maximal proper time for free fall from event horizon to the singularity of the Schwarzschild black hole of mass M ([94], p. 836).

In the case of the quadrupole distortion (2.52), the integral in (2.66) can be

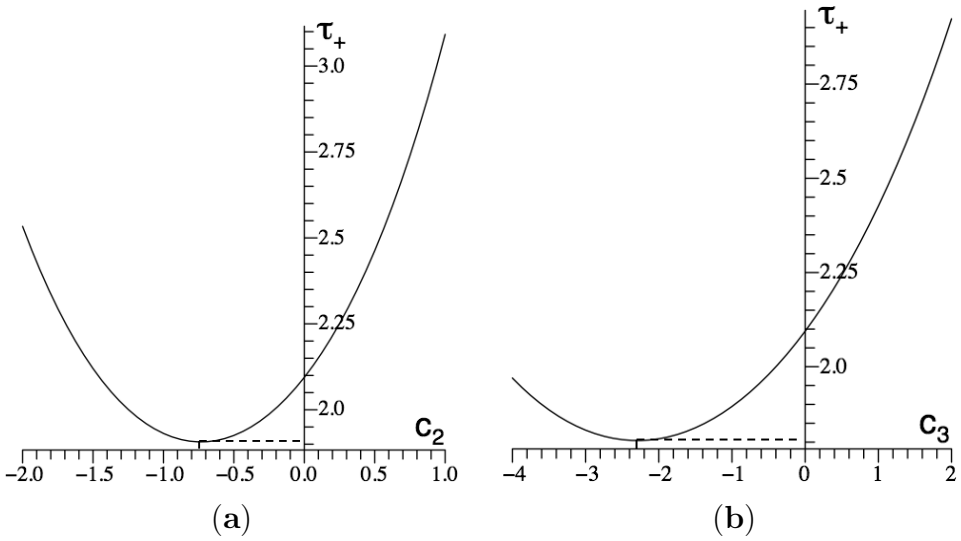

Figure 2.6: Free fall along the axis of symmetry from the outer to the inner horizon surface for $p' = 1/2$. (**a**) Dimensionless proper time τ_+ for different values of the quadrupole moment c_2. Here, the minimal value of the dimensionless proper time $\tau_{+min} \approx 1.91$ corresponds to $c_{2min} \approx -0.734$. (**b**) Dimensionless proper time τ_+ for different values of the octupole moment c_3, for the fall from the north pole. Here, the minimal value of the dimensionless proper time $\tau_{+min} \approx 1.80$ corresponds to $c_{3min} \approx -2.29$, where c_{3min} does not depend on the value of p'. For the RN black hole $\tau_+ = 2\pi/3 \approx 2.09$.

calculated analytically:

$$\tau_+ \;=\; \frac{\pi}{2} I_0(c_2/2)[e^{c_2/2} + \delta e^{-c_2/2}], \tag{2.67}$$

where $I_0(x)$ is the modified Bessel function (see, e.g., [3], p. 374). Note, that because of the reflection symmetry of the horizon surfaces with respect to the plane $\theta = \pi/2$ the proper time is the same for the fall from the north and the south poles. For the octupole distortion we evaluate the integral numerically. From expressions (2.52) and (2.66) we see that the change in sign of the octupole moment corresponds to the change of the poles as the starting points of the fall. The dimensionless proper time calculated for $p' = 1/2$ is presented in Figure 2.6.

2.8 Spacetime invariants

For distorted vacuum black holes there exists a remarkable relation between the Kretschmann scalar calculated on the surface of the event horizon $\mathcal{K}^{(+)}$ and the Gaussian curvature of the horizon $K^{(+)}$ calculated at the same point (see Eq. (1.99) representing such a relation in dimensionless form)

$$\mathcal{K}^{(+)} = 12K^{(+)^2}. \tag{2.68}$$

The proof of this relation for a more general case of electrostatic solution is given in Appendix E. This relation shows that the 4D curvature invariant of the spacetime calculated on the black hole horizon is correlated with the shape of the horizon surface. In a region where the horizon is sharper the 4D curvature invariant is larger than in a region where the horizon is smoothed out. In order to prove the property (2.68) one uses the fact that the horizon $\mathcal{H}^{(+)}$ surface is a *totally geodesic* surface.

The general analysis by Boyer [13], and, in particular, his conclusion saying that a bifurcate Killing horizon contains a totally geodesic 2D surface, which is in fact independent of the field equations, can be applied to the case of the charged distorted black hole. For this reason one can expect the existence of a relation similar to (2.68) and generalizing the latter (see Appendix E for details). In this section, we discuss this problem.

First of all, let us emphasize that in the presence of the electromagnetic field $F_{\alpha\beta}$ there exist an additional 4D invariant $F^2 = F_{\alpha\beta}F^{\alpha\beta}$ characterizing the strength of the field. For the distorted black hole the calculations give the following value of this invariant on the outer horizon [see Eqs. (2.38), (2.39), (2.40), (1.71) and (1.73)]

$$F^{(+)^2} = -\frac{2}{M'^2}\frac{(1-p')}{(1+p')^3}, \tag{2.69}$$

where M' and p' are defined by Eq. (2.31) and Eq. (2.32) respectively. Note, that $F^{(+)^2}$ is a constant over the outer horizon. The minus sign on the right-hand side reflects the fact that we are dealing with an electric (not magnetic) field. The Kretschmann scalar $\mathcal{K}$ and the Weyl invariant $\mathcal{C}^2$ are related as follows:

$$\mathcal{K} = \mathcal{C}^2 + 2(F^2)^2. \tag{2.70}$$

In the presence of matter, in order to characterize the 'strength' of the gravitational field, it is more convenient to use the Weyl invariant. The calculations presented in Appendix E give for the Weyl invariant on the event horizon the following

expression [cf. Eqs. (E.40) and (E.41)]:

$$\mathcal{C}^{2(+)} = 12\left[K^{(+)} - \frac{1}{2}F^{(+)2}\right]^2 . \tag{2.71}$$

It is evident that in vacuum, when F^2 vanishes and the Kretschmann invariant coincides with the Weyl invariant, this relation reduces to Eq. (2.68). The second term in the square brackets is constant on the horizon [see Appendix E, and Eq. (2.76) below]. Using Eqs. (2.36) and (2.27) we can present the expression in the square brackets in the following form

$$K^{(+)} - \frac{1}{2}F^{(+)2} = \frac{4K^{(+)}|_{p=1}}{(1+p)^2} - \frac{1}{2}F^{(+)2}, \tag{2.72}$$

where $K^{(+)}|_{p=1}$ is the Gaussian curvature of the horizon surface of a distorted Schwarzschild black hole. Thus, the Gaussian curvature of the horizon surface of a distorted RN black hole is related to that of a distorted Schwarzschild black hole by the linear transformation (2.72).

The relations similar to (2.69) and (2.71) are valid for the inner horizon,

$$F^{(-)2} = -\frac{2}{M'^2}\frac{(1+p')}{(1-p')^3}, \tag{2.73}$$

$$\mathcal{C}^{2(-)} = 12\left[K^{(-)} - \frac{1}{2}F^{(-)2}\right]^2 . \tag{2.74}$$

Using Eq. (2.70) we can calculate the ratio of the Kretschmann invariants on the black hole horizons:

$$k = \frac{\mathcal{K}^{(+)}}{\mathcal{K}^{(-)}} = \delta^4\frac{3(K_+ + \delta)^2 + 2\delta^2}{3(K_- + \delta^{-1})^2 + 2\delta^{-2}}, \tag{2.75}$$

where δ is defined by Eq. (2.30). This ratio calculated for $p' = 1/2$ is presented in Figure 2.7. The behavior of the curves is very similar to those for the Gaussian curvature illustrated in Figure 2.4.

Finally, we present the expressions for the curvature and the electromagnetic field invariants at the vicinity of the black hole horizons. We use the expressions (E.44), (E.40) and (E.45) given in Appendix E. The expansion of the electromagnetic field invariant near the black hole horizons reads

$$F_\pm^2 = -2\delta^{\pm1} \pm 4\delta^{\pm1}e^{\pm2u_\pm}(K_\pm - \delta^{\pm1})(\eta \mp 1) + \dots . \tag{2.76}$$

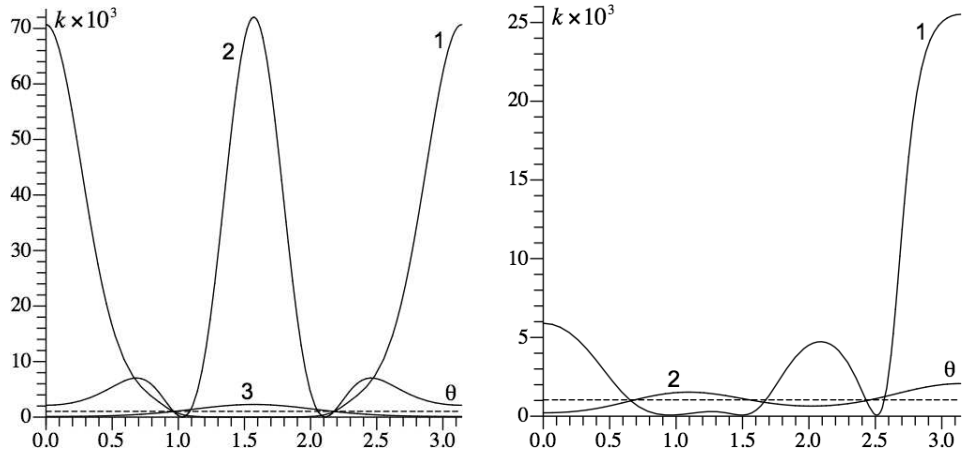

Figure 2.7: Ratio k for $p' = 1/2$. Plot (**a**) illustrates the ratio for the quadrupole distortion of $c_2 = -2/3$, line (1), $c_2 = 2/3$, line (2) and $c_2 = 1/9$, line (3). Plot (**b**) illustrates the ratio for the octupole distortion of $c_3 = -2/3$, line (1), and $c_3 = 1/9$, line (2). The dashed horizontal line corresponds to the RN black hole.

The expansion of the Weyl invariant near the black hole horizons is

$$\begin{aligned} \mathcal{C}^2_{\pm} &= 12K^2_{e\pm} \mp 4\left(3K^2_{e\pm}[3K_{\pm} - 2\delta^{\pm 1}]e^{\pm 2u_{\pm}} - 2[K_{\pm,\theta}]^2\right. \\ &+ \left. 3K_{e\pm}[K_{\pm,\theta\theta} + \cot\theta K_{\pm,\theta}]\right)(\eta \mp 1) + \dots , \end{aligned} \tag{2.77}$$

where $K_{e\pm} = (K_{\pm} - \delta^{\pm 1})$.

2.9 Discussion

In this chapter, we studied the interior of a distorted, static, axisymmetric, electrically charged black hole. The corresponding metric was derived by the Harrison-Ernst transformation applied to the metric of a distorted, static, axisymmetric vacuum black hole, whose interior was discussed in Chapter 1. We established the special duality relations between the properties of the inner and the outer horizons of the distorted charged black hole. These duality relations allow one to make a conclusion about the inner (Cauchy) horizon structure, which is based on the structure of the outer (event) horizon of the black hole. In particular, regions of positive and negative Gaussian curvature and its values on the outer horizon surface are correlated with those on the inner horizon surface. There is a correlation

between the shapes of the horizon surfaces as well.

We derived expansion of the curvature and electromagnetic field invariants near the black hole horizons, which is expressed in terms of the Gaussian curvature, electrostatic field, and their derivatives calculated on the horizon surfaces. Thus, the established duality relations show that the spacetime geometry near the inner (Cauchy) horizon is correlated with the spacetime geometry near the outer (event) horizon. This implies that if the distortion leaves the outer horizon regular, the inner horizon remains regular as well.

The duality between the outer and the inner horizons seems important. Apparently, according to the mass inflation phenomenon [107] such duality breaks in the case of dynamical perturbation of the RN black hole. Namely, due to the presence of the outgoing flux the inner apparent horizon and the Cauchy horizon become separated. The infinite grow of the mass parameter induced by the blueshift of the ingoing flux on the Cauchy horizon is not canceled by the redshift of the ingoing flux on the apparent horizon. As a result, the Cauchy horizon becomes singular. This does not happen in the case of static, axisymmetric distortion. One may think of the static distortion in the dynamical region between the black hole horizons as represented by 'standing' waves. According to the duality relations between the horizons, initial and boundary values of the waves should be dual as well.

Quite possibly, the axisymmetric, static distortion due to remote charged masses and fields cannot affect much the interior of a charged black hole. In such a situation nothing enters, or leaves (through the Cauchy horizon into other 'universes') the black hole. Thus, the black hole inner horizon remains regular due to such a type of distortion. Nevertheless, as our analysis shows, such 'serene' distortion can in fact deform the interior of the black hole to create regions of high local curvature. Moreover, the distortion noticeably affects the maximal proper time of free fall of a test particle moving along the axis of symmetry in the black hole interior. An important question of whether the Cauchy horizon of an electrically charged black hole is regular for an arbitrary static, external distortion remains open. It would be interesting to study a general class of electromagnetic distortion fields, as well as more general class of rotating charged distorted black holes which admit the Weyl form of the metric (see, e.g., [16]).

Chapter 3

5D electrically charged black string

3.1 Introduction

In attempts to resolve the hierarchy problem, the existence of large extra spatial dimensions was proposed in modern theoretical models [6, 8]. The existence of large compact extra dimensions opens an interesting possibility of mini black hole production in future LHC experiments (see, e.g., [26, 53, 125]). In addition, in spacetimes with large compact extra dimensions, a large variety of topologically different black objects may exists: black holes, black rings, black branes, black strings, etc. (see, e.g., [66]). The study of such objects, especially topological phase transitions between them, is a subject of high interest.

In this chapter we study static electric black strings in 5D spacetime with one large compact dimension and compare their thermodynamical and dynamical properties with static magnetic black strings. The topology of the horizon of the black string is different from the spherical topology of a black hole solution, which is another possible topological phase. A vacuum black string solution can be obtained from a lower dimensional, spherically symmetric, static, vacuum black hole solution by adding a flat compact extra dimension. In the case of more than one, say p, extra dimensions, the solution is called a black p-brane. Simple analysis shows that for a given size of extra dimensions, there exists a critical value of the mass M_{cr}. If $M > M_{cr}$, the entropy of the black string or black brane is larger than the entropy of the black hole, while for $M < M_{cr}$ the situation is opposite.

Based on this simple argument, Gregory and Laflamme (GL) [57] came to a conclusion that a black string (brane) must be unstable if its mass is smaller than some critical value. Studying S-wave gravitational perturbations of black strings, they discovered the classical instability of these objects. Namely, they obtained a dispersion relation between the imaginary part Ω of the frequency, and the wave

number k of the perturbation field mode, which clearly illustrates the instability. The dispersion relation allows one to find a rate of decay corresponding to a given wave number k. The instability starts at the special value k_{cr}. Ω vanishes for this threshold mode. Positive values of Ω correspond to values of the wave numbers smaller than k_{cr}. Finally, the zero-value wave number corresponds to $\Omega = 0$, which indicates the stability of the D-dimensional Schwarzschild-Tangherlini black hole.

The existence of the critical (maximal) wave number k_{cr} in the instability spectrum corresponds to the minimal wavelength $\lambda_{cr} = 2\pi/k_{cr}$ of the perturbation threshold mode. The modes with smaller values of the wavelength are stable. This behavior is similar to the classical Jeans instability (see [60, 66, 82] and [121], p. 562). If there exist compact extra spatial dimensions with a size smaller than the minimal wavelength L_{cr}, then unstable modes cannot fit into the compact dimensions, and the instability does not arise. In the opposite case, compactified black string (brane) solutions are unstable.

The GL instability is a generic property of black objects in spacetime with compact extra dimensions. This effect was studied by many authors. For example, in [58] the GL instability for a dilaton black string with magnetic charge was demonstrated. The instability in magnetically charged black strings was studied in [95]. It was found that for a certain range of magnetic charge values, the string becomes stable, if compared with a neutral one. The instability in boosted strings was studied in [75]. It was found that in the frame comoving with the string, results are largely unchanged if compared with a static black string. However, in the frame where the string is moving along its length, the instability strongly depends on the velocity of the string. For example, the threshold mode appears as a wave traveling with the boost velocity along the string. New AdS black string solutions were discovered in [91]. Analysis of the GL instability for these solutions showed that small AdS black strings are unstable; however, black strings with relatively large values of the event horizon radius, as well as topological black strings, are classically stable [17].

Numerical evolution of a perturbed, unstable black string was studied in [24]. It was found that at an intermediate time of the evolution a nonuniform black string forms. This string is reminiscent of a distorted spherical black hole connected to a thin black string. Topological transitions between black strings in 5D and 6D, and the corresponding Kaluza-Klein black holes, were studied in [86]. It was found that the black string and the black hole phases merge at a topology-changing transition. Large D asymptotics of a marginally stable black string were studied in [88]. Detailed reviews on the phase transitions between black strings and black holes and the GL instability issue are given in [87] and [66], respectively.

There is an interesting relation between the dynamical instability of a black brane and off-shell instability of the corresponding Euclidean black hole. For example, the threshold unstable mode of a neutral black brane corresponds to the

Euclidean Schwarzschild black hole negative mode [60]. Namely, $k_{cr}^2 = -\lambda$, where λ is the negative eigenvalue of the spectral problem related to the Euclidean black hole off-shell perturbations. A general analysis of such relations is given in [111]. Negative modes of a 4D Reissner-Nordström black hole with magnetic charge corresponding to the threshold unstable mode of a 5D black string were found in [96].

In a general case, the size of extra compact dimensions is a spacetime parameter which is fixed at an asymptotically flat region. However, the proper length of the extra compact dimensions at the vicinity of a black object generally depends on the matter and fields present. The matter or fields may increase or decrease the local size of the compact dimensions, changing the black object instability spectrum. This effect is illustrated on several types of black strings. For example, the presence of magnetic and dilaton fields tends to stabilize the black string [58]. A similar behavior of the critical wave number for a black string in a spacetime of arbitrary dimension $D \geqslant 5$ with magnetic or electric charge was observed in [95] and [112], respectively.

Here, we shall study the GL instability of an electrically charged 5D black string. The corresponding dimensionally reduced solution is S-dual to the dimensionally reduced solution for a 5D black string with a magnetic charge [95]. We consider static S-wave perturbation of the charged black string and search for the threshold mode. The existence of the threshold mode implies existence of the instability spectrum. We construct a critical curve in a topological phase transition diagram. The curve corresponds to a nonuniform black string and separates the charged black string phase and the corresponding charged Kaluza-Klein black hole phase. The shape of the curve illustrates that electric charge tends to destabilize the black string. Similar behavior can be inferred from the global thermodynamic equilibrium condition between the charged black string and charged black hole. The main results discussed here were published in [46].

3.2 5D charged black string solution

3.2.1 5D theory

In this section, we describe a solution for 5D electrically charged, compactified black string. Let us consider the following action

$$S = \frac{1}{16\pi G_{(5)}} \int_0^L dz \int dx^4 \sqrt{-g} \left(R - \frac{1}{4} F^2 \right), \tag{3.1}$$

where

$$F_{\mu\nu} = \nabla_\mu A_\nu - \nabla_\nu A_\mu. \tag{3.2}$$

Here A_μ is the 5D electromagnetic vector potential, and L is the size of the compact dimension. The corresponding Einstein-Maxwell equations read

$$R_{\mu\nu} - \frac{1}{2} g_{\mu\nu} R = \frac{1}{2} T^{(em)}_{\mu\nu}, \tag{3.3}$$

$$\nabla_\nu F^{\mu\nu} = 0\,, \;\; \nabla_{[\lambda} F_{\mu\nu]} = 0. \tag{3.4}$$

The 5D electromagnetic field energy-momentum tensor is given by

$$T^{(em)}_{\mu\nu} \;\; = \;\; F_\mu{}^\lambda F_{\nu\lambda} - \frac{1}{4} g_{\mu\nu} F^2. \tag{3.5}$$

Here and in what follows, ∇_μ denotes a covariant derivative defined with respect to the 5D metric $g_{\mu\nu}$, whereas a comma stands for a partial derivative.

In a general case, the electric charge Q associated with the d-form $F_{(d)}$ is defined as follows:

$$Q \;\; = \;\; (-1)^{1+d(D-d)} \int_{V_{(D-d)}} \star F_{(D-d)}, \tag{3.6}$$

where the Hodge dual to $F_{(d)}$ is defined by

$$\star F^{\mu_1 \ldots \mu_{(D-d)}} = \frac{\varepsilon^{\mu_1 \ldots \mu_{(D-d)} \nu_1 \ldots \nu_d}}{d! \sqrt{-g}} F_{\nu_1 \ldots \nu_d}. \tag{3.7}$$

The magnetic charge P is defined by

$$P \;\; = \;\; \int_{V_{(d)}} F_{(d)}. \tag{3.8}$$

The integral over the d-form $F_{(d)}$ and the corresponding volume element $V_{(d)}$ are defined as follows:

$$\int_{V_{(d)}} F_{(d)} \;\; = \;\; \int_{V_{(d)}} F_{|\mu_1 \ldots \mu_d|} dx^{\mu_1} \ldots dx^{\mu_d}\,, \;\; V_{(d)} = \int_{V_{(d)}} \star 1, \tag{3.9}$$

where $|\mu_1 \ldots \mu_d| = \mu_1 < \ldots < \mu_d$ means proper orientation, and $\varepsilon^{|\mu_1 \ldots \mu_{(D-d)} \nu_1 \ldots \nu_d|} = +1$. In our case $d = 2$.

The Komar mass of a black object is defined by (see, e.g., [98])

$$M = \frac{1}{16\pi G_{(D)}} \frac{D-2}{D-3} \int_{V^\infty_{(D-2)}} d^{D-2} \Sigma_{\mu\nu} \nabla^\mu k^\nu, \tag{3.10}$$

where k^μ is the timelike Killing vector normalized at spatial infinity as $k^\mu k_\mu = -1$. Another definition of the mass of a black object in spacetime with compact dimensions was given in [68].

For a spacetime with compact extra dimensions of asymptotic size L, the D-dimensional and 4D gravitational constants are related as follows

$$G_{(D)} = G_{(4)} L^{D-4}. \tag{3.11}$$

We consider a 5D metric of the following form:

$$ds^2 = -f_1 dt^2 + \frac{dr^2}{f_1 f_2} + f_2 dz^2 + f_3(d\theta^2 + \sin^2\theta d\phi^2), \tag{3.12}$$

where $f_i = f_i(r)$, $i = 1, 2, 3$, and z is the coordinate of the compact dimension of size L. In the next subsection, we shall see that this metric can be derived by oxidizing (uplifting) a 4D dimensional solution, which does not depend on the compact coordinate z, to the 5D spacetime of the charged black string [102]. Such a 4D solution is related to solutions of the so-called a-model. In our case, this is a 4D electrically charged dilaton black hole.

3.2.2 *a*-model

Here, we discuss the 4D a-model solution representing a dilaton black hole with electric charge. Let us start from the 4D a-model action [102]

$$\bar{S} = \frac{1}{16\pi G_{(4)}} \int d^4x \sqrt{-\bar{g}} \left(\bar{R} - \frac{1}{2}(\bar{\nabla}\varphi)^2 - \frac{1}{4} e^{-2a\varphi} \bar{F}^2 \right), \tag{3.13}$$

where $\bar{R}$ is the Ricci scalar of the 4D spacetime, φ is the dilaton field, and a is the dilaton-electromagnetic field coupling constant. The electromagnetic field tensor is

$$\bar{F}_{ij} = \bar{\nabla}_i \bar{A}_j - \bar{\nabla}_j \bar{A}_i, \tag{3.14}$$

where $\bar{A}_i$ is the 4D electromagnetic vector potential. Here and in what follows, $\bar{\nabla}_i$ denotes a covariant derivative defined with respect to the 4D metric $\bar{g}_{ij}$, and $i, j, k = 0, 1, 2, 3$.

The Einstein-Maxwell-dilaton equations read ($16\pi G = c = 1$)

$$\bar{R}_{ij} - \frac{1}{2}\bar{g}_{ij}\bar{R} = \frac{1}{2}\left(\bar{T}^{(d)}_{ij} + e^{-2a\varphi} \bar{T}^{(em)}_{ij} \right), \tag{3.15}$$

$$\bar{\nabla}_j \left(e^{-2a\varphi} \bar{F}^{ij} \right) = 0\,, \;\; \bar{\nabla}_{[k} \bar{F}_{ij]} = 0, \tag{3.16}$$

$$\bar{\nabla}^2 \varphi + \frac{a}{2} e^{-2a\varphi} \bar{F}^2 = 0. \tag{3.17}$$

Here the dilaton and the 4D electromagnetic field energy-momentum tensors are given by

$$\bar{T}^{(d)}_{ij} = (\bar{\nabla}_i\varphi)(\bar{\nabla}_j\varphi) - \frac{1}{2}\bar{g}_{ij}(\bar{\nabla}\varphi)^2, \tag{3.18}$$

$$\bar{T}^{(em)}_{ij} = \bar{F}_i{}^k\bar{F}_{jk} - \frac{1}{4}\bar{g}_{ij}\bar{F}^2, \tag{3.19}$$

respectively.

We are interested in static, spherically symmetric solutions of the equations. One of such solutions is a dilaton black hole with electric charge. The corresponding metric is [102]

$$d\bar{s}^2 = -\frac{r^{v-1}(r-w)}{(r+h)^v}dt^2 + \frac{(r+h)^v}{r^{v-1}(r-w)}dr^2 + r^{2-v}(r+h)^v(d\theta^2+\sin^2\theta d\phi^2), \tag{3.20}$$

where $v = 2/(1+4a^2)$. The electromagnetic vector potential and the dilaton field are given by

$$\bar{A}_i = \mp\frac{\sqrt{vh(4w+h)}}{\sqrt{2}(r+h)}\delta_i{}^t, \quad \varphi = -2av\ln\left(1+\frac{h}{r}\right), \tag{3.21}$$

respectively. In the particular case of zero coupling constant, $a = 0$, the solution is the 4D Reissner-Nordström black hole [see Eq. (2.1)].

To proceed with the oxidation [102], let us consider the 5D metric (3.12) in the following form:

$$ds^2 = e^{-\frac{\varphi}{\sqrt{3}}}d\bar{s}^2 + e^{\frac{2\varphi}{\sqrt{3}}}dz^2, \tag{3.22}$$

where $d\bar{s}^2$ is the 4D metric (3.20). The following relations between the 5D and the 4D objects hold:

$$R = e^{\frac{\varphi}{\sqrt{3}}}\left(\bar{R} - \frac{1}{2}(\bar{\nabla}\varphi)^2 + \sqrt{3}\bar{\nabla}^2\varphi\right), \tag{3.23}$$

$$\sqrt{-g} = e^{-\frac{\varphi}{\sqrt{3}}}\sqrt{-\bar{g}}, \quad F^2 = e^{\frac{2\varphi}{\sqrt{3}}}\bar{F}^2. \tag{3.24}$$

Applying these relations to the action (3.1), integrating over z, and using the relationship (3.11) between the gravitational constants in 5D and 4D spacetimes, we derive

$$\bar{S} = \frac{1}{16\pi G_{(4)}}\int dx^4\sqrt{-\bar{g}}\left(\bar{R} - \frac{1}{2}(\bar{\nabla}\varphi)^2 - \frac{1}{4}e^{\frac{\varphi}{\sqrt{3}}}\bar{F}^2\right). \tag{3.25}$$

This is exactly the 4D action (3.13) with $a = -1/(2\sqrt{3})$.

3.2.3 5D electrically charged black string

An oxidation of the dilaton black hole with electric charge to a 5D spacetime gives us the electric black string solution (3.12) (see, e.g., [86], and [112] for $D = 5$) with

$$f_1 = \frac{r(r-w)}{(r+h)^2}\,,\;\; f_2 = 1+\frac{h}{r}\,,\;\; f_3 = r(r+h)\,,\;\; A_\mu = \mp\frac{\sqrt{3h(w+h)}}{r+h}\delta_\mu{}^t. \quad (3.26)$$

Note that for the 5D black string and the 4D black hole solutions $r > 0$, $h > 0$, and the corresponding event horizons are defined by $r = w > 0$. The parameters h and w can be expressed in terms of the mass and the electric charge of the black string.

The definition (3.10) and the relation (3.11) give us the black string mass, which in our units is

$$M \;=\; 6\pi(w+2h). \quad (3.27)$$

Using the definition of electric charge (3.6) for $d = 2$, we derive

$$Q \;=\; \pm 4\pi L\sqrt{3h(w+h)}. \quad (3.28)$$

Expressions (3.27) and (3.28) give

$$w \;=\; \frac{1}{6\pi}\sqrt{M^2-3(Q/L)^2}\,,\;\; h = \frac{1}{12\pi}\left(M-\sqrt{M^2-3(Q/L)^2}\right). \quad (3.29)$$

Thus, the magnitude of the black string electric charge is defined within the range

$$0 \leqslant |Q| \leqslant \frac{ML}{\sqrt{3}}. \quad (3.30)$$

Calculating the energy-momentum tensor components in a local tetrad frame, we derive the following energy density ρ, and the principal pressures p_i, $(i = r, z, \theta, \phi)$:

$$\rho = -p_r = p_z = p_\theta = p_\phi = \frac{3h(w+h)}{2r(r+h)^3}. \quad (3.31)$$

Thus, all but the radial principal pressures are positive.

3.3 Static perturbations of the black string

3.3.1 S-wave static perturbations

To study the GL instability of a 5D charged black string, we consider gravitational perturbations $h_{\mu\nu} \ll 1$ of the metric $g_{\mu\nu}$, given by (3.12), (3.26). In general, for a 5D metric we have 15 components of the gravitational perturbation field $h_{\mu\nu}$. Following [57], we consider S-wave perturbations only. In this case, the perturbation field has 7 components

$$h_{\mu\nu} = \{h_{tt}, h_{tr}, h_{tz}, h_{rr}, h_{rz}, h_{\theta\theta}, h_{\phi\phi} = h_{\theta\theta}\sin^2\theta, h_{zz}\}. \tag{3.32}$$

Such gravitational perturbation in general induces a perturbation in the electromagnetic field $F_{\mu\nu}$. In the case of the electric black string, $F_{\mu\nu}$ has in general the following induced components:

$$\delta F_{\mu\nu} = \{\delta F_{tr}, \delta F_{tz}, \delta F_{rz}\}, \tag{3.33}$$

which depend on the (t, r, z) coordinates.

The Fourier mode of the S-wave propagating in z direction along the black string reads

$$h_{\mu\nu} = \mathrm{Re}\left\{a_{\mu\nu}(r)e^{-i\omega t+ikz}\right\}. \tag{3.34}$$

This mode is unstable if $\omega = i\Omega$, where $\Omega > 0$. The threshold of GL instability corresponds to the time-independent (critical) mode with $\Omega = 0$. We shall study static S-wave perturbations of the black string and search for the critical GL mode.

In the case of static S-wave as a result of the symmetry $t \to -t$, the number of the metric perturbation field components reduces to 5,

$$h_{\mu\nu} = \{h_{tt}, h_{rr}, h_{rz}, h_{\theta\theta}, h_{\phi\phi} = h_{\theta\theta}\sin^2\theta, h_{zz}\}. \tag{3.35}$$

The perturbed electromagnetic field (3.33) has δF_{tr} and δF_{tz} components only, which depend on (r, z) coordinates. Using the electromagnetic gauge freedom the corresponding vector potential can be cast into the form $A_\mu = A_t(r, z)\delta_\mu{}^t$.

Thus, we can present the perturbed 5D charged black string solution (3.12), (3.26) as follows:

$$ds^2 = -f_1 e^{2\tau}dt^2 + \frac{e^{2\sigma}dr^2}{f_1 f_2} + f_2 e^{2\beta}(dz - \alpha dr)^2 + f_3 e^{2\gamma}(d\theta^2 + \sin^2\theta d\phi^2), \tag{3.36}$$

$$A_\mu = [A_t(r) + a_t(r, z)]\delta_\mu{}^t. \tag{3.37}$$

Here, the components $\{\tau, \sigma, \beta, \alpha, \gamma, a_t\} \ll 1$ are functions of r and z only.

Because of the freedom in coordinate choice in general relativity, there is a gauge

freedom in the perturbation field. To fix the gauges we have to fix infinitesimal diffeomorphisms ξ^μ in the coordinate transformations $x^\mu = x^{\mu'} + \xi^\mu$. In our case, $\xi^\mu = [\xi^r(r,z), \xi^z(r,z)]$. These diffeomorphisms induce gauge transformations in the metric $g_{\mu\nu}$ and in the vector potential A_μ as follows:

$$\delta g_{\mu\nu} = (\mathcal{L}_\xi \mathbf{g})_{\mu\nu} = \nabla_\mu \xi_\nu + \nabla_\nu \xi_\mu, \tag{3.38}$$

$$\delta A_\mu = (\mathcal{L}_\xi \mathbf{A})_\mu = A_{\mu,\nu}\xi^\nu + A_\nu \xi^\nu{}_{,\mu}. \tag{3.39}$$

As a result, the components of the perturbation field transform in the following way:

$$\delta\tau = \frac{1}{2}\xi_r f_{1,r} f_2\,, \;\; \delta\sigma = \xi_{r,r} f_1 f_2 + \frac{1}{2}\xi_r (f_1 f_2)_{,r}, \tag{3.40}$$

$$\delta\gamma = \frac{1}{2}\xi_r f_1 f_2 f_3^{-1} f_{3,r}\,, \;\; \delta\beta = \xi_{z,z} f_2^{-1} + \frac{1}{2}\xi_r f_1 f_{2,r}, \tag{3.41}$$

$$\delta\alpha = f_2^{-2}(\xi_z f_{2,r} - \xi_{z,r} f_2 - \xi_{r,z} f_2). \tag{3.42}$$

In the case of the 5D electric black string the only non-vanishing induced electromagnetic perturbation, a_t, transforms as

$$\delta a_t = \xi_r f_1 f_2 A_{t,r}. \tag{3.43}$$

The induced electromagnetic perturbation a_t corresponds to the perturbation of the timelike (electrostatic) component of A_μ.

Our system of equations contains 6 'field' variables $\{\tau, \sigma, \beta, \alpha, \gamma, a_t\}$ with the gauge freedom (3.40)-(3.43) generated by 2 functions ξ^r and ξ^z of 2 variables r and z. As usual for such a case, there exist $6 - 2 \cdot 2 = 2$ 'physical' degrees of freedom (see, e.g., [27]). We shall demonstrate that one can choose γ and a_t as such physical degrees of freedom. Namely, we show that these objects obey 2 decoupled, second order ordinary differential equations. As we show later, one of the equations (for a_t) does not have unstable modes, while the other one, the master equation for γ, is responsible for the existence of the GL unstable threshold mode.

3.3.2 Master equation for the electric black string

Here we use the same gauge as in [95]. Namely, we define $\tau = \tau' + \delta\tau = 0$, which fixes ξ^r through Eq. (3.40). This gauge preserves the gravitational redshift function f_1 under the perturbation field. The next gauge choice is $\beta = \beta' + \delta\beta = 0$, which fixes ξ^z through Eq. (3.41). This gauge preserves the metric along the z coordinate. Thus, we are left with $\{\sigma, \alpha, \gamma, a_t\}$. Assuming that the amplitudes in the Fourier modes (3.34) of the perturbation field are real-valued functions, we

have

$$\sigma = \tilde{\sigma}(r)\cos(kz)\,, \quad \alpha = -\tilde{\alpha}(r)k\sin(kz), \tag{3.44}$$

$$\gamma = \tilde{\gamma}(r)\cos(kz)\,, \quad a_t = \tilde{a}_t(r)\cos(kz). \tag{3.45}$$

Here, the form of the Fourier mode of α reflects the fact that $\delta\alpha$ is an antisymmetric function of z.

Our goal is to derive the master equation corresponding to the perturbation field. Currently we have three components of the gravitational perturbation field, $\{\sigma, \alpha, \gamma\}$, and one component of the induced electrostatic perturbation, a_t. They solve system of the Einstein-Maxwell equations.

We employed the GRTENSORII package to derive a reduced system of the Einstein-Maxwell equations for the first order gravitational perturbation of metric (3.12), (3.26) corresponding to the electric black string. As a result, we have five components, $\{tt, rr, rz, \theta\theta, zz\}$, of the Einstein equations and one, $\{t\}$, component of the Maxwell equations $\nabla_\nu F^{\mu\nu} = 0$. The Maxwell equations $\nabla_{[\lambda}F_{\mu\nu]} = 0$ are satisfied identically. Using the $\{rz\}$ component of the Einstein equations, we can express $\tilde{\sigma}$ in terms of $\tilde{\gamma}$ and $\tilde{a}_t$,

$$\tilde{\sigma} = \frac{16\pi L(r-w)(r\tilde{\gamma}_{,r} + \tilde{\gamma}) - Q\tilde{a}_t}{4\pi L(4r-3w)}, \tag{3.46}$$

substitute the result into the $\{rr\}$ component of the Einstein equations, and solve it for $\tilde{\alpha}$ in terms of $\tilde{\gamma}$ and $\tilde{a}_t$,

$$\tilde{\alpha} = -\frac{2w(2r-3w)\tilde{\gamma}_{,r} - [4w - 4k^2r^2(4r-3w)]\tilde{\gamma}}{k^2(4r-3w)^2} + \frac{Q[(4r-3w)\tilde{a}_{t,r} + 4\tilde{a}_t]}{4\pi L k^2(4r-3w)^2}. \tag{3.47}$$

Thus, we can express $\tilde{\sigma}$ and $\tilde{\alpha}$ in terms of $\tilde{\gamma}$ and $\tilde{a}_t$. Substituting the result into the remaining Einstein-Maxwell equations, we see that the $\{zz\}$ component is satisfied identically, whereas the components $\{tt\}$ and $\{\theta\theta\}$ together with the $\{t\}$ component of the Maxwell equation represent a system of three mutually compatible equations for $\tilde{\gamma}$ and $\tilde{a}_t$. An analysis of the equations shows that we can eliminate $\tilde{\gamma}$ and derive a single equation for $\tilde{a}_t$,

$$\frac{r-w}{r}\tilde{a}_{t,rr} + \frac{2(r-w)(w+2h)}{r(wr+2hr-wh)}\tilde{a}_{t,r} = k^2\tilde{a}_t. \tag{3.48}$$

Thus, the electrostatic perturbation decouples from the gravitational one. As we illustrate in Appendix F, there are no unstable threshold modes. Thus we can take $\tilde{a}_t = 0$.

As a result, the $\{tt\}$ and $\{\theta\theta\}$ components of the Einstein equations and the $\{t\}$ component of the Maxwell equations become equivalent and give us the master equation for the static S-wave gravitational perturbation of the electric black string,

$$\frac{r-w}{r}\tilde{\gamma}_{,rr} - \frac{w(2r-3w)}{r^2(4r-3w)}\tilde{\gamma}_{,r} + \frac{2w}{r^2(4r-3w)}\tilde{\gamma} = k^2\tilde{\gamma}. \tag{3.49}$$

Remarkably, this equation has only one parameter w, whereas the black string metric (3.12), (3.26) has two, w and h.

3.4 Numerical analysis

We shall integrate the master equation (3.49) numerically, applying the shooting method [108]. To proceed we map the semi-infinite interval $r \in [w, +\infty)$ into a finite one and rewrite the master equation in a dimensionless form using the following transformations:

$$r = \frac{w}{1-x}, \quad k = \frac{\kappa}{w}, \tag{3.50}$$

where $x \in [0, 1]$. Here, $x = 0$ corresponds to the black string event horizon. The master equation (3.49) takes the form

$$x^2\tilde{\gamma}_{,xx} + xP(x)\tilde{\gamma}_{,x} + Q(x)\tilde{\gamma} = 0, \tag{3.51}$$

where

$$P(x) = -\frac{(3x^2+6x-1)}{(1-x)(1+3x)}, \tag{3.52}$$

$$Q(x) = \frac{2x}{(1-x)(1+3x)} - \frac{x\kappa^2}{(1-x)^4}. \tag{3.53}$$

This equation has a regular singular point at $x = 0$ and an irregular singular point at $x = 1$. We are looking for regular solutions which are finite everywhere, together with their derivatives, and which vanish at infinity. Namely, $\tilde{\gamma}(1) = 0$. Applying the method of Frobenius, we can construct an approximate solution near the horizon. The solution reads

$$\tilde{\gamma}(x) \approx C_0 - C_0(2-\kappa^2)x + \cdots, \tag{3.54}$$

where C_0 is an arbitrary constant, which we take to be equal to one. From (3.54) we derive the following boundary conditions on the black string event horizon:

$$\tilde{\gamma}(0) = 1\,, \;\; \tilde{\gamma}_{,x}(0) = \kappa^2 - 2. \tag{3.55}$$

Using the boundary conditions and implementing the shooting code written in FORTRAN, we found $\kappa_{cr} \approx 0.876$ for the critical GL mode. This result coincides with that of [75] for a neutral 5D black string.

To obtain a critical wave number k_{cr}, we use the transformations (3.50), and derive

$$k_{cr} \;\; = \;\; \frac{\kappa_{cr}}{w(M,Q)}. \tag{3.56}$$

Here, $w(M,Q)$ is given by Eq. (3.29). The critical unstable mode corresponds to the highest mode in the instability spectrum $\Omega = \Omega(k)$, i.e., to the lowest frequency $\Omega = 0$. For the second order equations for the static spacetime (3.12), (3.26) the dispersion relation $\Omega = \Omega(k)$ has two roots, $k = 0$ and $k = k_{cr}$. The region $k \in [0, k_{cr}]$ defines the instability spectrum. If we set the asymptotic size of the compact dimension $L = L_{cr} \equiv 2\pi/k_{cr}$, then for such a spacetime (with fixed M and Q) there will be only one unstable mode, the critical one. For spacetime with $L > L_{cr}$, additional unstable modes are possible, and for spacetime with $L < L_{cr}$, there are no unstable modes at all. The relation (3.56) can be presented in the following dimensionless form:

$$\mu \;\; = \;\; \sqrt{9\kappa_{cr}^2 + 3q^2}. \tag{3.57}$$

Here we introduced the dimensionless mass $\mu = M/L$ and the dimensionless electric charge $q = Q/L^2$. Line (1) in Figure 3.1 represents this relation for the dimensionless critical wave number $\kappa_{cr} \approx 0.876$. We see that addition of electric charge to a neutral 5D black string makes it less stable. Namely, for a given mass $M > M_{cr}$ corresponding to a stable neutral black string, gradual addition of electric charge shifts the black string close to the critical curve, and for $Q > Q_{cr}(M_{cr})$ the black string becomes unstable.

3.5 Thermodynamics of the black strings

Black strings are higher dimensional objects which have an event horizon. Thus, as in the case of a black hole, they can be considered as thermodynamical systems which have entropy and temperature (see, e.g., [116]). The entropy is defined as

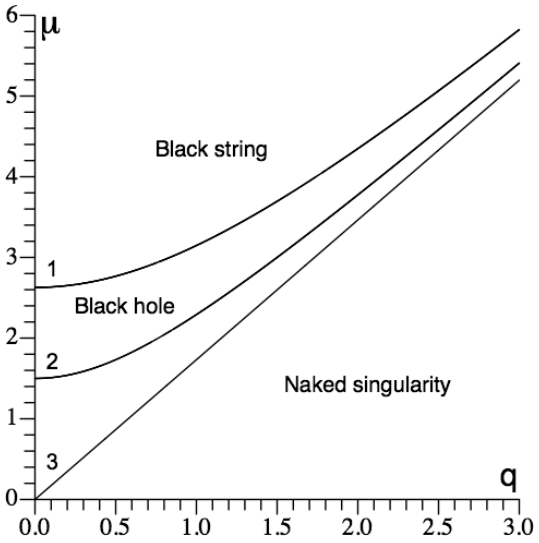

Figure 3.1: Dynamical critical curve (1) for the electric black string−electric black hole topological phase transition corresponding to $\kappa_{cr} \approx 0.876$. Here, $\mu = M/L$, $q = Q/L^2$. The thermodynamical curve (2) corresponds to the relation (3.66). Line (3), $\mu = q\sqrt{3}$, corresponds to the extreme value of the electric charge [see Eqs. (3.30), (3.64)]. Curves (1) and (2) asymptotically approach line (3). The region above curve (1) represents dynamically stable black string topological phase, whereas the region between the curves (1) and (3) represents dynamically stable black hole topological phase. Analogously, curve (2) separates the regions of thermodynamically stable black string topological phase (above the curve), and the region of thermodynamically stable black hole topological phase [below the curve, up to the line (3)]. The region below the line (3) represents naked spacetime singularities.

follows:

$$S = \frac{\mathcal{A}_{\mathcal{H}}}{4G_{(D)}}, \tag{3.58}$$

where A_H is the event horizon surface area. For the electric black string we have

$$S_{EBS} = 16\pi^2\sqrt{w}(w+h)^{\frac{3}{2}} = \frac{\sqrt{2}}{9}\left[M^2 - 3(Q/L)^2\right]^{\frac{1}{4}}\left[M + \sqrt{M^2 - 3(Q/L)^2}\right]^{\frac{3}{2}}. \tag{3.59}$$

We assume that an unstable 5D electric black string may undergo a topological phase transition into an electrically charged 5D black hole. We can compare the

entropy (3.59) with that of the electrically charged black hole S_{EBH}, and define the micro-canonical equilibrium condition for the electric black string as $S_{EBS} > S_{EBH}$. The corresponding critical curve is defined as $S_{EBS} = S_{EBH}$.

Unfortunately, an exact solution of a 5D electrically charged black hole in spacetime with one compact dimension is unknown. Analytical approximations for an electrically neutral black hole are given in [55, 56, 84]. However, we can make an estimate for the micro-canonical critical curve by comparing the electric black string entropy, S_{EBS}, with that of a 5D Reissner-Nordström black hole. We take the mass and the electric charge of the black hole equal to those of the black string and use the relation (3.11).

The 5D Reissner-Nordström black hole metric is (see, e.g., [102])

$$ds^2 = -\frac{r^2(r^2-\tilde{w})}{(r^2+\tilde{h})^2}dt^2 + \frac{r^2+\tilde{h}}{r^2-\tilde{w}}dr^2 + (r^2+\tilde{h})(d\psi^2+\sin^2\psi[d\theta^2+\sin^2\theta d\phi^2]), \tag{3.60}$$

where $\psi \in [0,\pi]$ is the third angular coordinate for a 3D round sphere. The corresponding electromagnetic vector potential is given by

$$A_\mu = \mp\frac{\sqrt{3\tilde{h}(\tilde{w}+\tilde{h})}}{r^2+\tilde{h}}\delta_\mu{}^t. \tag{3.61}$$

The black hole horizon is located at $r = \sqrt{\tilde{w}}$. The Komar mass (3.10) and the electric charge (3.6) are

$$M = \frac{6\pi^2}{L}(\tilde{w}+2\tilde{h}), \;\; Q = \pm 4\pi^2\sqrt{3\tilde{h}(\tilde{w}+\tilde{h})}. \tag{3.62}$$

Thus, we have

$$\tilde{w} = \frac{L}{6\pi^2}\sqrt{M^2-3(Q/L)^2}, \;\; \tilde{h} = \frac{L}{12\pi^2}\left(M-\sqrt{M^2-3(Q/L)^2}\right). \tag{3.63}$$

Hence, the black hole electric charge is defined within the range

$$0 \leqslant |Q| \leqslant \frac{ML}{\sqrt{3}}. \tag{3.64}$$

For the 5D Reissner-Nordström black hole we have

$$S = \frac{8\pi^3}{L}(\tilde{w}+\tilde{h})^{\frac{3}{2}} = \frac{L^{\frac{1}{2}}}{3\sqrt{3}}\left[M+\sqrt{M^2-3(Q/L)^2}\right]^{\frac{3}{2}}. \tag{3.65}$$

According to expressions (3.30) and (3.64), the electric charge of the black string and the black hole is defined in the same range. Approximating S_{EBH} with expression (3.65), we derive the micro-canonical critical curve. In dimensionless form the curve is given by

$$\mu = \sqrt{9/4+3q^2}. \tag{3.66}$$

This curve is shown in Figure 3.1 [curve (2)] together with the critical curve (3.57) of the dynamical perturbation. These curves are hyperbolae. They have qualitatively similar behavior and illustrate that an electrically charged black string is less stable than a neutral one. Let us note that line (1) for the dynamical instability is always higher than line (2).

3.6 5D extremal electrically charged black string

In this section, we discuss a 5D extremal electrically charged black string. An extremal black p-brane with dilaton and charge associated with n-form was studied in [59]. It was demonstrated that such a p-brane is stable against S-wave gravitational perturbations.

Let us consider the limiting case of the expression (3.30),

$$|Q| = \frac{ML}{\sqrt{3}}, \tag{3.67}$$

which corresponds to the extremal electrically charged black string. In this case, the parameters of the black string are the following:

$$w = 0\,,\;\; h = \frac{M}{12\pi}, \tag{3.68}$$

and the corresponding solution is given by (3.12), where

$$f_1 = \frac{r^2}{(r+h)^2}\,,\;\; f_2 = 1+\frac{h}{r}\,,\;\; f_3 = r(r+h)\,,\;\; A_\mu = \mp\frac{\sqrt{3}h}{r+h}\delta_\mu{}^t. \tag{3.69}$$

This solution belongs to the family of 5D extremal electrically charged solutions

discussed in [97]. According to the theorem proven in [97], all higher dimensional ($D \geqslant 5$) extremal solutions, except a sequence of any number of extremal Reissner-Nordström black holes, have singular event horizons. This theorem is an extension of the theorem by Hartle and Hawking, which was proven in [70] for 4D spacetimes. We present the 5D compactified extremal Reissner-Nordström black hole solution in Appendix G. The energy-momentum tensor components in a local tetrad frame are [cf. Eq. (3.31)]

$$\rho = -p_r = p_z = p_\theta = p_\phi = \frac{3h^2}{2r(r+h)^3}. \tag{3.70}$$

Here we consider S-wave static gravitational perturbations of the spacetime (3.12), (3.69) and search for an unstable threshold mode. The extremal black string horizon is defined by $r = 0$. One can check that the surface horizon area is zero, and so is the black string entropy. Thus, we may expect that the spacetime is unstable. To study S-wave static perturbations of the spacetime, one can follow the procedure presented in Section 3.3, or one can take the limit $w \to 0$ in the expressions therein, which gives the same result. For $w = 0$, expressions (3.46)-(3.49) read

$$\tilde{\sigma} = r\tilde{\gamma}_{,r} + \tilde{\gamma} - \frac{Q\tilde{a}_t}{4\pi L}, \tag{3.71}$$

$$\tilde{\alpha} = -r\tilde{\gamma} + \frac{Q(r\tilde{a}_{t,r} + \tilde{a}_t)}{16\pi L k^2 r^2}, \tag{3.72}$$

$$\tilde{a}_{t,rr} + \frac{2}{r}\tilde{a}_{t,r} = k^2\tilde{a}_t, \tag{3.73}$$

$$\tilde{\gamma}_{,rr} = k^2\tilde{\gamma}. \tag{3.74}$$

We shall look for solutions to these equations which are finite at the horizon $r = 0$ and which vanish at asymptotically flat infinity, $r \to +\infty$. The general solution to Eq. (3.73) has the following form

$$\tilde{a}_t = \frac{C_1}{r}\sin(\sqrt{-k^2}r) + \frac{C_2}{r}\cos(\sqrt{-k^2}r), \tag{3.75}$$

where C_1 and C_2 are arbitrary constants. Imposing the following boundary conditions,

$$\tilde{a}_t|_{r\to 0} = const = 1\,, \;\; \tilde{a}_t|_{r\to+\infty} = 0, \tag{3.76}$$

we derive

$$\tilde{a}_t = \frac{\sin(\sqrt{-k^2}r)}{\sqrt{-k^2}r}, \tag{3.77}$$

where $\sqrt{-k^2}$ is real, i.e., k is imaginary. Thus, there are no unstable threshold

modes for nontrivial induced electrostatic perturbation $\tilde{a}_t$. As in the case of the non-extremal electrically charged black string, we take $\tilde{a}_t = 0$. The general solution to the master equation (3.74) is

$$\tilde{\gamma} = \tilde{C}_1 e^{\sqrt{k^2}r} + \tilde{C}_2 e^{-\sqrt{k^2}r}, \tag{3.78}$$

where $\tilde{C}_1$ and $\tilde{C}_2$ are arbitrary constants. Imposing the following boundary conditions

$$\tilde{\gamma}|_{r\to 0} = const = 1\,, \;\; \tilde{\gamma}|_{r\to+\infty} = 0, \tag{3.79}$$

we derive

$$\tilde{\gamma} = e^{-\sqrt{k^2}r}, \tag{3.80}$$

where $\sqrt{k^2}$ is real, i.e., k is real. For a fixed asymptotic size of the compact dimension L, we have the maximal wave number $k_{max} = 2\pi/L$ in the instability spectrum. According to the solution (3.80), there is a continuous spectrum of unstable threshold modes defined by $k \in (0, k_{max}]$. Using expressions (3.71), (3.72), and (3.44) we derive the following perturbation fields

$$\begin{aligned} \tau &= 0\,, \;\; \sigma = (1-kr)e^{-kr}\cos(kz)\,, \;\; \beta = 0, \\ \alpha &= kre^{-kr}\sin(kz)\,, \;\; \gamma = e^{-kr}\cos(kz)\,, \;\; \tilde{a}_t = 0. \end{aligned} \tag{3.81}$$

The continuous spectrum of the unstable threshold modes indicates that the corresponding system, the 5D extremal electrically charged black string, is highly unstable, as we expected because of its zero entropy. In fact, we have a highly unstable spacetime with a naked singularity. According to the expressions (3.69) and (3.70), the proper length along the compact dimension and the energy momentum tensor components diverge at the horizon of the extremal electrically charged black string. An analysis of dynamical evolution of such a singular spacetime, especially its final state, is an interesting open question.

3.7 5D magnetic black string

It is interesting to compare the obtained topological phase diagram (Figure 3.1) with a similar diagram for a 5D magnetically charged black string. Let us recall some properties of the 5D magnetic black string, which was studied (in the case of general $D \geqslant 5$) in [95]. The magnetic black string metric can be derived as follows. The dimensionally reduced magnetic black string gives a 4D dilaton black hole with magnetic charge which is another solution to the 4D a-model discussed above. This solution is S-dual to the 4D dilaton black hole with electric charge,

Eqs. (3.20)-(3.21). Applying the S-duality transformation [102]

$$\bar{F}' = e^{-2a\varphi} \star \bar{F}\,, \quad \varphi' = -\varphi, \tag{3.82}$$

to the 4D dilaton black hole with electric charge, one derives the electromagnetic potential and the dilaton field

$$\bar{A}_i = \pm\sqrt{vh(4w+h)}\cos\theta\delta_i{}^{\phi}\,, \quad \varphi = 2av\ln\left(1+\frac{h}{r}\right), \tag{3.83}$$

of the 4D dilaton black hole with magnetic charge. The duality transformation does not change the 4D metric (3.20). Oxidizing the metric to a 5D spacetime, we derive the magnetic black string solution (3.12) (see, e.g., [95] for $D=5$), where

$$f_1 = \frac{r-w}{r+h}\,, \quad f_2 = \frac{r}{r+h}\,, \quad f_3 = (r+h)^2\,, \quad A_\mu = \pm\sqrt{3h(w+h)}\cos\theta\delta_\mu{}^{\phi}. \tag{3.84}$$

Using Eqs. (3.10), (3.11) and (3.8), we derive the mass M and the magnetic charge P of the black string,

$$M = 6\pi(w+h)\,, \quad P = \mp 4\pi\sqrt{3h(w+h)}. \tag{3.85}$$

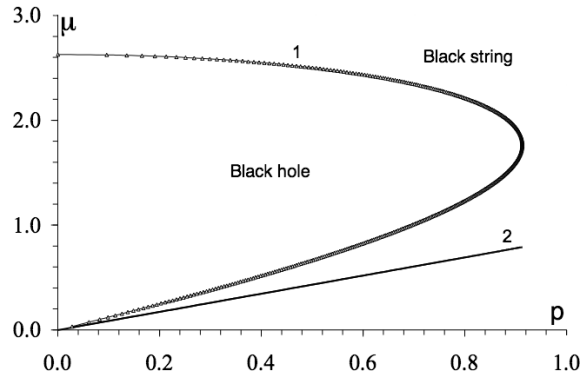

Figure 3.2: Dynamical critical curve (1) for the magnetic black string−black hole topological phase transition. Here, $\mu = M/L$, $p = P/L$. Line (2) corresponds to $p = 2\mu/\sqrt{3}$. The region enclosed by the curve (1) represents a dynamically stable black hole topological phase, whereas the region outside the curve (1) represents a dynamically stable black string topological phase.

We take the magnetic black string mass equal to the mass of the electric black

string. Using (3.85), we derive

$$w = \frac{1}{6\pi M}\left(M^2 - \frac{3}{4}P^2\right), \quad h = \frac{P^2}{8\pi M}. \tag{3.86}$$

To preserve the spacetime signature, we define $w \geqslant 0$ corresponding to

$$0 \leqslant |P| \leqslant \frac{2M}{\sqrt{3}}. \tag{3.87}$$

The energy-momentum tensor components calculated in a local tetrad frame are

$$\rho = -p_r = p_\theta = p_\phi = -p_z = \frac{3h(w+h)}{2(r+h)^4}. \tag{3.88}$$

Thus, in contrast to the electric black string [see Eq. (3.31)], the principal pressure p_z is negative.

To present the critical mode of the magnetic black string in the (M, P) parameter space, we have to construct a relation between the dimensionless mass $\mu = M/L$ and the dimensionless magnetic charge $p = P/L$ for $L = L_{cr}$. We use Eq. (3.86) and the numerical results of [95]. The relation has the following parametric form:

$$\mu = \frac{3\kappa_{cr}(m)}{1-m}, \quad p = \frac{2\kappa_{cr}(m)\sqrt{3m}}{1-m}, \tag{3.89}$$

where

$$m = \frac{h}{h+w}. \tag{3.90}$$

Figure 3.2 illustrates the relation (3.89). We see that in contrast to electric charge, magnetic charge tends to stabilize black string.

We do not know the final state of the topological phase transition of the magnetically charged black string. A 5D magnetic black hole, dual to a 5D Reissner-Nordström black hole, does not belong to the same theory. Namely, the corresponding electromagnetic tensor is a 3-form, whereas for the 5D magnetic black string considered above it is a 2-form. One may propose a scenario where the final state of the topological phase transition is a neutral black hole pierced by a magnetically charged string which wraps around the compact dimension. Such a scenario tacitly assumes that the topology of the magnetic charge is stable.

3.8 Discussion

The thermodynamical and dynamical correspondence observed for the electric black string (see Figure 3.1) shows that as in the case of a neutral black string

discussed in [57], one may expect a decay of an electric black string into the corresponding Kaluza-Klein black hole. But as it is in the case of a neutral black string, the question whether such a transition is possible remains open [74]. One may expect that because such a transition is associated with extreme spacetime curvatures of a nonuniform black string horizon at the pinch regions (see, e.g., the 4D compactified Schwarzschild black hole discussed in Section 1.9), to describe such a transition quantum gravity considerations may be necessary.

Our results show that, in contrast to the magnetic black string, the electric black string is less stable than a neutral one. Namely, an electric charge tends to destabilize black string, whereas a magnetic charge makes it more stable. This can be deduced from the form of g_{zz} components of the corresponding metrics. For the electric black string, $g_{zz} = f_2 \geqslant 1$, [see Eq. (3.26)] which makes the proper length along the compact dimension greater than L_{cr}. As a result, the electric black string is thinner than a neutral one, and hence less stable. For the magnetic black string, $g_{zz} = f_2 \leqslant 1$, [see Eq. (3.84)] which makes the proper length along the compact dimension smaller than L_{cr}, and as a result, the string is thicker than a neutral one, and hence more stable. This may also be related to the fact that the principal pressure p_z is positive for the electric black string and negative for the magnetic black string [see Eqs. (3.31) and (3.88)].

The S-duality transformation (3.82), between dimensionally reduced versions of the electric and magnetic black strings, is broken after oxidization. In fact, we have such symmetry only in 4D spacetimes for black holes, in 6D spacetimes for black strings, etc. [102]. It is interesting to study whether there remains any connection between the instability spectrum properties of the electric and magnetic black strings induced by this S-duality.

Finally, it is interesting to analyze the relation between the threshold unstable mode of the electrically charged black string and the negative mode of the corresponding Euclidean dilaton black hole with electric charge. To do this one can follow the procedure given in [111]. However, our gauge is not suitable for such analysis.

Conclusion

Let us now summarize the main results presented in this thesis.

In the first two chapters we studied the interior of 4D Schwarzschild and Reissner-Nordström black holes distorted by external, static, axisymmetric fields. We found that in the case of a Schwarzschild black hole, there is a duality relation between its event horizon and singularity. A similar relation exists for distorted Reissner-Nordström black hole between its event and Cauchy horizons. One may expect that, if the electric charge of the Reissner-Nordström black hole vanishes, the black hole becomes Schwarzschild, and the duality relation between the event and Cauchy horizons 'transforms' into the duality relation of the Schwarzschild black hole between its event horizon and singularity. As we illustrated, in the case of a distorted Reissner-Nordström black hole, such a duality relation plays a crucial role in the Cauchy horizon stability. Namely, it shows that the spacetime geometry near the event horizon is correlated with the spacetime geometry near the Cauchy horizon. This correlation implies that the Cauchy horizon remains regular for such type of distortion. Whenever the Cauchy horizon remains regular for a more general type of static distortion is an interesting open question. One may conjecture that the instability of the Cauchy horizon is purely dynamical by nature. However, to prove such a conjecture is a rather nontrivial problem. In addition, it would be interesting to study the interior of a rotating charged distorted black hole, which admits the Weyl form of the metric.

We found, with the examples of octupole and quadrupole distortions, that such distortion fields noticeably change the proper time of free fall of a test particle from the event horizon to the singularity of a distorted Schwarzschild black hole, as well as the proper time of a free fall from the event to the Cauchy horizon of a distorted Reissner-Nordström black hole.

An analysis of the distorted Schwarzschild black hole near its singularity shows that the corresponding metric has the Kasner form of an undistorted Schwarzschild black hole. It is an interesting open question if an asymmetric, static distortion will preserve the Kasner form of the metric near the corresponding black hole singularity.

We demonstrated, with the example of a compactified 4D Schwarzschild black hole, that the *physical singularity* becomes naked when the north and the south

poles of the black hole come close to each other. It is important to study whether this happens for a higher-dimensional compactified black hole, which may be a topological phase of the corresponding unstable black string. If this is the case, we may question the validity of the classical analysis of the merger transition between the black string and the compactified black hole.

In Chapter 3 we studied the Gregory-Laflamme instability of a 5D black string with magnetic or electric charge. We illustrated that an electric charge tends to destabilize black string, whereas a magnetic charge makes it more stable. This result may be related to the fact that the principal pressure p_z is positive for the electric black string and negative for the magnetic black string. It may be stimulating to analyze which properties of the matter field are responsible for such an effect.

The analysis of the Gregory-Laflamme instability of a 5D extremal electrically charged black string shows the presence of a continuous spectrum of the unstable threshold modes. This indicates that the black string, which has a singular event horizon, is highly unstable. It would be interesting to study the dynamical evolution of such extremal black string.

Bibliography

[1] S. Abdolrahimi, V. P. Frolov, and A. A. Shoom, Phys. Rev. D **80**, 024011 (2009).

[2] A. M. Abrahams, G. B. Cook, S. L. Shapiro, and S. A. Teukolsky, Phys. Rev. D **49**, 5153 (1994).

[3] M. Abramowitz and I. A. Stegun, *Handbook of Mathematical Functions with Formulas, Graphs, and Mathematical Tables*, Dover Publications, Inc., New York (1970).

[4] C. Amsler *et al.* (Particle Data Group), Phys. Lett. B **667**, 1 (2008).

[5] M. Ansorg and J. Hennig, Class. Quantum Grav. **25**, 222001 (2008).

[6] I. Antoniadis, N. Arkani-Hamed, S. Dimopoulos, G. Dvali, Phys. Lett. B **436**, 257 (1998).

[7] G. Arfken, *Mathematical Methods for Physicists*, Academic Press, Inc., New York and London (1968).

[8] N. Arkani-Hamed, S. Dimopoulos, G. Dvali, Phys. Lett. B **429**, 263 (1998).

[9] J. M. Bardeen, B. Carter, and S. W. Hawking, Commun. Math. Phys. **31**, 161 (1973).

[10] R. Beig and W. Simon, J. Math. Phys. **24**, 1163 (1983).

[11] A. R. Bogojevic and L. Perivolaropoulos, Mod. Phys. Lett. A **6**, 369 (1991).

[12] A. Bonanno, S. Droz, W. Israel and S. Morsink, Can J. Phys. **72**, 755 (1994).

[13] R. H. Boyer, Proc. Roy. Soc. London, **A311**, 245 (1969).

[14] P. Brady and J. Smith, Phys. Rev. Lett. **75**, 1256 (1995).

[15] N. Bretón, T. E. Denisova, and V. S. Manko, Physics Letters A **230**, 7 (1997).

[16] N. Bretón, A. A. García, and V. S. Manko, T. E. Denisova, Phys. Rev. D **57**, 3382 (1998).

[17] Y. Brihaye, T. Delsate, and E. Radu, Phys. Lett. B **662**, 264 (2008).

[18] L. M. Burko, Int. J. Mod. Phys. D **11**, 1561 (2002).

[19] L. M. Burko, Phys. Rev. D **66**, 024046 (2002).

[20] L. M. Burko, Phys. Rev. Lett. **90**, 121101 (2003).

[21] L. M. Burko, Phys. Rev. Lett. **90**, 249902 (E) (2003).

[22] S. Chandrasekhar, *The Mathematical Theory of Black Holes*, Clarendon Press, Oxford, (1983).

[23] S. Chandrasekhar and J. B. Hartle, Proc. Roy. Soc. London, **A384**, 301 (1982).

[24] M. Choptuik, L. Lehner, I. Olabarrieta, R. Petryk, F. Pretorius, and H. Villegas, Phys. Rev. D **68**, 044001 (2003).

[25] S. Cotsakis and D. Barrow, arXiv: gr-qc/0608137.

[26] S. Dimopoulos, G. Landsberg, Phys. Rev. Lett. **87**, 161602 (2001).

[27] P. A. M. Dirac, *Lectures on Quantum Mechanics*, Belfer Graduate School of Science Monographs Series, Number 2 (1964).

[28] S. S. Doeleman et al., Nature, **455**, 78 (2008).

[29] A. G. Doroshkevich, Ya. B. Zel'dovich, and I. D. Novikov, Zh. Eksp. Teor. Fiz. **49**, 170 (1965).

[30] J. Ehlers, *Grundlagenprobleme der modernen Physik*, edited by J. Nitsch, J. Pfarr, and E. W. Stachov, BI-Verlag, Mannheim, (1981).

[31] L. P. Eisenhart, *Riemannian Geometry*, Princeton University Press, Princeton, New Jersey, (1993).

[32] G. F. R. Ellis and A. R. King, Commun. Math. Phys. **38**, 119 (1974).

[33] F. J. Ernst, Phys. Rev. **168**, 1415 (1968).

[34] S. Fairhurst and B. Krishnan, Int. J. Mod. Phys. D **10**, 691 (2001).

[35] L. Ferrarese and D. Merritt, Physics World, **15**, 41 (2002).

[36] E. Flanagan and A. Ori, Phys. Rev. D **54**, 6233 (1996).

[37] J. L. Friedman, K. Schleich, and D. M. Witt, Phys. Rev. Lett. **71**, 1486 (1993).

[38] V. P. Frolov, Phys. Rev. D **73**, 064021 (2006).

[39] V. P. Frolov, *Black Hole Physics*, Lecture Notes, (2008).

[40] A. V. Frolov and V. P. Frolov, Phys. Rev. D **67**, 124025 (2003).

[41] A. V. Frolov, K. R. Kristjansson, and L. Thorlacius, Phys. Rev. D **72**, 021501 (2005).

[42] A. V. Frolov, K. R. Kristjansson, and L. Thorlacius, Phys. Rev. D **73**, 124036 (2006).

[43] V. Frolov and I. Novikov, *Black Hole Physics: Basic Concepts and Recent Developments*, Kluwer Academic Publishers, Dodrecht-Boston-London (1998).

[44] V. P. Frolov and N. Sanchez, Phys. Rev. D **33**, 1604 (1986).

[45] V. P. Frolov and A. A. Shoom, Phys. Rev. D **76**, 064037 (2007).

[46] V. P. Frolov and A. A. Shoom, Phys. Rev. D **79**, 104002 (2009).

[47] V. P. Frolov, A. I. Zel'nikov, Phys. Rev. D **35**, 3031 (1987).

[48] R. Geroch, J. Math. Phys. **11**, 1955 (1970).

[49] R. Geroch, J. Math. Phys. **11**, 2580 (1970).

[50] R. Geroch and J. B. Hartle, J. Math. Phys. **23**, 680 (1982).

[51] R. Geroch, E. H. Kronheimer, R. Penrose, Proc. Roy. Soc. London, **A327**, 545 (1972).

[52] S. B. Giddings, Phys. Rev. D **76**, 064027 (2007).

[53] D. M. Gingrich, Int. J. Mod. Phys. A **21**, 6653 (2006).

[54] M. L. Gnedin and N. Y. Gnedin, Class. Quantum Grav. **10**, 1083 (1993).

[55] D. Gorbonos and B. Kol, JHEP, **06**, 053 (2004).

[56] D. Gorbonos and B. Kol, Class. Quantum Grav. **22**, 3935 (2005).

[57] R. Gregory and R. Laflamme, Phys. Rev. Lett. **70**, 2837 (1993).

[58] R. Gregory and R. Laflamme, Nucl. Phys. B **428**, 399 (1994).

[59] R. Gregory and R. Laflamme, Phys. Rev. D **51**, R305 (1995).

[60] D. J. Gross and M. J. Perry, L. G. Yaffe, Phys. Rev. D **25**, 330 (1982).

[61] Y. Gürsel, Gen. Relativ. Gravit. **15**, 737 (1983).

[62] Y. Gürsel, I. D. Novikov, V. D. Sandberg, and A. A. Starobinsky, Phys. Rev. D **20**, 1260 (1979).

[63] A. J. S. Hamilton, arXiv: 0903.2021.

[64] A. J. S. Hamilton and P. P. Avelino, arXiv: 0811.1926.

[65] R. O. Hansen, J. Math. Phys. **15**, 46 (1974).

[66] T. Harmark, V. Niarchos, and N. A. Obers, Class. Quantum Grav. **24**, R1 (2007).

[67] T. Harmark and N. A. Obers, JHEP, **05**, 032 (2002).

[68] T. Harmark and N. A. Obers, Class. Quantum Grav. **21**, 1709 (2004).

[69] B. K. Harrison, J. Math. Phys. **9**, 1744 (1968).

[70] J. B. Hartle and S. W. Hawking, Commun. Math. Phys. **26**, 87 (1972).

[71] S. W. Hawking, Commun. Math. Phys. **25**, 152 (1972).

[72] S. W. Hawking & G. F. R. Ellis, *The large scale structure of space-time*, Cambridge University Press, Cambridge (1973).

[73] J. Hennig and M. Ansorg, arXiv: 0904.2071.

[74] G. T. Horowitz and K. Maeda, Phys. Rev. Lett. **87**, 131301 (2001).

[75] J. L. Hovdebo and R. C. Myers, Phys. Rev. D **73**, 084013 (2006).

[76] S. A. Hughes, C. R. Kreeton II, P. Walker, K. T. Walsh, S. L. Shapiro, and S. A. Teukolsky, Phys. Rev. D **49**, 4004 (1994).

[77] W. Israel, Phys. Rev. **164**, 1776 (1967).

[78] W. Israel, Commun. Math. Phys. **8**, 245 (1968).

[79] W. Israel, Lett. Nuovo Cimento **6**, 267 (1973).

[80] W. Israel and K. A. Khan, Nuovo Cimento **33**, 331 (1964).

[81] T. Jacobson and S. Venkataramani, Class. Quantum Grav. **12**, 1055 (1995).

[82] J. H. Jeans, Phil. Trans. Roy. Soc. A **199**, 1 (1902).

[83] H. Jeffreys and B. Jeffreys, *Methods of Mathematical Physics*, Cambridge University Press, Cambridge, Third Edition, (1956).

[84] D. Karasik, C. Sahabandu, P. Suranyi, and L. C. R. Wijewardhana, Phys. Rev. D **71**, 024024 (2005).

[85] A. R. King, Phys. Rev. D **11**, 763 (1975).

[86] B. Kleihaus, J. Kunz, and E. Radu, JHEP **06**, 016 (2006).

[87] B. Kol, Phys. Rep. **422**, 119 (2006).

[88] B. Kol and E. Sorkin, Class. Quantum Grav. **21**, 4793 (2004).

[89] R. Kulkarni and N. Dadhich, Phys. Rev. D **33**, 2780 (1986).

[90] V. S. Manko, Class. Quantum Grav. **7**, L209 (1990).

[91] R. B. Mann, E. Radu, C. Stelea, JHEP **09**, 073 (2006).

[92] R. A. Matzner, N. Zamorana, and V. D. Sandberg, Phys. Rev. D **19**, 2821 (1979).

[93] J. M. McNamara, Proc. Roy. Soc. London, **A358**, 499 (1978).

[94] C. W. Misner, K. S. Thorne, and J. A. Wheeler, *Gravitation*, W. H. Freeman and Co., San Francisco, (1973).

[95] U. Miyamoto, Phys. Lett. B **659**, 380 (2008).

[96] R. Monteiro and J. E. Santos, Phys. Rev. D **79**, 064006 (2009).

[97] R. C. Myers, Phys. Rev. D **35**, 455 (1987).

[98] R. C. Myers and M. J. Perry, Annals of Physics **172**, 304 (1986).

[99] L. A. Mysak and G. Szekeres, Can. J. Phys. **44**, 617 (1966).

[100] I. D. Novikov and A. A. Starobinsky, Sov. Phys. JETP **51**, 1 (1980); Zh. Eksp. Teor. Fiz. **78**, 3 (1980).

[101] A. Ori, Phys. Rev. Lett. **67**, 789 (1991).

[102] T. Ortín, *Gravity and Strings*, Cambridge University Press, Cambridge, p. 350 (2006).

[103] D. N. Page, arXiv: hep-th/9305040.

[104] D. Papadopoulos and B. C. Xanthopoulos, Il Nuovo Cim. **83B**, 113 (1984).

[105] R. Penrose, *Structure of space-time*, in Battelle Rencontres, ed. C. M. de Witt and J. A. Wheeler, Benjamin, New York, (1968).

[106] P. C. Peters, J. Math. Phys. **20**, 1481 (1979).

[107] E. Poisson and W. Israel, Phys. Rev. D **41**, 1796 (1990).

[108] W. H. Press, S. A. Teukolsky, W. T. Vetterling, and B. P. Flannery, *Numerical Recipes in FORTRAN*, 2nd edition, Cambridge University Press, Cambridge (1992).

[109] A. P. Prudnikov, Yu. A. Brychkov, and O. I. Marichev, *Integrals and Series* V. I, Gordon and Breach Science Publishers (1986).

[110] H. Quevedo, Phys. Rev. D **39**, 2904 (1989).

[111] H. S. Reall, Phys. Rev. D **64**, 044005 (2001).

[112] O. Sarbach, L. Lehner, Phys. Rev. D **71**, 026002 (2005).

[113] S. L. Shapiro, S. A. Teukolsky, and J. Winicour, Phys. Rev. D **52**, 6982 (1995).

[114] L. Smarr, Phys. Rev. D **7**, 289 (1973).

[115] H. Stephani, D. Kramer, M. Maccallum, C. Hoenselaers, and E. Herlt, *Exact Solutions to Einstein's Field Equations*, 2nd edition, Cambridge University Press, Cambridge (2003).

[116] A. Strominger and C. Vafa, Phys. Lett. B **379**, 99 (1996).

[117] W. Suen, Phys. Rev. D **34**, 3617 (1986).

[118] W. Suen, Phys. Rev. D **34**, 3633 (1986).

[119] K. S. Thorne, Rev. Mod. Phys. **52**, 299 (1980).

[120] M. Visser, *Lorentzian wormholes: from Einstein to Hawking*, Springer-Verlag New York, Inc., (1996).

[121] S. Weinberg, *Gravitation and Cosmology*, Jonh Wiley & Sons, Inc., New York (1972).

[122] W. J. Wild, R. M. Kerns, Phys. Rev. D **21**, 332 (1980).

[123] W. J. Wild, R. M. Kerns, and W. F. Drish, Jr., Phys. Rev. D **23**, 829 (1981).

[124] S. S. Yazadjiev, Class. Quantum Grav. **18**, 2105 (2001).

[125] H. Yoshino and Y. Nambu, Phys. Rev. D **67**, 024009 (2003).

[126] D. M. Zipoy, J. Math. Phys. **7**, 1137 (1966).

Appendix A

Relation between the multipole moments

In this appendix, we present the relation between two different representations of the distortion field $\hat{U}$ given by expressions (1.42) and (1.44). Using the expansion of the Legendre polynomials of the first kind (see, e.g., [7], p. 419),

$$P_l(x) = \frac{1}{2^l} \sum_{k=0}^{\lfloor l/2 \rfloor} \frac{(-1)^k (2l-2k)!}{k!(l-k)!(l-2k)!} x^{l-2k}, \tag{A.1}$$

where $\lfloor x \rfloor$ is the floor function (see List of Symbols and Abbreviations), we derive

$$R^n P_n(\eta \cos\theta / R) \;\; = \;\; \sum_{s=0}^{n} A_{s,n} P_s(\eta) P_s(\cos\theta), \tag{A.2}$$

where $R = (\eta^2 - \sin^2\theta)^{1/2}$. Here, according to the property of the Legendre polynomials, $P_n(\pm 1) = (\pm 1)^n$, the coefficients $A_{s,n}$ satisfy the relation

$$\sum_{s=0}^{n} A_{s,n} = 1, \tag{A.3}$$

where the sum is over even s if n is even, and it is over odd s if n is odd. These coefficients can be calculated with the aid of the following recurrence expressions:

for even n, $A_{0,0}=1$, and for $n \geqslant 2$,

$$A_{n-2q,n} = 2^{n-4q}\left[\frac{(n-2q)!(n-2q)!}{(2n-4q)!}\right]^2 \times\Bigg[\sum_{m=0}^{\min\{n/2-q,q\}} \frac{(2n-2q-2m)!}{m!m!(q-m)!(n-q-m)!(n-2q-2m)!} - \sum_{s=n/2-q+1}^{n/2} A_{2s,n}\left(\frac{(n+2s-2q)!}{2^{2s-n/2}(n-2q)!(s-n/2+q)!(s+n/2-q)!}\right)^2\Bigg], \quad (A.4)$$

where the integer $q \in [1, n/2]$, and

$$A_{n,n} = \frac{n!n!2^n}{(2n)!}; \quad (A.5)$$

for odd n, $A_{1,1}=1$, and for $n \geqslant 3$,

$$A_{n-2q,n} = 2^{n-4q}\left[\frac{(n-2q)!(n-2q)!}{(2n-4q)!}\right]^2 \times\Bigg[\sum_{m=0}^{\min\{(n-1)/2-q,q\}} \frac{(2n-2q-2m)!}{m!m!(q-m)!(n-q-m)!(n-2q-2m)!} - \sum_{s=(n+1)/2-q}^{(n-1)/2} \frac{A_{2s+1,n}[(n+2s+1-2q)!]^2}{[2^{2s-n/2+1}(n-2q)!(s-(n-1)/2+q)!(s+(n+1)/2-q)!]^2}\Bigg], \quad (A.6)$$

where $q \in [1, (n-1)/2]$, and

$$A_{n,n} = \frac{n!n!2^n}{(2n)!}. \quad (A.7)$$

Thus, we have the following relation [see Eqs. (1.42), (1.44), and (A.2)]

$$\hat{U}(\eta,\theta) \;=\; \sum_{n=0}^{N} c_n \sum_{s=0}^{n} A_{s,n} P_s(\eta) P_s(\cos\theta) = \sum_{n=0}^{N} a_n P_s(\eta) P_s(\cos\theta), \quad (A.8)$$

where N is the order of approximation of the distortion field. The multipole moments a_n's and c_n's are uniquely related to each other though the following formulas:

for even $N \geqslant 0$, and the even multipole moments,

$$a_{2n} = \sum_{k=n}^{N/2} c_{2k} A_{2n,2k}\,, \quad n \in \left[0,\, \frac{N}{2}\right], \tag{A.9}$$

for $N \geqslant 2$, and the odd multipole moments,

$$a_{2n+1} = \sum_{k=n}^{N/2-1} c_{2k+1} A_{2n+1,2k+1}\,, \quad n \in \left[0,\, \frac{N}{2} - 1\right], \tag{A.10}$$

for odd $N \geqslant 1$,

$$a_{2n} = \sum_{k=n}^{(N-1)/2} c_{2k} A_{2n,2k}\,, \quad n \in \left[0,\, \frac{N-1}{2}\right], \tag{A.11}$$

$$a_{2n+1} = \sum_{k=n}^{(N-1)/2} c_{2k+1} A_{2n+1,2k+1}\,, \quad n \in \left[0,\, \frac{N-1}{2}\right]. \tag{A.12}$$

The multipole moments c_n's can be defined in terms of a_n's by the following recurrence formulas:
for $N = 0$, $c_0 = a_0$, and for even $N \geqslant 2$, and the even multipole moments,

$$c_{2n} = A^{-1}_{2n,2n} \left[a_{2n} - \sum_{k=n+1}^{N/2} c_{2k} A_{2n,2k} \right], \quad n \in \left[0,\, \frac{N}{2} - 1\right], \quad c_N = \frac{a_N}{A_{N,N}}, \tag{A.13}$$

for $N \geqslant 4$, and the odd multipole moments,

$$c_{2n+1} = A^{-1}_{2n+1,2n+1} \left[a_{2n+1} - \sum_{k=n+1}^{N/2-1} c_{2k+1} A_{2n+1,2k+1} \right], \quad n \in \left[0,\, \frac{N}{2} - 2\right], \quad c_{N-1} = \frac{a_{N-1}}{A_{N-1,N-1}}; \tag{A.14}$$

for $N = 1$, $c_0 = a_0$, $c_1 = a_1$, and for odd $N \geqslant 3$, and the even multipole moments,

$$c_{2n} = A^{-1}_{2n,2n} \left[a_{2n} - \sum_{k=n+1}^{(N-1)/2} c_{2k} A_{2n,2k} \right], \quad n \in \left[0,\, \frac{N-3}{2}\right], \quad c_{N-1} = \frac{a_{N-1}}{A_{N-1,N-1}}, \tag{A.15}$$

and for the odd multipole moments,

$$c_{2n+1} = A^{-1}_{2n+1,2n+1}\left[a_{2n+1} - \sum_{k=n+1}^{(N-1)/2} c_{2k+1}A_{2n+1,2k+1}\right],$$
$$n \in \left[0,\, \frac{N-3}{2}\right],\ c_N = \frac{a_N}{A_{N,N}}. \tag{A.16}$$

These relations together with conditions (1.50) and (1.51) imply the following expressions:

$$\sum_{n=0}^{\lfloor (N-1)/2 \rfloor} a_{2n+1} = \sum_{n=0}^{\lfloor (N-1)/2 \rfloor} c_{2n+1} = 0, \tag{A.17}$$

and

$$\sum_{n=0}^{\lfloor N/2 \rfloor} a_{2n} = \sum_{n=0}^{\lfloor N/2 \rfloor} c_{2n}. \tag{A.18}$$

These expressions imply,

$$\sum_{n=0}^{N} a_n = \sum_{n=0}^{N} c_n = u_0. \tag{A.19}$$

Example: Octupole approximation

Let us preset the relation (A.8) for an octupole approximation, $N = 3$. We start with the representation (1.44):

$$\hat{U} = c_0 + c_1 R P_1(\eta\cos\theta/R) + c_2 R^2 P_2(\eta\cos\theta/R) + c_3 R^3 P_3(\eta\cos\theta/R), \tag{A.20}$$

where according to the conditions (1.50) and (1.51), $c_1 = -c_3$. Applying Eqs. (A.4)-(A.7) we derive

$$A_{0,0} = A_{1,1} = 1\,,\ A_{0,2} = \frac{1}{3}\,,\ A_{2,2} = \frac{2}{3}\,,\ A_{1,3} = \frac{3}{5}\,,\ A_{3,3} = \frac{2}{5}, \tag{A.21}$$

and Eqs. (A.11), (A.12) give

$$a_0 = c_0 + \frac{1}{3}c_2\,,\ a_2 = \frac{2}{3}c_2\,,\ a_1 = -a_3 = -\frac{2}{5}c_3. \tag{A.22}$$

The conditions (A.17) and (A.18) are easily verified. Finally, with the aid of Eq. (A.8) we derive

$$\hat{U} = a_0 - a_3 P_1(\eta) P_1(\cos\theta) + a_2 P_2(\eta) P_2(\cos\theta) + a_3 P_3(\eta) P_3(\cos\theta), \qquad \text{(A.23)}$$

where a_n's are defined through c_n's by the relations (A.22). The inverse relations are

$$c_0 = a_0 - \frac{1}{2} a_2 \,, \;\; c_2 = \frac{3}{2} a_2 \,, \;\; c_1 = -c_3 = -\frac{5}{2} a_3. \qquad \text{(A.24)}$$

Appendix B

Expansions of the distortion fields $\mathcal{U}$ and $\hat{V}$

In this appendix, we present expansions of the distortion fields $\mathcal{U}$ and $\hat{V}$ near the horizon and the singularity of the distorted Schwarzschild black hole. Using the the transformations (1.58), we present Eq. (1.34) in the following form:

$$D_\psi \hat{U} = D_\theta \hat{U}\,, \tag{B.1}$$

$$D_\psi \hat{U} = \hat{U}_{,\psi\psi} + \cot\psi\, \hat{U}_{,\psi}\,, \tag{B.2}$$

$$D_\theta \hat{U} = \hat{U}_{,\theta\theta} + \cot\theta\, \hat{U}_{,\theta}\,. \tag{B.3}$$

Then, from Eq. (B.2) we see that $D_\psi \hat{U} = D_{-\psi}\hat{U}$. Thus, a solution to Eq. (B.1) can be presented as a sum of two solutions, one being odd and the other being an even function of ψ. Because of the presence of the factor $\cot\psi$ in D_ψ, this operator is singular at $\psi = 0$. Hence, the solution regular at the horizon must be an even function of ψ. Indeed, using the transformations (1.58) the solution (1.42) reads

$$\hat{U}(\psi,\theta) = \sum_{n\geqslant 0} a_n P_n(\cos\psi) P_n(\cos\theta), \tag{B.4}$$

The solution (B.4) can be used to find the asymptotic behavior of $\mathcal{U}$ near the horizon, $\psi = 0$, and the singularity, $\psi = \pi$. To deal with both the cases simultaneously, we denote $\psi_+ = \psi$ and $\psi_- = \pi - \psi$. The function $\mathcal{U}$ is an even function of ψ_σ ($\sigma = \pm$), and it has the following expansion:

$$\mathcal{U} = \sum_{n=0}^{\infty} U_\sigma^{(2n)}\, \psi_\sigma^{2n}\,. \tag{B.5}$$

Here $U_\sigma^{(2n)}$ are functions of the angular variable θ. The operator D_ψ in (B.2) has the same form D_σ for both the variables ψ_σ,

$$D_\sigma = \partial_{\psi_\sigma}^2 + \cot\psi_\sigma\, \partial_{\psi_\sigma}\,. \tag{B.6}$$

Using the series expansion for $\cot\psi_\sigma$,

$$\cot\psi_\sigma = \psi_\sigma^{-1}[1 - \sum_{m=1}^{\infty} c_{2m}\psi_\sigma^{2m}]\,,\;\; c_{2m} = \frac{(-1)^{m-1}2^{2m}B_{2m}}{(2m)!}\,, \tag{B.7}$$

where B_{2m} are the Bernoulli numbers,

$$B_2 = \frac{1}{6}\,,\;\; B_4 = -\frac{1}{30}\,,\;\; B_6 = \frac{1}{42}\,\ldots\,, \tag{B.8}$$

the relation

$$D_\sigma\psi_\sigma^{2n} = 4n^2\psi_\sigma^{2(n-1)} - 2n\sum_{m=1}^{\infty} c_{2m}\psi_\sigma^{2(n+m-1)}, \tag{B.9}$$

and equation (B.1), one obtains

$$\begin{aligned}
U_\sigma^{(0)} &= u_\sigma\,, && \text{(B.10)}\\
U_\sigma^{(2)} &= \frac{1}{4}(u_{\sigma,\theta\theta} + \cot\theta u_{\sigma,\theta})\,, && \text{(B.11)}\\
U_\sigma^{(4)} &= \frac{1}{16}\left(U_{\sigma,\theta\theta}^{(2)} + \cot\theta U_{\sigma,\theta}^{(2)} + \frac{2}{3}U_\sigma^{(2)}\right)\,, && \text{(B.12)}\\
&\vdots\\
U_\sigma^{(2n+2)} &= \frac{1}{4(n+1)^2}[D_\theta U_\sigma^{(2n)} + 2\sum_{m=1}^{n}(n-m+1)c_{2m}U_\sigma^{(2(n-m+1))}]\,. && \text{(B.13)}
\end{aligned}$$

Similarly, the asymptotic expression for $\hat{V}$ near the horizon and the singularity can be written in the form

$$\hat{V} = \sum_{n=0}^{\infty} V_\sigma^{(2n)}\psi_\sigma^{2n}\,, \tag{B.14}$$

where $V_\sigma^{(2n)}$ are functions of the angular variable θ. Substituting the expansion (B.5) into Eqs. (1.35), (1.36), and integrating with the boundary condition (1.74)

one can determine the functions $V_\sigma^{(2n)}$. The first three of these functions are

$$V_\sigma^{(0)} = 2\sigma u_\sigma \,, \tag{B.15}$$

$$V_\sigma^{(2)} = 2\sigma U_\sigma^{(2)} - \sigma \cot\theta u_{\sigma,\theta} + \frac{1}{2}(u_{\sigma,\theta})^2 = \frac{1}{2}[\sigma(u_{\sigma,\theta\theta} - \cot\theta u_{\sigma,\theta}) + (u_{\sigma,\theta})^2] \,, \tag{B.16}$$

$$\begin{aligned} V_\sigma^{(4)} &= \frac{1}{12}\{\sigma[24U_\sigma^{(4)} + 6(1+2\cot^2\theta)U_\sigma^{(2)} - 6\cot\theta U_{\sigma,\theta}^{(2)} - (5+6\cot^2\theta)\cot\theta\, u_{\sigma,\theta}] \\ &+ 6u_{\sigma,\theta}U_{\sigma,\theta}^{(2)} + (1+3\cot^2\theta)(u_{\sigma,\theta})^2 - 12\cot\theta U_\sigma^{(2)} u_{\sigma,\theta} + 12(U_\sigma^{(2)})^2\} \,. \end{aligned} \tag{B.17}$$

Appendix C

Geodesic motion near the singularity

In this appendix, we derive an approximate solution for 'radial' timelike geodesic motion near the singularity of the distorted Schwarzschild black hole. For a free particle moving in the black hole interior there exist two integrals of motion related to the spacetime symmetry,

$$E = -p_T = -\xi^\alpha_{(T)} p_\alpha = const\,, \;\; L = p_\phi = \xi^\alpha_{(\phi)} p_\alpha = const\,. \tag{C.1}$$

The first integral has the meaning of the conserved momentum p_T along the T axis, and the second one is the angular momentum p_ϕ.

Consider a point $(\psi^o_-, \theta^o, T^o, \phi^o)$ near the singularity of a distorted black hole. What is the proper time τ^o required to fall from this point to the singularity? This time depends on the value of E and L. We consider the proper time for the special value of these parameters $E = L = 0$. In this case, for a moving particle $T = const$ and $\phi = const$. For the Schwarzschild geometry this is radial motion. We also call the motion in the interior of a distorted black hole 'radial' when $E = L = 0$. This type of motion is a geodesic in the 2D metric

$$d\gamma^2 = B_-(d\theta^2 - d\psi_-^2)\,, \tag{C.2}$$

obtained by dimensional reduction ($T = const, \phi = const$) from the metric (1.100). Let us denote

$$\alpha = \frac{1}{2}(\ln B_-)_{,\psi_-}\,, \;\; \beta = \frac{1}{2}(\ln B_-)_{,\theta}\,. \tag{C.3}$$

Then the Christoffel symbols for the metric $d\gamma^2$ are

$$\Gamma^{\psi_-}_{\psi_-\psi_-} = \Gamma^{\theta}_{\;\theta\psi_-} = \Gamma^{\psi_-}_{\theta\theta} = \alpha\,, \tag{C.4}$$

$$\Gamma^{\theta}_{\;\psi_-\psi_-} = \Gamma^{\theta}_{\;\theta\theta} = \Gamma^{\psi_-}_{\theta\psi_-} = \beta\,. \tag{C.5}$$

The geodesic equation

$$\ddot{x}^\alpha + \Gamma^\alpha_{\beta\gamma}\,\dot{x}^\beta\dot{x}^\gamma = 0 \tag{C.6}$$

for the metric (C.2) takes the following form:

$$\ddot{\psi}_- + \alpha(\dot{\psi}_-^2 + \dot{\theta}^2) + 2\beta\dot{\psi}_-\dot{\theta} = 0\,, \tag{C.7}$$

$$\ddot{\theta}_- + \beta(\dot{\psi}_-^2 + \dot{\theta}^2) + 2\alpha\dot{\psi}_-\dot{\theta} = 0\,. \tag{C.8}$$

Here the over-dot denotes a derivative with respect to the proper time τ. These equations obey the constraint

$$B_-(\dot{\psi}_-^2 - \dot{\theta}^2) = 1\,, \tag{C.9}$$

that is, the normalization condition, $u_\alpha u^\alpha = -1$, for the 4-velocity u^α.

Using the expansions (1.101)-(1.103) for the metric (1.100) near the singularity, we derive

$$\ln B_- = 4\ln\psi_- - 6u_- - \ln 16 + O(\psi_-^2)\,. \tag{C.10}$$

Thus, in the leading order $\alpha \approx 2/\psi_-$ and $\beta \approx -3u_{-,\theta}$. In the leading order the geodesic equations (C.7) and (C.8) and the constraint (C.9) take the following form:

$$\psi_-\ddot{\psi}_- + 2(\dot{\psi}_-^2 + \dot{\theta}^2) - 6u_{-,\theta}\psi_-\dot{\psi}_-\dot{\theta} \approx 0, \tag{C.11}$$

$$\psi_-\ddot{\theta} - 3u_{-,\theta}\psi_-(\dot{\psi}_-^2 + \dot{\theta}^2) + 4\dot{\psi}_-\dot{\theta} \approx 0, \tag{C.12}$$

$$e^{-6u_-}\psi_-^4(\dot{\psi}_-^2 - \dot{\theta}^2) \approx 16, \tag{C.13}$$

respectively. According to the expansion (C.10), the order of approximation in the geodesic equations corresponds to the order of approximation of the metric (1.100).

We use the ambiguity in the choice of τ to put $\tau = 0$ at the singularity for each of the 'radial' geodesics approaching the singularity. Since τ grows along geodesics directed to the singularity, it is negative before the geodesic reaches the singularity.

The point $\tau = 0$ is a singular point of equations (C.11)-(C.13). To find an approximate solution to the geodesic equations one can apply the method of asymptotic splittings described in [25]. A 'radial' geodesic approaching the singularity is uniquely determined by the limiting value $\theta_0 = \theta$ at $\tau = 0$. The asymptotic expansions of ψ_- and θ near $\tau = 0$ have the following form:

$$\psi_- = \tilde{\tau}^{1/3} + \frac{2}{5}u_{-,\vartheta}^2(\vartheta)\tilde{\tau} + O(\tilde{\tau}^{4/3})\,, \tag{C.14}$$

$$\theta = \theta_0 + \frac{1}{2}u_{-,\vartheta}(\vartheta)\tilde{\tau}^{2/3} + O(\tilde{\tau}^{4/3})\,,\ \ \tilde{\tau} = -12e^{3u_-(\vartheta)}\tau\,. \tag{C.15}$$

Appendix D

Newtonian picture

In this appendix, we consider a static axisymmetric Newtonian gravitational potential $\hat{U}_N$ at point A due to point-like masses m_1, m_2, and a thin ring of mass m and radius $\mathtt{r}_0$, as it is shown in Figure D.1.

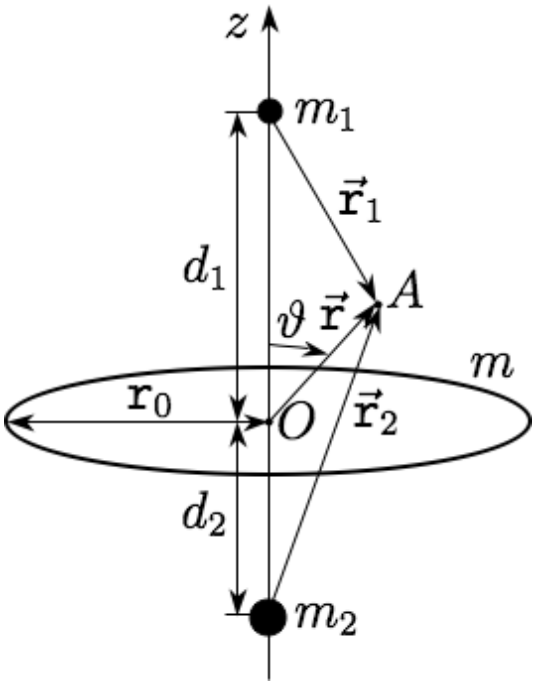

Figure D.1: Scheme for calculation of the gravitational potential at point A due to the point-like masses m_1 and m_2 located on the axis Oz, and the thin ring of mass m and radius $\mathtt{r}_0$ located in the plane perpendicular to the axis.

The potential is

$$\begin{aligned}\hat{U}_N &= -\frac{m_1}{\sqrt{\mathtt{r}^2+d_1^2-2\mathtt{r}d_1\cos\vartheta}}-\frac{m_2}{\sqrt{\mathtt{r}^2+d_2^2+2\mathtt{r}d_2\cos\vartheta}}\\ &- \frac{2mK(k)}{\pi\sqrt{\mathtt{r}^2+\mathtt{r}_0^2+2\mathtt{r}\mathtt{r}_0\sin\vartheta}}\,,\ k=\frac{2\sqrt{\mathtt{r}\mathtt{r}_0\sin\vartheta}}{\sqrt{\mathtt{r}^2+\mathtt{r}_0^2+2\mathtt{r}\mathtt{r}_0\sin\vartheta}},\end{aligned}\tag{D.1}$$

where $\mathtt{r}=|\vec{\mathtt{r}}|$ and $K(k)$ is the complete elliptic integral of the first kind, $K(0)=\pi/2$.

We consider an octupole approximation of the potential assuming that the sources are remote, i.e., $\mathtt{r}/l\ll 1$, where $l=\min\{\mathtt{r}_0,d_1,d_2\}$. The approximation reads

$$\hat{U}_N \approx \alpha_0+\alpha_1\mathtt{r}P_1(\cos\vartheta)+\alpha_2\mathtt{r}^2P_2(\cos\vartheta)+\alpha_3\mathtt{r}^3P_3(\cos\vartheta),\tag{D.2}$$

where the Newtonian multipole moments are given by

$$\begin{aligned}\alpha_0 &= -\frac{m_1}{d_1}-\frac{m_2}{d_2}-\frac{m}{\mathtt{r}_0}\,,\ \alpha_1=\frac{m_2}{d_2^2}-\frac{m_1}{d_1^2},\\ \alpha_2 &= \frac{m}{2\mathtt{r}_0^3}-\frac{m_1}{d_1^3}-\frac{m_2}{d_2^3}\,,\ \alpha_3=\frac{m_2}{d_2^4}-\frac{m_1}{d_1^4}.\end{aligned}\tag{D.3}$$

Here, α_0 is the monopole, α_1 is the dipole, α_2 is the quadrupole, and α_3 is the octupole moment.

In general, for arbitrary values of the masses we can have any values for the moments; however, the condition that $\hat{U}_N\leqslant 0$ should be satisfied. Note, that α_0 is always negative.

Appendix E

Calculation of the spacetime invariants

In this appendix, we obtain expressions for the curvature and the electromagnetic field invariants near horizons of a static, arbitrary (not necessary axisymmetric) distorted black hole with electric charge. The procedure is similar to that presented in [78]. We start our construction in the regions where the Killing vector $\boldsymbol{\xi}$ is timelike, namely outside of the horizons. The final expressions of the invariants will be valid in the region between the horizons as well.

The simplest curvature invariant is the Kretschmann scalar, which for Einstein-Maxwell 4D spacetime admits the following decomposition

$$\mathcal{K} = R_{\alpha\beta\gamma\delta}R^{\alpha\beta\gamma\delta} = \mathcal{C}^2 + 2R_{\alpha\beta}R^{\alpha\beta}, \tag{E.1}$$

where $\mathcal{C}^2 = C_{\alpha\beta\gamma\delta}C^{\alpha\beta\gamma\delta}$ is the Weyl scalar. The Weyl invariant characterizes properties of a 'pure' gravitational field, while the square of the Ricci tensor $R_{\alpha\beta}R^{\alpha\beta}$ is determined in our case by the electrostatic field. In this appendix, we derive an expansion of these invariants near the black hole horizons. In the main text of Chapter 2, we use these results for a special case, when the static spacetime is axisymmetric. A similar analysis for a vacuum distorted black hole can be found in [44] and [77]. The results presented in [44] are the particular case (corresponding to zero electrostatic field) of the results given in this appendix.

It is convenient to start with the form of the metric proposed in [77]. Namely, we consider static spacetime which has timelike, hypersurface orthogonal Killing vector $\boldsymbol{\xi}$. We assume that in the region under consideration $\nabla_\alpha(\boldsymbol{\xi}^2)$ does not vanish. Following [77] we write our metric, $g_{\alpha\beta}$ $(\alpha, \beta, \ldots = 0, \ldots, 3)$ in this region in the form

$$ds^2 = -k^2dt^2 + d\gamma^2\,,\;\; d\gamma^2 = \gamma_{AB}dy^Ady^B = \kappa^{-2}(k,\theta^c)dk^2 + h_{ab}(k,\theta^c)d\theta^ad\theta^b\,. \tag{E.2}$$

Here, $k = (-\xi_\alpha \xi^\alpha)^{1/2}$; $A, B, \ldots = 1, 2, 3$; $a, b, c, \ldots = 2, 3$,

$$\kappa^2 = -\frac{1}{2}(\nabla^\beta \xi^\alpha)(\nabla_\beta \xi_\alpha)\,, \tag{E.3}$$

and h_{ab} is the metric on 'equipotential' 2D surfaces $k = const$ spanned by θ^a coordinates. At the horizon of a static black hole, that is for $k = 0$, κ coincides with the surface gravity. In a static spacetime the Weyl invariant can be written as follows [47]

$$\mathcal{C}^2 \equiv C_{\alpha\beta\gamma\delta}C^{\alpha\beta\gamma\delta} = 8\Pi_{\alpha\beta}\Pi^{\alpha\beta} + 8\Pi_{\alpha\beta}\Lambda^{\alpha\beta} + 4\Lambda_{\alpha\beta}\Lambda^{\alpha\beta} - (\Pi + \Lambda)^2 - 2R_{\alpha\beta}R^{\alpha\beta}\,, \tag{E.4}$$

where

$$\Pi_{\alpha\beta} = R_{\alpha\gamma\delta\beta}\zeta^{\gamma\delta}\,,\ \ \Pi \equiv \Pi_\alpha{}^\alpha = -\zeta_{\alpha\beta}R^{\alpha\beta}\,, \tag{E.5}$$

$$\Lambda_{\alpha\beta} = R_{\alpha\beta} + \zeta_{\alpha\beta}\Pi\,,\ \ \Lambda \equiv \Lambda_\alpha{}^\alpha = R + \Pi\,. \tag{E.6}$$

Here, $\zeta_{\gamma\delta} = -\xi_\gamma\xi_\delta/\boldsymbol{\xi}^2$. For a static spacetime $\Pi_{00} = \Pi_{0A} = 0$. To calculate $\mathcal{C}^2$, it is convenient to use the Gauss-Codazzi equations (see [77])

$$R_{ABCD} = \mathcal{R}_{ABCD} + \varepsilon[\mathcal{S}_{AD}\mathcal{S}_{BC} - \mathcal{S}_{AC}\mathcal{S}_{BD}]\,, \tag{E.7}$$

$$n^\alpha R_{\alpha BCD} = \mathcal{S}_{BC|D} - \mathcal{S}_{BD|C}\,, \tag{E.8}$$

$$kR_{A\gamma\delta B}n^\gamma n^\delta = -k\Pi_{AB} = \gamma_{AC}\mathcal{S}_B{}^C{}_{,t} + \varepsilon k_{|AB} + k\mathcal{S}_{AC}\mathcal{S}_B{}^C\,. \tag{E.9}$$

Here, $n^\alpha = \xi^\alpha/k$ is the unit normal to a hypersurface $t = const$, $\varepsilon = \boldsymbol{n}^2 = -1$, $\mathcal{S}_{AB}$ is the extrinsic 3D curvature of the hypersurface $t = const$, $\mathcal{R}_{ABCD}$ is its 3D intrinsic curvature defined with respect to the metric $d\gamma^2$, while $\mathcal{R}$ is the 3D scalar curvature. The stroke stands for a covariant derivative with respect to this metric.

Relations (E.7)-(E.9) imply

$$2G_{\alpha\beta}n^\alpha n^\beta = -\varepsilon\mathcal{R} - \mathcal{S}_{AB}\mathcal{S}^{AB} + \mathcal{S}^2\,, \tag{E.10}$$

$$R_{\alpha\beta}n^\alpha n^\beta = -\mathcal{S}_{AB}\mathcal{S}^{AB} - \varepsilon k^{-1}k_{|A}{}^{|A} - k^{-1}\mathcal{S}_{,t}\,, \tag{E.11}$$

$$G_{\alpha B}n^\alpha = R_{\alpha B}n^\alpha = -\mathcal{S}_{,B} + \mathcal{S}_B{}^C{}_{|C}\,, \tag{E.12}$$

$$R_{AB} = \mathcal{R}_{AB} - \varepsilon\mathcal{S}\mathcal{S}_{AB} - k^{-1}k_{|AB} - \varepsilon k^{-1}\gamma_{AC}\mathcal{S}_B{}^C{}_{,t}\,. \tag{E.13}$$

Here $\mathcal{S} = \gamma^{AB}\mathcal{S}_{AB}$ is twice the mean curvature. Since the metric (E.2) is static, the extrinsic curvature defined as

$$\mathcal{S}_{AB} = \frac{1}{2}k^{-1}\gamma_{AB,t} \tag{E.14}$$

vanishes. Thus, Eqs. (E.7)-(E.13) imply

$$\Pi_{AB} = k^{-1}k_{|AB}\,,\ \ \Pi = k^{-1}k_{|A}{}^{|A}\,, \tag{E.15}$$

$$\Lambda_{AB} = \mathcal{R}_{AB} - k^{-1}k_{|AB}\,,\ \ \Lambda = \mathcal{R} - k^{-1}k_{|A}{}^{|A}\,, \tag{E.16}$$

$$\Lambda_{00} = 0\,,\ \ \Lambda_{0A} = 0\,. \tag{E.17}$$

The Einstein equations $G_{\alpha\beta} = 8\pi T_{\alpha\beta}$ give

$$\mathcal{R} = 16k^{-2}\pi T_{00}\,,\ \ T_{0A} = 0\,,\ \ G_{AB} = 8\pi T_{AB} + k^{-1}k_{|AB} - k^{-1}\gamma_{AB}k_{|A}{}^{|A}. \tag{E.18}$$

Thus, the Weyl invariant (E.4) written in terms of 3D objects related to hypersurface $t = const$ is

$$\mathcal{C}^2 \ \ = \ \ 2k^{-2}\left(k_{|AB}k^{|AB} - 3k_{|A}{}^{|A}k_{|B}{}^{|B}\right) + 2\left(\mathcal{R}_{AB} + 2k^{-1}k_{|AB}\right)\mathcal{R}^{AB}\,. \tag{E.19}$$

The next step is a $(2+1)$ decomposition. We use the following expression for the 3D metric

$$d\gamma^2 = \kappa^{-2}(k,\theta^c)dk^2 + h_{ab}(k,\theta^c)d\theta^a d\theta^b\,. \tag{E.20}$$

We denote a covariant derivative with respect to the 2D metric h_{ab} as $(\ldots)_{:a}$. A unit vector orthogonal to the equipotential 2D surface $k = const$ is $n^A = \kappa\delta^A_k$, $\varepsilon = \boldsymbol{n}^2 = 1$. The extrinsic curvature of the surface is

$$S_{ab} = \frac{\kappa}{2}h_{ab,k}. \tag{E.21}$$

Using the metric (E.20) we derive

$$k_{|kk} \ \ = \ \ \kappa^{-1}\kappa_{,k}\,,\ \ k_{|ka} = \kappa^{-1}\kappa_{:a}\,,\ \ k_{|ab} = \kappa S_{ab}\,,\ \ k_{|A}{}^{|A} = \kappa S + \kappa\kappa_{,k}\,,\ \ S = h^{ab}S_{ab}\,. \tag{E.22}$$

To project the Einstein equations on the $2D$ surface we have to define the stress-energy tensor of the electrostatic field. The electrostatic potential is given by $\Phi = \Phi(k,\theta^a)$. The corresponding electric field vector defined with respect to the Schwarzschild time t on the hypersurface $t = const$ reads

$$E_A = -k^{-1}F_{0A} = -k^{-1}\Phi_{,A}. \tag{E.23}$$

We are interested in deformation of the equipotential 2D surfaces. Thus, it is convenient to define the component of the electric field vector orthogonal to the surfaces separately. The electric field vector components in an orthonormal frame

are

$$E_{\hat{k}} = -\kappa\, k^{-1}\Phi_{,k}\,,\;\; E_a = k^{-1}\Phi_{:a}\,. \tag{E.24}$$

Thus, in our notations

$$\vec{E}^2 = E_{\hat{k}}^2 + k^{-2}\Phi_{:a}\Phi^{:a}. \tag{E.25}$$

The energy-momentum tensor of the field is

$$8\pi T_{\alpha\beta} = 2\xi_\alpha\xi_\beta k^{-2}\vec{E}^2 - 2E_\alpha E_\beta + g_{\alpha\beta}\vec{E}^2. \tag{E.26}$$

Using the relations (E.10)-(E.13) for the metric (E.20) together with the relations (E.18), we derive the Einstein equations projected onto the 2D equipotential surfaces:

$$\begin{aligned}
\kappa^3\, S_a^{\;b}{}_{,k} &= \kappa^2[K - E_{\hat{k}}^2 - k^{-2}\Phi_{:c}\Phi^{:c}]\delta_a^{\;b} - \kappa^3 k^{-1} S_a^{\;b} \\
&+ \kappa\kappa_{:a}^{\;\;:b} - 2\kappa_{:a}\kappa^{:b} - \kappa^2 S S_a^{\;b} + 2\kappa^2 k^{-2}\Phi_{:a}\Phi^{:b}, && \text{(E.27)}\\
\kappa^3\, S_{,k} &= \kappa^2\left[\kappa k^{-1} S - S_a^{\;b} S_b^{\;a} - 2k^{-2}\Phi_{:a}\Phi^{:a}\right] + \kappa\kappa_{:a}^{\;\;:a} - 2\kappa_{:a}\kappa^{:a}, && \text{(E.28)}\\
k^{-1}\kappa\,\kappa_{,k} &= -\kappa k^{-1} S + E_{\hat{k}}^2 + k^{-2}\Phi_{:a}\Phi^{:a}, && \text{(E.29)}\\
\kappa^2\, E_{\hat{k}\,,k} &= -\kappa S E_{\hat{k}} - \kappa_{:a} k^{-1}\Phi^{:a} + \kappa\, k^{-1}\Phi_{:a}^{\;\;:a}. && \text{(E.30)}
\end{aligned}$$

The corresponding constraints are

$$\begin{aligned}
0 &= S^2 - S_a^{\;b} S_b^{\;a} - 2K + 2[\kappa k^{-1} S + E_{\hat{k}}^2 - k^{-2}\Phi_{:a}\Phi^{:a}], && \text{(E.31)}\\
0 &= [S_{:a} - S_a^{\;\;b}{}_{:b}]k + 2E_{\hat{k}}\Phi_{:a} + \kappa_{:a}. && \text{(E.32)}
\end{aligned}$$

Here, K is the Gaussian curvature of a 2D equipotential surface $k = const$.

The square of the Ricci tensor $R_{\alpha\beta}R^{\alpha\beta}$ is equal to the squared electromagnetic field invariant

$$R_{\alpha\beta}R^{\alpha\beta} = (F^2)^2 = (F_{\alpha\beta}F^{\alpha\beta})^2. \tag{E.33}$$

According to Eqs. (E.23) and (E.25), F^2 has the following form:

$$F^2 = -2\vec{E}^2 = -2[E_{\hat{k}}^2 + k^{-2}\Phi_{:a}\Phi^{:a}]. \tag{E.34}$$

Using the expressions (E.18), (E.24)-(E.30), we derive

$$\begin{aligned}
\mathcal{R}_{kk} &= k^{-1}\kappa^{-1}\kappa_{:k} + \kappa^{-2}[\vec{E}^2 - 2E_{\hat{k}}^2],\\
\mathcal{R}_{ak} &= k^{-1}\kappa^{-1}[\kappa_{:a} + 2E_{\hat{k}}\Phi_{:a}],\\
\mathcal{R}_{ab} &= k^{-1}\kappa S_{ab} + h_{ab}\vec{E}^2 - 2k^{-2}\Phi_{:a}\Phi_{:b},\\
\mathcal{R} &= 2\vec{E}^2 = 2k^{-1}\kappa[S + \kappa_{:k}]. && \text{(E.35)}
\end{aligned}$$

Using Eqs. (E.19), (E.1), (E.34), and expressions (E.22) and (E.35), we have

$$\begin{aligned}\frac{1}{8}\mathcal{C}^2 &= [\kappa^2 S_a{}^b S_b{}^a + 2\kappa_{:a}\kappa^{:a} + \kappa^2 S^2 + 2\vec{E}^2\Phi_{:a}\Phi^{:a}]k^{-2} \\ &+ 4E_{\hat{k}}\kappa_{:a}\Phi^{:a}k^{-2} - 2\kappa\,[S_a{}^b\Phi_{:b} + S\Phi_{:a}]\Phi^{:a}k^{-3}. \qquad \text{(E.36)}\end{aligned}$$

The hypersurface-orthogonal Killing vector field ξ^α by definition is null on the Killing horizon, which is bifurcate ($\kappa \neq 0$). A bifurcate Killing horizon contains a 2D spacelike, totally geodesic surface [13]. In our coordinates, this equipotential surface is defined by $t = const$ and $k = 0$. On the other side, a necessary and sufficient condition that a hypersurface is totally geodesic is its vanishing extrinsic curvature defined in the corresponding enveloping space [31]. Thus, for the equipotential surfaces $t = const$, $k = 0$, we have $S_{ab} = 0$. For a regular horizon, its 2D surface has everywhere finite Gaussian curvature, and the electrostatic field on the surface is finite as well. Thus, we can deduce from the constraints (E.31) and (E.32) that on the horizon $\Phi_{:a} = \kappa_{:a} = 0$. Hence, the electrostatic field potential Φ is constant on the black hole horizon. This implies that the horizon surface is an equipotential surface of the electrostatic field; thus, according to Eq. (E.24),

$$E_a|_H = k^{-1}\Phi_{:a}|_H = 0\,. \qquad \text{(E.37)}$$

Here and below $(...)|_H$ means calculated on the horizon. The constancy of κ on the horizon is nothing but the zeroth law of black hole thermodynamics [9].

Projecting the first of the Einstein equations (E.27) on the horizon, we derive

$$\kappa\left[S_a{}^b{}_{,k} + S_a{}^b k^{-1}\right]\big|_H = \delta_a{}^b[K - E_{\hat{k}}^2]\big|_H\,. \qquad \text{(E.38)}$$

Expanding the extrinsic curvature near the horizon, $S_a{}^b \approx S_a{}^b\big|_H\, k$, we present the expression (E.38) in the following form:

$$2\kappa S_a{}^b k^{-1}\big|_H = \delta_a{}^b[K - E_{\hat{k}}^2]\big|_H\,. \qquad \text{(E.39)}$$

Thus, using Eqs. (E.33), (E.34), (E.36) and (E.39), we derive the following expressions for the spacetime invariants calculated on the horizon:

$$F^4\big|_H = R_{\alpha\beta}R^{\alpha\beta}\big|_H = 4E_{\hat{k}}^4\big|_H\,, \qquad \text{(E.40)}$$

and

$$\mathcal{C}^2\big|_H = 12[K - E_{\hat{k}}^2]^2\big|_H\,. \qquad \text{(E.41)}$$

This is the generalization of the relation between the Gaussian curvature and the Kretschmann scalar calculated on the event horizon surface of an arbitrary

distorted Schwarzschild black hole [45], [44].

We can expand the metric and the electrostatic field in a series near the horizon and substituting these expansions into Eqs. (E.34) and (E.36), to derive expressions of the spacetime invariants near the horizon. There are two types of quantities, even and odd in k, which we denote by $A = \{\kappa, h_{ab}, K, \Phi, E_{\hat{k}}, F^2, \mathcal{C}^2\}$, and $B = \{S_a^{\ b}, S\}$, respectively. The series expansions of A and B read

$$A = \sum_{n\geqslant 0} A^{[2n]} k^{2n}, \quad B = \sum_{n\geqslant 0} B^{[2n+1]} k^{2n+1}. \tag{E.42}$$

Here, $A^{[0]} \equiv A|_H$. We can express higher order coefficients in the expressions in terms of these on the horizon substituting Eq. (E.42) into the Einstein equations (E.27)-(E.32). The necessary coefficients to calculate the first order expansion of the spacetime invariants are the following:

$$\begin{aligned}
\kappa^{[2]} &= \frac{1}{2\kappa^{[0]}}[2E^{[0]2}_{\hat{k}} - K^{[0]}], \quad \Phi^{[2]} = -\frac{E^{[0]}_{\hat{k}}}{2\kappa^{[0]}}, \\
S_a^{\ b[1]} &= \frac{\delta_a^{\ b}}{2\kappa^{[0]}}[K^{[0]} - E^{[0]2}_{\hat{k}}], \quad S^{[1]} = \frac{1}{\kappa^{[0]}}[K^{[0]} - E^{[0]2}_{\hat{k}}], \\
S_a^{\ b[3]} &= \frac{1}{8\kappa^{[0]2}}[2\kappa^{[2]:b}_{:a} + \kappa^{[2]:a}_{:a}\delta_a^{\ b} - \kappa^{[0]} S^{[1]2}\delta_a^{\ b}] \\
&+ \frac{1}{16\kappa^{[0]3}}[2E^{[0]}_{\hat{k}:a}E^{[0]:b}_{\hat{k}} - 3E^{[0]}_{\hat{k}:c}E^{[0]:c}_{\hat{k}}\delta_a^{\ b}], \\
S^{[3]} &= \frac{1}{4\kappa^{[0]2}}[2\kappa^{[2]:a}_{:a} - \kappa^{[0]}S^{[1]2}] - \frac{1}{4\kappa^{[0]3}}E^{[0]}_{\hat{k}:a}E^{[0]:a}_{\hat{k}}, \\
E^{[3]}_{\hat{k}} &= -\frac{1}{4\kappa^{[0]2}}[2\kappa^{[0]}S^{[1]}E^{[0]}_{\hat{k}} + E^{[0]:a}_{\hat{k}:a}].
\end{aligned} \tag{E.43}$$

Finally, we derive the first-order expansions of the spacetime invariants near the horizon:

$$F^2 \approx -2E^2_{\hat{k}}\big|_H + \frac{1}{2\kappa^2}\big[4K_e E^2_{\hat{k}} + E^{2\ :a}_{\hat{k}:a} - 3E_{\hat{k}:a}E^{\ :a}_{\hat{k}}\big]\Big|_H k^2, \tag{E.44}$$

$$\begin{aligned}
\mathcal{C}^2 &\approx 12K_e^2\big|_H - \frac{1}{\kappa^2}\big[6K_e^2[3K_e - 2E^2_{\hat{k}}] - [2K_e - E^2_{\hat{k}}]_{:a} \\
&\times [2K_e - E^2_{\hat{k}}]^{:a} + 6K_e[K_{e:a}^{\ \ :a} - 2E_{\hat{k}}E^{\ :a}_{\hat{k}:a}]\big]\big|_H k^2,
\end{aligned} \tag{E.45}$$

where $K_e|_H = [K - E^2_{\hat{k}}]|_H$.

Appendix F

Induced electrostatic perturbation

I this appendix, we discuss the existence of threshold modes in the electrostatic perturbation equation (3.48). Using the transformations (3.50) and (3.90), we present the equation in the following form:

$$x^2\tilde{a}_{t,xx} + \frac{2mx^2}{1+mx}\tilde{a}_{t,x} - \frac{\kappa^2 x}{(1-x)^4}\tilde{a}_t = 0. \tag{F.1}$$

Applying the method of Frobenius we derive the following boundary conditions

$$\tilde{a}_t(0) = 0\,,\ \ \tilde{a}_{t,x}(0) = \kappa^2\,,\ \ \tilde{a}_t(1) = 0. \tag{F.2}$$

Using the boundary conditions and implementing the shooting code written in FORTRAN [108], we found no indication of unstable threshold modes.

This result can be inferred from analytical consideration of the equation. Let us present (F.1) in the self-adjoint form

$$\left[(1+mx)^2\tilde{a}_{t,x}\right]_{,x} - \frac{\kappa^2(1+mx)^2}{x(1-x)^4}\tilde{a}_t = 0. \tag{F.3}$$

Multiplying this equation by $\tilde{a}_t$, integrating the result by parts, and using the boundary conditions (F.2), we derive

$$\int_0^1 \left((1+mx)^2\tilde{a}_{t,x}^2 + \frac{\kappa^2(1+mx)^2}{x(1-x)^4}\tilde{a}_t^2\right) dx = 0. \tag{F.4}$$

This equation has the nontrivial solution $\tilde{a}_t$ only if $\kappa^2 < 0$. Thus, there are no unstable threshold modes.

Appendix G

5D compactified extremal RN black hole

In this appendix, we consider a static, extremal RN black hole in 5D spacetime with one compact dimension of asymptotic size L (see, e.g., [97]). The corresponding metric is

$$ds^2 = -U^{-2}(\rho,z)dt^2 + U(\rho,z)dl^2, \tag{G.1}$$

$$U(\rho,z) = 1 + \frac{4M}{3\rho}\frac{\sinh(2\pi\rho/L)}{\cosh(2\pi\rho/L) - \cos(2\pi z/L)}, \tag{G.2}$$

$$dl^2 = d\rho^2 + dz^2 + \rho^2(d\theta^2 + \sin^2\theta d\phi^2)\,., \tag{G.3}$$

and the coordinate ranges are

$$t \in (-\infty,\infty)\,,\ \ \rho \in [0,\infty)\,,\ \ z \in [0,L]\,,\ \ \theta \in [0,\pi]\,,\ \ \phi \in [0,2\pi). \tag{G.4}$$

The corresponding electrostatic potential vanishing at asymptotic infinity is

$$A_\alpha = \sqrt{3}[U(\rho,z)^{-1} - 1]\delta_\alpha{}^t. \tag{G.5}$$

The Komar mass and the electric charge of the black hole are the same as those of the corresponding 5D extremal RN black hole. The equipotential hypersurfaces $U = const$ are schematically illustrated in Figure G.1.

The black hole horizon is defined by $\rho = z = 0$. As it is shown in the figure, the horizon is a point. This is just a manifestation of coordinate singularity. One can check that none of the spacetime invariants $C_{\alpha\beta\gamma\delta}C^{\alpha\beta\gamma\delta}$, $R_{\alpha\beta}R^{\alpha\beta}$ diverges there. Therefore, we can perform an analytical continuation through the point $(\rho = 0, z = 0)$. We consider the following analytical continuation in the (ρ, z) plane:

$$\rho = i\tilde{\rho}\,,\ \ z = i\tilde{z}, \tag{G.6}$$

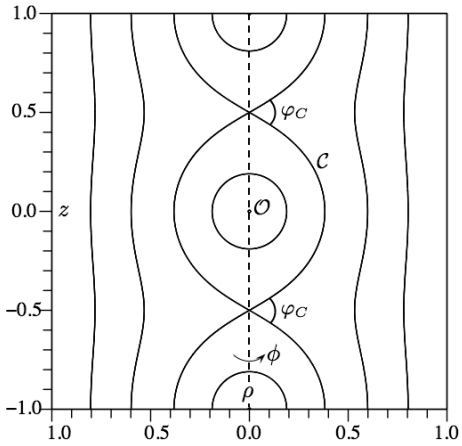

Figure G.1: Rotational curves corresponding to 2D slices $\theta = \pi/2$ of equipotential 3D hypersurfaces $U = const$ are shown for $M = L = 1$ in the corresponding covering space. 5D extremal black holes are located along the dashed vertical line. Point $\mathcal{O}$ indicates horizon of one of such black holes. The critical curve $\mathcal{C}$ separates equipotential hypersurfaces of different topology and corresponds to $U = 1+4\pi/3$. The angle of the cone of the critical surface is $\varphi_C = 60^\circ$ (see [39]).

where $\tilde{\rho}$ and $\tilde{z}$ are real coordinates. In the new coordinates $(\tilde{\rho}, \tilde{z})$ the metric function (G.2) reads

$$\widetilde{U}(\tilde{\rho}, \tilde{z}) = 1 + \frac{4M}{3\tilde{\rho}} \frac{\sin(2\pi\tilde{\rho}/L)}{\cos(2\pi\tilde{\rho}/L) - \cosh(2\pi\tilde{z}/L)}. \tag{G.7}$$

The equipotential hypersurfaces $\widetilde{U} = const$ are schematically illustrated in Figure G.2. Analysis of the spacetime invariants shows that the true spacetime singularity corresponds to $\widetilde{U} = 0$. The singularity is timelike. It is illustrated in Figure G.2 by the curve $\mathcal{S}$. However, as one can check from the metric (G.1), it is a point of zero 4D volume.

Finally, we can calculate the Bekenstein-Hawking entropy of the black hole [see Eq. (3.58)],

$$\mathcal{S} = \frac{4M^{3/2}}{3\sqrt{3}} \sqrt{\pi L}. \tag{G.8}$$

We see that the entropy, and hence the horizon area, is nonzero, despite the fact that the horizon surface is a point in (ρ, z) coordinates. From expression (G.8) we see that the entropy of a single compactified RN black hole is greater than the entropy of an assemblage of such black holes of the same total mass M.

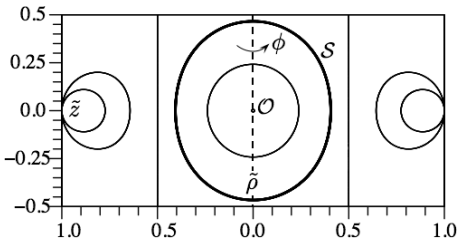

Figure G.2: Rotational curves corresponding to 2D slices $\theta = \pi/2$ of equipotential 3D hypersurfaces $\widetilde{U} = const$ are shown for $M = L = 1$. The point $\mathcal{O}$ indicates the black hole horizon. The spacetime singularity $\widetilde{U} = 0$ is illustrated by the curve $\mathcal{S}$, which separates equipotential hypersurfaces of negative (inside the curve) and positive (outside the curve) values of $\widetilde{U} = const$.